PART A:
IRIDIUM CATALYZED C-H BORYLATION OF ARENES; ENGINEERING SELECTIVITY BY LIGAND DESIGN.
PART B:
Z-SELECTIVE PALLADIUM CATALYZED CROSS COUPLING OF E-VINYL GERMANES.

By

Susanne L. Miller

A DISSERTATION

Submitted to
Michigan State University
in partial fulfillment of the requirements
for the degree of

Chemistry-Doctor of Philosophy

2017

ABSTRACT

PART A: IRIDIUM CATALYZED C-H BORYLATION OF ARENES; ENGINEERING SELECTIVITY BY LIGAND DESIGN.

By

Susanne L. Miller

Iridium catalyzed C-H borylation has gained popularity as a means to functionalize simple aromatic and heterocyclic substrates under mild conditions which tolerate a variety of functional groups. Initial efforts to develop this chemistry made use of sterically driven selectivity to achieve contra-electronic substitution patterns of aromatic and heterocyclic building blocks that were not easily obtainable by conventional organic chemistry prevalent before the discovery of this chemistry in 1999. As methodology and substrate scope rapidly expanded, steric selectivity became a limitation, as more diverse substitution patterns and higher selectivities were sought. These limitations were partially overcome by the extensive development of directing groups which enabled more traditional ortho substitution patterns to be accessed by the same mild conditions that made Ir-C-H borylation popular. While steric limitations that result in mixtures by the standard borylation protocols can now be overcome by directing groups, a serious challenge remains for the meta-functionalization of substrates which lack common directing groups or have small substituents. This work seeks to address this limitation by ligand-directed selectivity which can be instituted by the rational design of catalysts and ligands to achieve different selectivity outcomes depending on the desired product. The design and development of ligands which make use of either steric or electronic properties to achieve a given outcome was realized, and borylation meta to fluorine in simple arenes which lack directing groups was achieved. By varying the substituents on this ligand framework, the selectivity of the borylation can be shifted from steric to electronic selectivity.

PART B: Z-SELECTIVE PALLADIUM CATALYZED CROSS COUPLING OF E-VINYL GERMANES.

Germanium cross coupling reactions were born out of efforts to replace toxic organo-tin reagents used in the Stille cross coupling reaction for the construction of C-C bonds. Initial interest in germanium as a transmetalation partner peaked in the mid to late 1990s, but eventually waned due to poor reactivity of organo-germanium reagents and the harsh conditions needed to activate Ge-C bonds towards cross coupling. One such effort from the Maleczka group in the early 2000s, although suffering from poor conversion and unreliable results, gained modest attention by displaying a reactivity distinct from typical Stille coupling selectivity. Instead of retention of geometry, the major product of the E-vinyl germanium coupling reaction exhibited inverted Z-olefin geometry. In the reverse case, Z-vinylgermanes likewise gave inverted E-olefins as the major coupling products. Early studies of the reaction led to the hypothesis of a Heck-like insertion with subsequent germyl elimination to form the inverted product. The proposed mechanism featured a palladium-germyl elimination in preference to a possible β-H elimination. Based on the substrate scope and the organo-germane's required possession of a tertiary allylic alcohol, the Pd-Ge elimination theory was discarded in favor of the formation of a reactive epoxide intermediate, which eliminated germanium upon carbopalladation. The observation of the unactivated cross coupling of allylic germanium epoxides with iodo-arenes supported this hypothesis. Expansion of this chemistry was hampered by inconsistent results and a very narrow substrate scope. Further investigation suggested involvement of Pd nanoparticles.

I dedicate this dissertation to my parents, Bob and Mary, who never gave me any reason to think there is anything I can't do. I also dedicate this dissertation to my sisters, Lorenda, Dianne and Judy, smart and lovely women who are strong, positive role models for their baby sister. I also thank my husband Mitch for his mostly constructive criticism and unwavering support, and my kids, Fred and Milton, who taught me the fine art of work-life triage.

ACKNOWLEDGMENTS

I would like to acknowledge the chemists who influenced me the most in my early years and gave me a firm foundation on which I built my current knowledge and deep appreciation for science. Thanks to Dean Lantero, my undergraduate mentor, who taught me the art of air-free Schlenk-line techniques, mastery of laboratory equipment and the skills to follow any experimental procedure. Thanks to G. Abbas Chotana who guided me through my first C-H borylation and taught me how the results of one experiment flow into the design of the next. Thanks to Luis Sanchez and Monica Norberg for teaching an inorganic chemist the finer points of organic synthesis, and to Rob Maleczcka for teaching me how to run a proper silica gel flash chromatography column. Thanks to Paul Herrinton, my former supervisor and colleague at BoroPharm, who taught me how to scale up reactions safely, how to stream line and improve procedures, and most importantly, when to throw a reaction away and start over. He helped me prioritize projects to make the best use of my time, because, as he would tell me often, time is always the most expensive reagent.

I would also like to acknowledge the world-class support staff at MSU, most notably Dr. Dan Holmes, a true NMR genius, and his talented assistant Dr. Li Xie. They helped me set up and run no-D NMR kinetic studies and, most importantly, kept the instruments running so I always had access to a spectrometer when I needed crucial data. Dr. Holmes has helped me design and interpret numerous NMR experiments, and this thesis would not be the same without his help.

I also would like to acknowledge Dr. Richard Staples, a crystallographer of extraordinary talent, for solving all the crystal structures produced in my graduate work. I am grateful for the opportunity to work with him and learn from him.

I also wish to acknowledge Dr. Dan Jones, director of the Mass Spectrometry and Metabolomic Core Facility at MSU, and his assistant Lijun Chen, in addition to Todd Liddick, the director of the biochemistry mass spec facility in the Chemistry Building, and my colleague Yu-Ling Lien, all of whom helped me help collect HRMS data. Thanks also to Olivia Chesniak for her invaluable help with transmission electron microscopy, and to Olivia and Yu-Ling for their help in preparing samples for TEM analysis.

Many thanks are due to Scott Bankroff in the glass shop and Glenn Weseley in the machine shop. An integral part of my research is contingent on having a good vacuum line and manifold, and I have depended on Scott to keep my vacuum manifold free of leaks and Glenn to change my worn-out drive belts. Thanks also to Dean Shooltz for rebuilding my pump and keeping it running like new. Without their support, I could not do the same high caliber work.

I must also acknowledge the Computer and Technology office for saving the day during several computer emergencies. Thanks to Tom Carter for help with poster design and printing, and helping me to set up a backup drive. Thanks to Paul Reed for keeping our ancient GC computer running on the network, and for helping me fix rogue printers, find lost emails and solve networking problems. Thanks to Chris Pfeiffer for helping with posters, web posting and email issues.

This section would not be complete without acknowledging the many specialists and support staff that keep the department running with a high level of efficiency and professionalism so that students can focus on research and teaching. I would like to acknowledge the main office and graduate office staff, the purchasing and business office staff, and building staff for keeping me on track and our labs in good functioning order. Thanks especially to Marvy Olson and Beth McGaw in purchasing; and Bob Rasico, Eric Smariege, Bill Flick, and Melissa Parsons of the

building staff. A special thanks to Heidi Warden in the graduate office for always knowing what the actual MSU policy is and what I needed to do to follow it!

I would also like to acknowledge the many supportive lab-mates, friends and colleagues who have made my life richer and more fun during my time in graduate school. Special thanks go to my boron project collaborators Behnaz Ghaffari and Jonathan Dannatt. Thanks to my germanium project collaborators, Kio Tanemura, Shawn Haldar and Maryam Abbas. Thanks also to my favorite current and former coworkers Damith Perera, Kristin Gore, Tim Shannon, Yu-Ling Lien, Hao Li, Ruwi Jayasundara, Olivia Chesniak, Rosario Amado-Hennessey, Aaron Baker, Fangyi Shen, Luis Mori, Pepe Montero, Badru-Deen Barry, David Vogelsang, Gayanthi Attanayake, Buddhadeb Chattopadhayay, Dmitry Sabasovs, Jon Fritz, Jacob Stricker, and Beth Schoen.

Many thanks go out to my committee members, all of whom are accomplished chemists and good people whose work I admire. They have inspired and challenged me professionally and personally, and they are truly great teachers, role models, and friends. Thanks to Rob Maleczka, my advisor, Aaron Odom, my second reader, Ned Jackson, Tom Hamann and Viktor Poltavets.

My final acknowledgements go out to Dr. Steve Carlson from Lansing Community College and Dr. Todd Zahn from BoroPharm, guys who trusted me enough to hire me as a chemist at different times in my life. Those jobs gave me valuable confidence and experience that allowed me to get where I wanted to go.

TABLE OF CONTENTS

LIST OF TABLES

LIST OF FIGURES

LIST OF SCHEMES

KEY TO ABBREVIATIONS

Ac	Acetate
AIBN	Azobisisobutyronitrile
Ar	Aryl
-BCat	Catecholate Ester of Boron, also called Catechol boronate
HBCat	Catechol Borane
-Bpin	Pinacolate Ester of Boron, also called Pinacol boronate
HBpin	Pinacol Borane
B_2pin_2	Bispinacolatodiborane
Bn	Benzyl
Bozo	2,2'-Bis-2-oxazoline
Bnbozo	2,2′-Bis[(4S)-4-benzyl- -2-oxazoline]
bpy	Bipyridine
BQ	1,4-Benzoquinone
Br	Bromine atom
Bu	Butyl
Bu_4NBr	Tetrabutyl Ammonium Bromide
t-Bu	Tertiary Butyl, also called tert-Butyl
°C	Degrees Celsius
Cp	Cyclopentadiene or Cyclopentadienyl
Cp*	Pentamethyl Cyclopentadiene or Pentamethyl Cyclopentadienyl
C-C	Carbon-Carbon Single Bond

C=C	Carbon-Carbon Double Bond
C-H	Carbon-Hydrogen Single Bond
C-F	Carbon-Fluorine Single Bond
C-Ge	Carbon-Germanium Single Bond
C-Si	Carbon-Silicon Single Bond
C-X	Carbon Singly Bonded to any Halogen (Group 7)
Si-H	Silicon-Hydrogen Single Bond
cal	Calorie
$CDCl_3$	Deuterated Chloroform, NMR solvent
Cy	Cyclohexane
cod	1,5-Cyclooctadiene
coe	cyclooctene
CHB	C-H Borylation
D	Deuterium atom
δ	delta, NMR Chemical shift
d	doublet, double peak in NMR spectrum
dd	doublet of doublets
dba	Dibenzylideneacetone
DCM	Dichloromethane
4-DMAP	4-Dimethylaminopyridine
dmadpm	Dimethylaminodipyridyl Methane
dpm	Dipyridyl Methane
dtbpy	4,4’-Di-tert-butyl-2,2’- bipyridine

dmpe	Dimethylphosphinoethane
DMG	Directed Metalation Group
D*o*M	Directed ortho Metalation
e^-	A Single Electron
E^+	Electrophile
-E	Electrophilic Group
(E)	*Trans*-Double Bond
EAS	Electrophilic Aromatic Substitution
EDG	Electron Donating Group
EDS	Energy Dispersive X-ray Spectroscopy
EI	Electron Impact
EI-MS	Electron Impact Mass Spectroscopy
EWG	Electron Withdrawing Group
F	Fluorine atom
FG	Functional Group
GC	Gas Chromatograph
GC-FID	Gas Chromatograph with Flame Ionizing Detector
GC-MS	Gas Chromatograph with Mass Spectrometer
H	Hydrogen atom
h	Hour
Hg	Mercury
Hz	Hertz (cycles per second)
ΔH	Enthalpy, or Change in Enthalpy

$\Delta\Delta H_s(Z)$	Steric Enthalpy of a Substituent, Z
HCl	Hydrochloric Acid
HRMS	High Resolution Mass Spectroscopy
Ir	Iridium atom
Ir CHB	Iridium-Catalyzed C-H Borylation
J	NMR Coupling Constant
KIE	Kinetic Isotope Effect
kcal	Kilocalorie
L	Ligand
LDA	Lithium Diisopropyl Amide
m	Multiplet peak in NMR spectrum
m-	meta-Substituted or directing to the meta position
M	Metal atom
M^+	Molecular Ion peak in Mass Spectrum
m/z	Mass divided by Charge of an ion in mass spectroscopy
Me	Methyl
MeCN	Acetonitrile
MHz	Mega Hertz
mol	Mole
NMP	N-Methyl pyrrolidone
NMR	Nuclear Magnetic Spectroscopy
Nu:	Nucleophile
o	ortho-Substituted or directing to ortho position

o/p	Directing to the ortho or para positions
P	Phosphorous atom
PCy_3	Tricyclohexyl Phosphine
Pd	Palladium Metal
$Pd(OAc)_2$	Palladium (II) Acetate
$Pd_2(dba)_3$	Tris(dibenzylidene)dipalladium (0)
Ph	Phenyl
PMe_3	Trimethyl Phosphine
PPh_3	Triphenyl Phosphine
PMHS	Polymethylhydroxysilane
QX	Quaternary Halogen Salt
rt	Room Temperature
s	singlet peak in NMR spectrum
SMAP	**S**ilica-constrained **M**onodentate tri**A**lkyl **P**hosphine
s	second
TBAB	Tetra Butyl Ammonium Bromide
TBAF	Tetra Butyl Ammonium Fluoride
TEM	Transmission Electron Microscope
TFA	Trifluoroacetic Acid
THF	Tetrahydrofuran
tmp	3,4,7,8-tetramethyl-1,10-phenanthroline
TNT	2,4,6-Trinitrotoluene
tol	Toluene

TPPO	Triphenyl Phosphine Oxide
(Z)	*Cis*-double bond

CHAPTER 1

INTRODUCTION

Ir-catalyzed borylation (Ir CHB) has been utilized in many applications for the production of fine chemicals,[1-2] but it is especially suitable for the construction of small molecule building blocks used in the fields of pharmaceutical, agricultural and advanced materials. There are many strategies for arene functionalization,[3] most of which have been improved and refined over decades and are still being reliably used in industry today. Ir-catalyzed C-H borylation is a new technology in comparison, and has earned its place in the top drawer of the synthetic chemist's tool box because it offers easy, one-step functionalization of arenes under mild conditions, and it provides a selectivity that many older methods of functionalization cannot easily achieve.[4]

The most widely used methods of aromatic functionalization are electrophilic or nucleophilic aromatic substitution, C-H deprotonation, and transition metal C-H activation-functionalization.[5] In recent years, innovations in all of these functionalization methodologies have developed at a rapid pace. Most selective functionalization methods make use of electronic properties resulting from the inductive or activating effects of existing electron-withdrawing or electron-donating substituents. Because the regiochemistry of Ir CHB is sterically driven, this methodology has been used as a complement to traditional selectivities that were unattainable by other types of arene functionalization. The mild conditions, high yields and simplicity of Ir CHB have resulted in efforts to develop methods that can attain all types of substitution patterns, including the ortho substitution patterns of EAS and D*o*M in order to avoid the harsh reagents or inconvenient reaction conditions of these older protocols.[6]

The selectivity of Ir CHB is primarily governed by sterics, but harnessing electronic factors to direct functionalization has also been a successful strategy. Most newer directed borylation

methodology has resulted in ortho functionalization by utilization of the conventional ortho/para directing effects of EAS chemistry[6-7]. Far less common is meta selective borylation of unhindered simple arenes lacking directing groups, and only since 2015 has meta-selective borylation been reported.[8] The origin of electronic effects lies in the properties of the arenes and their substituents, and to use these properties to gain an advantage in selectivity requires an understanding of how electronic effects arise from molecular structure.

Electrophilic Aromatic Substitution (EAS). The first method of aromatic C-H functionalization discovered is known as electrophilic aromatic substitution, (EAS).

The first report of EAS was made by Michael Faraday in 1825.[9] EAS involves an attack on the π-system of an aromatic ring by an electrophile, E^+, thus breaking the aromaticity of the ring and allowing cleavage of the C-H bond, as seen in Scheme 1.1

Scheme 1.1. Electrophilic Aromatic Substitution (EAS)

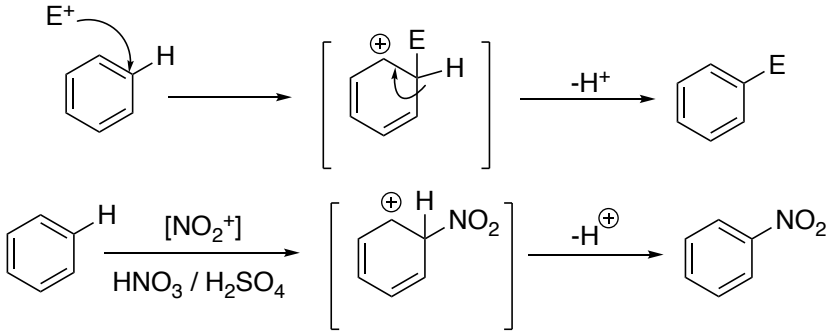

Scheme 1.1. Electrophilic aromatic substitution proceeds by an attack on the aromatic π-system. The first reported aromatic C-H functionalization was the nitration of benzene, reported in 1825 by Michael Faraday.

Substitution happens through interactions of the electronic properties of the reactants and any functional groups (FGs) that are already on the aromatic ring. Since benzene in Scheme 1.1 has no substituents, the NO_2 group can replace the H atom on any C atom of the benzene ring.

Once NO_2 is on the ring, however, where the next substituent goes will be determined by the rules of EAS.

Groups like NO_2 are referred to as Electron Withdrawing Groups (EWG) because they draw electron density out of the ring, causing incoming FGs to only substitute at the 3 or 5 positions on the ring. This is called meta substitution, also denoted by *m*.

In contrast to EWG, electron donating groups (EDG) donate π-electron density into the ring, making it more active towards substitution. This causes incoming FGs to substitute at 2, 4 and 6 positions on the ring. This is called ortho/para substitution, also denoted by *o/p*. Often *o/p* directors have lone pairs on the atom next to the ring, and although halogens are electron withdrawing, they also are *o/p* directors due to the presence of their unpaired electrons, and the ability of those electrons to donate into the ring via resonance. In order to effect substitution, reactants must be electron deficient and *electrophilic,* denoted as E^+. The positive E^+ group seeks electron density, and so substitution is not favorable at positions where there is a build-up of positive charge on the ring. Scheme 1.2 illustrates the substitution patterns of *ortho/para* and *meta* directing groups.

Scheme 1.2. Aromatic Substitution According to EAS

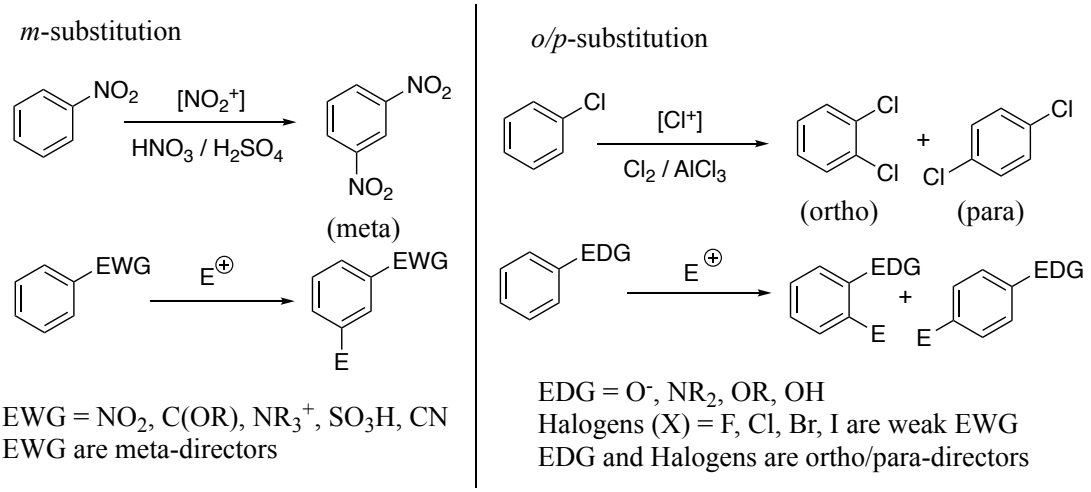

Scheme 1.2. Meta directors pull electron density out of the aromatic ring, thus partially deactivating it. Ortho/para directors release more electron density into the ring, thus partially activating it.

The selectivity rules of EAS are determined in large part by where electron density accumulates on the aromatic ring in conjunction with the steric accessibility of that site. In substrates with multiple FGs harboring contrasting steric and electronic properties, the accumulation of negative charge is a significant contributing factor in the substitution of the incoming substituent. When the electronics of two or more sites are similar, or if an electronically preferred site is sterically hindered, mixtures are often obtained.

Planning the synthesis of complex aromatic molecules around EAS rules can be very challenging, and for some combinations, EAS cannot produce the desired product, such as the meta substitution of structure **a** in Scheme 1.3. Particularly difficult is the functionalization of 1,3-dihaloarenes. Their synthesis is usually accessed from substitution of NO_2 meta directing groups which are then transformed into halogens through Sandmeyer reactions, which produce potentially explosive intermediates, and are generally avoided if possible.

Scheme 1.3. EAS Substitution Patterns

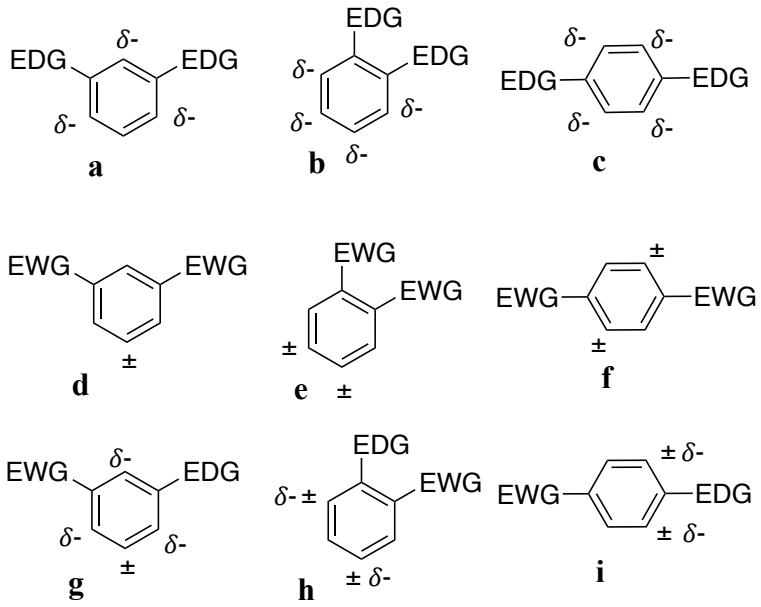

Scheme 1.3. Meta functionalized molecules like structure **a** are particularly challenging to prepare due to a lack of negative charge polarization at meta positions.

Directed ortho-Metalation. The second method of C-H activation offered an improvement in selectivity over EAS. Although aromatic C-H bonds have high pK_as that do not deprotonate with aqueous bases, they can be deprotonated by strong organometallic bases such as alkyl derivatives of lithium, sodium and potassium metals. This is known as metalation, defined broadly as the substitution reaction in which an acidic H atom is replaced by a metal to produce a true organometallic compound.[10] The metal-carbon bond is reactive and can be functionalized by trapping with an electrophile. The first C-H deprotonation and subsequent Li-functionalization was reported in 1928 by Schlenk, for whom the famous side-armed flask is named, and his student Bergmann.[11]

Scheme 1.4. The Selectivity of Directed Metalation, D*o*M

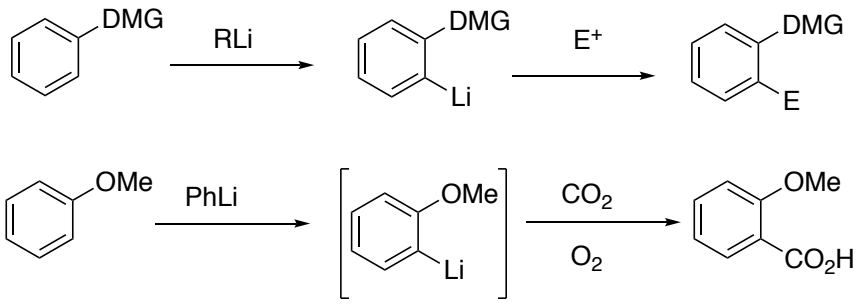

Scheme 1.4. D*o*M provides a selectivity advantages over EAS, but substitution is limited to ortho positions. Attempts to achieve meta substitution with combinations of directed metalation groups (DMGs) are substrate specific cannot be applied in a general way.

In 1930, work published by Zeigler made the preparation of standard organometallic reagents such as butyllithium and phenyllithium from alkyl halides routine,[12] and this led to a rapid development of metalation as a practical tool in organic synthesis. Early efforts of C-H deprotonation relied on functionalizing aromatic molecules with acidic protons, and lacked selectivity.

In 1938, the observation that methoxy-substituents coordinate to metals and direct selective deprotonation of C-H bonds ortho to the methoxy group was independently reported by Gilman[13]

and Wittig.[14] This led to rapid development of ortho-lithiation as a reliable method of C-H functionalization. This reactivity is summarized in Scheme 1.4. Groups that direct C-H deprotonation by chelation, such as the methoxy example, are called directed ortho metalation groups (DMGs).

Halogen substituents generally do not survive metalation with strong organolithium reagents, and instead undergo lithium halogen exchange. Exchange can be circumvented by the use of less basic and bulkier non-nucleophilic bases, such as lithium diisopropyl amide, LDA, which leaves halogens intact. Because of the inductive effects of halogen substituents, C-H bonds ortho to halogens are more acidic, thus halogens are themselves directing groups for metalation. Like EAS, selectivity in a molecule with two competing directing groups leads to mixtures.

Research into developing new DMGs has expanded rapidly in recent years and now includes diverse functionalities such as tertiary amines, amides, alcohols, oxazolines, mesylates, anilines, benzylamines and thiophenols, to name just a few of almost 50 classes of DMG groups.[15]

A complex set of rules based on DMG strength and number of DMGs present and the type of organometallic reagents employed along with reaction conditions can direct substitution in ingenious ways, providing enormous diversity in selectivity,[16] including complex substitutions and enantioselective transformations. Ortho directed metalation offers many options to build complex organic molecules, but it is not a general or mild method suitable for late stage functionalization. Often reagents are substrate specific and cannot be applied in a general way, and effective use of the most recent D*o*M advances requires specialization in medicinal chemistry. For basic functionalization of simple arenes like the example in Scheme 1.4, D*o*M groups still give useful alternate selectivity to EAS, although simple meta functionalization is not an option.

The Difficulty of Meta Substitution. The challenge of meta substitution is two-fold in that substituents which activate the ring, thus making it amenable to either EAS or D*o*M substitution, are ortho/para directors, and the accumulation of negative charge at the 2-, 4- and 6- positions poses serious competition to the unactivated sites at 3 and 5. When meta-directors are present, the presence of positive charge hampers reactions at the unactivated 3 and 5 sites, so meta functionalization is not easy even if there are no competing contra electronic substituents. This electronic effect is illustrated in Scheme 1.15.

Scheme 1.5. Electronic Effects Reinforce ortho Selectivity

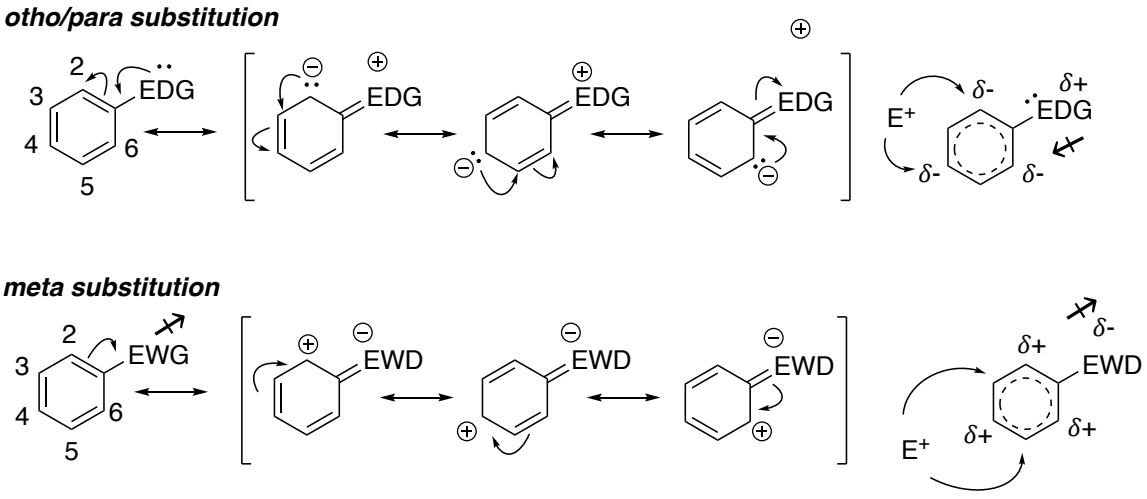

Scheme 1.5. Meta direction does not have electronic enhancement to reinforce sterically driven selectivity. Ortho/para direction enhances reactivity by accumulation negative charge at the 2, 4, and 6 positions thus reinforcing ortho direction.

Reliance on steric direction can only go so far, as the name implies, large or bulky substituents are required. When substituents are small, such as F, there is currently no way to achieve perfect steric selectivity. The best strategy to eliminate mixtures in the functionalization of arenes with F substituents is to direct ortho to F. Achieving direction meta to F is a serious challenge, and it is also a problem that has attracted the attention of medicinal chemists due to the importance of F atoms in pharmaceutical products.[17]

Metal Catalyzed C-H Activation - Functionalization. C-H activation offers an alternative to the traditional electronics based selectivity of EAS and DoM because it is a concerted process which takes place in one step without a chemical intermediate. Unlike EAS or D*o*M, which are step-wise, the stabilities of reactive intermediates, such as radicals or carbocations, do not govern formation of the products. (This selectivity is considered *kinetically determined* in contrast to *thermodynamically determined* selectivity of organic step-wise reactions).

It is necessary to differentiate between the terms C-H activation and C-H functionalization. C-H functionalization refers to breaking a C-H bond and replacing the H atom with a non-H substituent or functional group (FG). C-H functionalization is generally not reversible and transforms the substrate into a different compound.

Scheme 1.6. Arene Functionalization

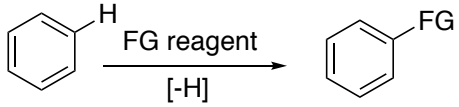

Scheme 1.6. C-H functionalization is the irreversible breaking of a C-H bond and the replacement of H with a non-H atom or functional group. Functionalization changes the substrate into a different molecule.

C-H activation, on the other hand, is not a precise or descriptive term; mid-century coordination chemistry pioneer, Lauri Vaska defined the term as a reversible binding of a substrate to a metal to form a metal-substrate complex. It was originally used to describe the behavior of enzymes or hemoglobin in the binding of small molecules. In the case of aromatic C-H activation, the metal inserts into the C-H bond to form an organic metal hydride complex[18-19] as shown in Scheme 1.7. In Ir CHB, this is the step where C-H bond scission happens. "Activation" is more precisely referred to as "Oxidative addition" for which Vaska is credited for describing. Oxidative addition describes the process whereby a low-valent metal inserts into a bond, thereby breaking

the bond and increasing in oxidation state by +2. "Activation" or oxidative addition in the case of C-H activation-borylation, only refers to the reversible formation of the metal hydride complex. Any additional reaction to form an organic product is the "functionalization," or in the case of Ir CHB, the reductive elimination is the "borylation" part.

Scheme 1.7. A Better Term for "Activation" is Oxidative Addition

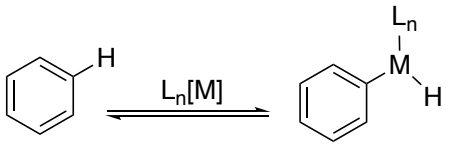

Scheme 1.7. C-H Activation (also called oxidative addition) is the insertion of a metal into a C-H bond and the subsequent reversible binding of the substrate to the metal to form a metal hydride-substrate complex. Activation is reversible and under favorable thermodynamic conditions the substrate can be regenerated again.

Oxidative addition has been known in the literature since the early 60s. One of the earliest examples of an isolated complex formed by metal-mediated C-H activation was reported by Chatt and Davidson in 1965.[20] Treatment of a dichloro-bis-dimethylphosphinoethane (dmpe) ruthenium complex, $[Ru(dmpe)_2Cl_2]$, with sodium naphthalide resulted in C-H activation of naphthalene onto the Ru metal center to form a naphthyl ruthenium hydride, which was isolated and characterized. Addition of 2 equiv HCl regenerated the complex and liberated naphthalene. Also observed was β-hydride elimination from the adjacent methyl of a dmpe ligand resulting in the liberation of naphthalene and the formation of a $Ru(dmpe)_2$ complex.

Scheme 1.8. Oxidative Addition of Naphthalene Reported in 1965

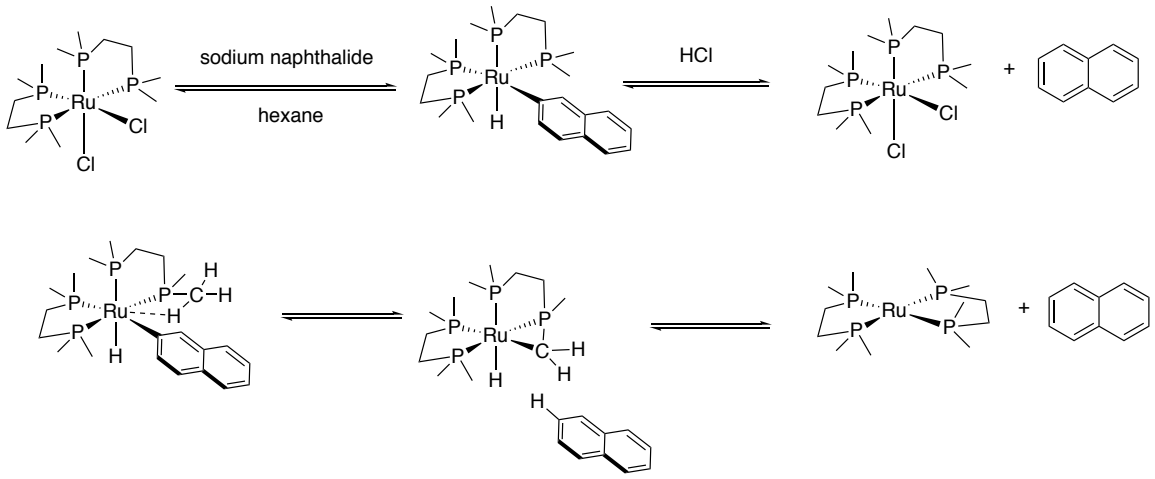

Scheme 1.8. C-H activation (oxidative addition) of naphthalene was observed by Chatt and Davidson in 1965. The oxidative addition was reversible by addition of HCl or by β-hydride elimination.

As mentioned before, the oxidative addition of substrates to coordinatively unsaturated low-valent metals is a concerted process, thus the electronic stability of intermediates does not play a role in selectivity, and metals favor activation of strong bonds over weak bonds. Hints of this concept were observed by Chatt and Ittel in 1976 with the report that the C-H activation of toluene by a phosphine ligated Fe complex did not take place at a benzylic position or ortho to methyl at the most substituted carbon, but at unsubstituted sites in a statistical 2:1 distribution with the methyl group meta or para to the metal.[21] Many examples of C-H activated metal hydride complexes were isolated and in the following years, but functionalization of activated complexes was not realized until much later in the 1980s.

Scheme 1.9. Oxidative Addition Exhibits Steric Selectivity

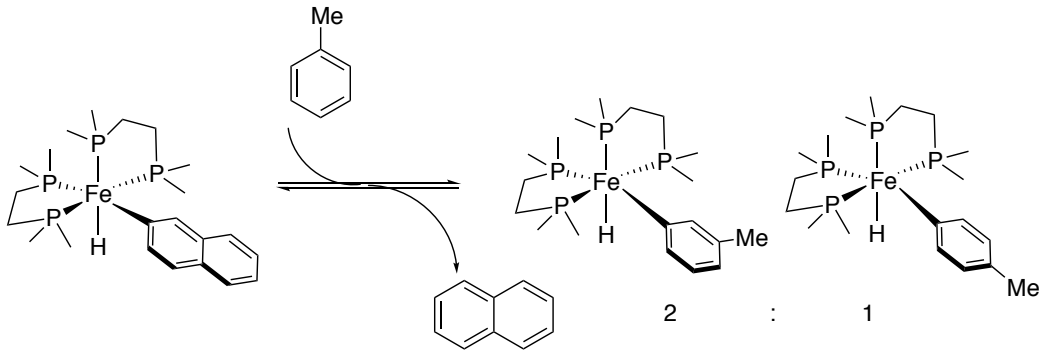

Scheme 1.9. Chatt and Ittel observed that oxidative addition of toluene does not take place at benzylic positions or the carbon of highest substitution like traditional organic chemistry selectivity, but at the least sterically hindered carbons resulting in a statistical mixture.

The first catalyzed functionalization of an activated organometallic arene complex was reported by Jones and Kosar[22] in 1986 using Chatt's $(dmpe)_2RuH(C_{10}H_7)$. Jones displaced naphthalene to add 2,6-dimethylphenylisocyanide, which underwent an intermolecular cyclometalation to make 7-methyl indole.

Scheme 1.10. First Reported Catalytic C-H Functionalization

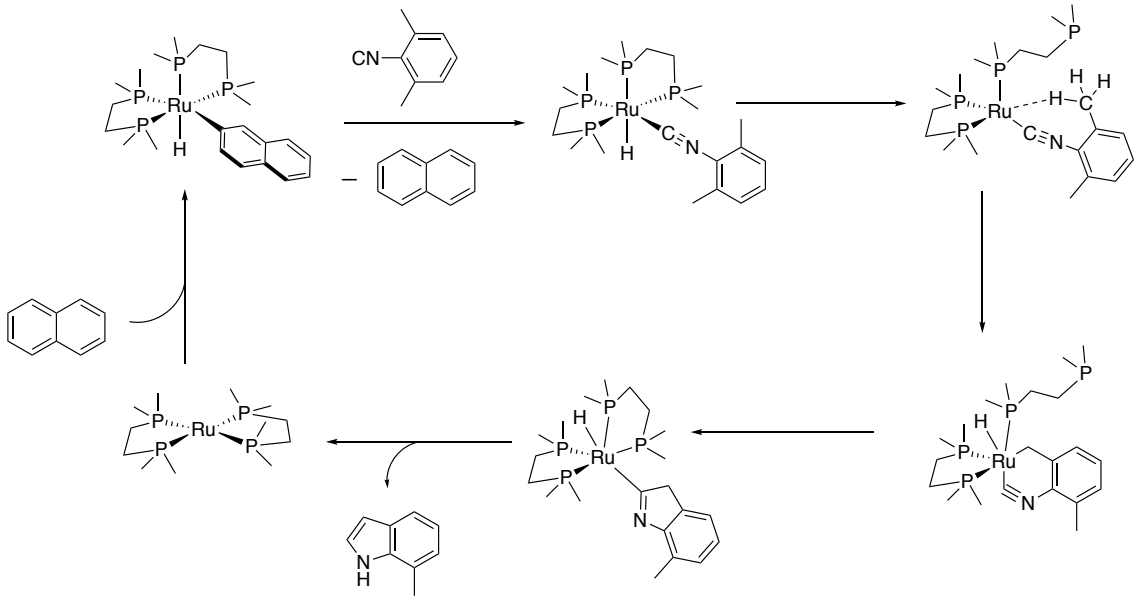

Scheme 1.10 The driving force for functionalization of the isocyanide complex is an intermolecular cyclometalation reaction in Jones and Kosar's 1986 synthesis of 7-methylindole.

Although research into C-H activation had advanced rapidly, and many kinds of organic compounds, including alkanes, had been activated and characterized, functionalization remained elusive with few examples until the 1990s. In 1995, the next breakthrough came when Hartwig reported that while irradiating Mn and Re pentacarbonyl complexes of catechol borane (Bcat) of the form $(CO)_5$M-Bcat (M = Mn or Re), stoichiometric functionalization of the solvent benzene was observed to give phenyl-Bcat, and a minor amount of HBcat.[23] When irradiation experiments were repeated in toluene, toluene was also functionalized to give a mixture of meta and para BCat substituted toluene along with some minor amounts of HBcat. Loss of a CO ligand enabled oxidative addition of the solvent and rapid functionalization to make a B-C bond from the C-H bond of an arene. These results led Hartwig to photolyze $CpFe(CO)_2$Bcat, which provided higher yields and greater efficiencies of stoichiometric Ph-Bcat generation, resulting only in the $[CpFe(CO)_2]_2$ dimer as the metal reaction product.

Scheme 1.11. First Stoichiometric Photolyzed Metal Mediated CHB

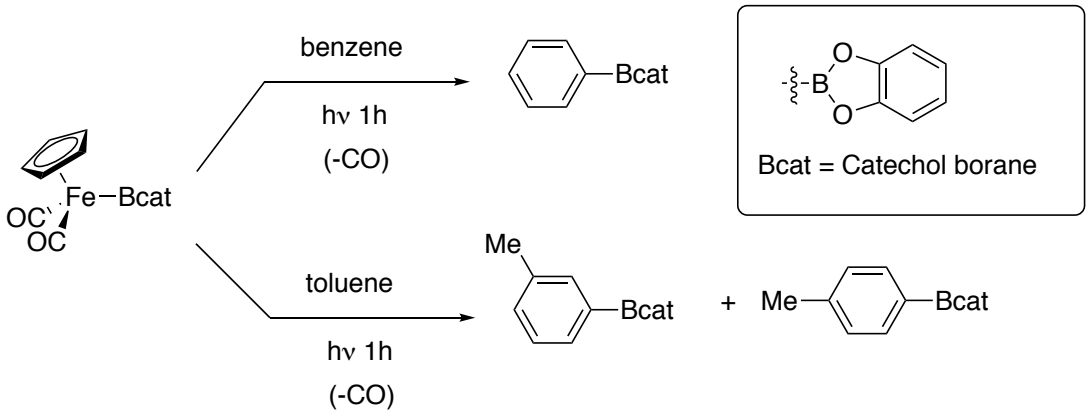

Scheme 1.11. Hartwig reported stoichiometric functionalization of benzene and toluene in 1995 by irradiation of metal carbonyl complexes.

C-H Activation by Iridium Catalyzed Borylation. At the end of the 90s and the early 2000s, rapid progress in catalyzed arene functionalization was made and many new developments were reported. In 1999, Smith reported the first thermal Ir-catalyzed thermal C-H

activation/functionalization of benzene with Cp*Ir(PMe_3)Bpin(H).[24] Although turnovers were low, this report provided the template for the successful development of catalytic C-H activation/functionalization efforts that followed.

Scheme 1.12. First Reported Catalytic Ir CHB of Benzene

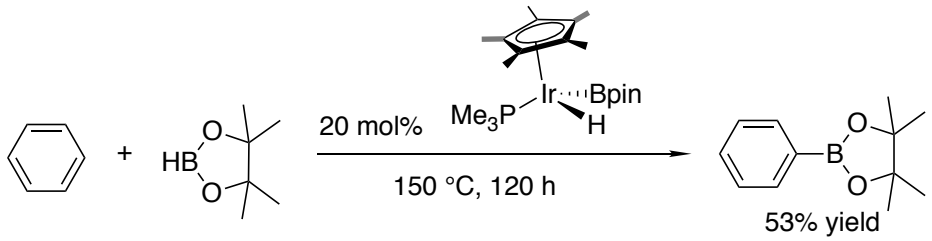

Scheme 1.12. In 1999 Iverson and Smith reported the first thermal Ir-catalyzed CH functionalization of an arene.

In that same year, Hartwig reported stoichiometric functionalization of alkanes and some arenes with W, Ru, and Re carbonyl complexes.[25-26] In 2000, Hartwig reported the catalytic functionalization of alkanes with Cp*Ru(η^4-C_6Me_6).[27] In the same year, Cho and Smith reported the first regioselectivity study of C-H borylation of arenes catalyzed by Cp*Ru(η^4-C_6Me_6), and compared the results obtained with a less active iridium precatalyst.[28] In this paper, the Smith and coworkers showed that the product distribution of isomers obtained in C-H borylation were kinetically determined, and the selectivity was primarily governed by the sterics of the substituents for both catalytic systems. Also of note was the first reported borylation of a heterocycle, 2,6-lutidine, and F substituted arenes.

Although the iridium catalyst was less active, the advantages became clear upon comparison. C-F bonds did not survive Rh catalysis, and underwent preferential oxidative addition over C-H bonds. Also Rh catalysis was less tolerant of benzylic C-H bonds, resulting in more benzylic activation of toluene, compared to the Ir catalyst. Although both systems exhibited roughly the same steric ratios of isomers for most substrates, some notable exceptions to statistical

distributions for anisole, esters and dimethylaniline were observed. Smith attributed these deviations to chelate directing effects, thus setting the stage for the investigation of competing steric and electronic directing effects in later C-H borylation studies.

In a 2001, Smith and Tse published a borylation overview aimed at a wider audience of synthetic organic chemists, in order to offer a practical guide for arene functionalization.[29] The use of an inert solvent, cyclohexane, rather than a large excess of substrate, was a marked improvement for those seeking to functionalize small amounts of material such as natural products or the late stage precursors of total synthesis, or the functionalization of expensive arenes where using the substrate as solvent would be impractical. A diverse substrate scope of 1,3-disubstituted arenes spanning a wide spectrum of electron-withdrawing to electron-donating functionality was featured to showcase the versatility of Ir CHB as a viable synthetic method.

In a subsequent 2002 Science paper,[30] Smith and Maleczka began a collaboration with the introduction of important synthetic refinements that propelled Ir CHB onto the radar screens of organic chemists seeking to find practical routes to improved arene functionalization. One-pot Suzuki coupling and polyphenylene synthesis examples were included, which demonstrated the high selectivity of C-H borylation towards aromatic C-H bonds, leaving the weaker C-X and benzylic C-H bonds untouched, unlike similar rhodium-based catalysis. In addition, the first putative mechanism for an Ir(III) to Ir(V) catalytic cycle was presented with the observations that supported it, as featured in Scheme 1.13 on the following page. Among the convincing evidence that cast doubt upon an Ir(I) to Ir(III) catalytic cycle was the observation that C-I bonds do not survive stoichiometric borylations with the Ir(I) complex $[Ir^{I}(H)(PMe_3)_4]$, but survived both stoichiometric borylation by $[Ir^{III}(Bpin)_3(PMe_3)_3]$ and catalytic borylation by other Ir(III) catalysts.

Scheme 1.13. 2002 Putative Catalytic Cycle of Ir CHB with Ir(III) to Ir(V) Manifold

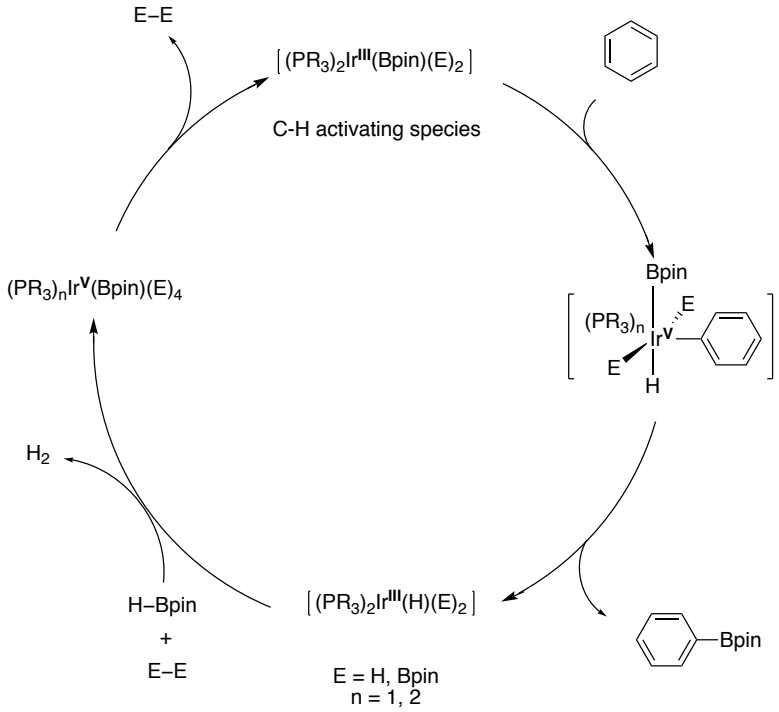

Scheme 1.13. In 2002, Smith and Cho offered a putative mechanism for Ir catalyzed CH borylation operating on an Ir(III) to Ir(V) catalytic manifold based on observations of reactivity.

Also reported in 2002 by Ishiyama and Hartwig was the introduction of Ir catalysis with bpy ligands, which soon became the most commonly used conditions for C-H borylation.[31] In 2003, Maleczka and Smith expanded on the development of practical applications of this new chemistry with their publication of one-pot synthesis of contra-electronically substituted phenols, which bore witness to the circumvention of long-standing electronic limitations in the preparation of contra-electronically substituted phenols.[32] This ground breaking synthesis is shown in Scheme 1.15.

Scheme 1.14. Old Fashioned EAS Synthesis of Contra-Electronic Phenol

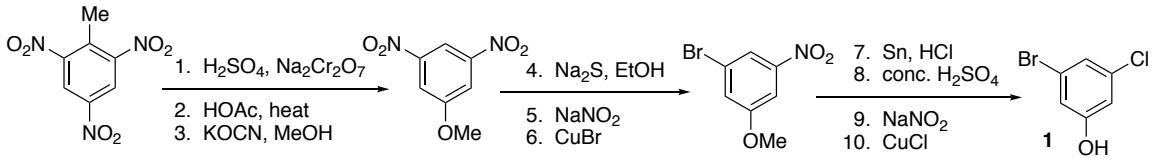

Scheme 1.14. The only synthesis of 3-bromo-5-chlorophenol reported before 2000 was published in 1926, featuring 10 steps starting from TNT and employing 4 potentially explosive Sandmeyer reactions.

The synthesis of 3,5-bromochlorophenol underscores the problem of functionalization meta to di-substituted 1,3-*o/p* directors, as shown in Scheme 1.14. The toxic and dangerous 10-step synthesis of this simple phenol provides a dramatic illustration of the advantages gained by the sterically driven regioselectivity of Ir CHB. Simple phenols such as **1** eluded synthetic chemists for almost a century. The preparation of 3-bromo-5-chlorophenol was reported only once, in 1926 following the 10-step process in Scheme 1.14 starting from the explosive material 2,4,6-trinitrotoluene, known commercially as TNT.[33] The next time it was reported was in 2001,[34] prepared in mg quantities from enzymatic hydroxylation.

Scheme 1.15. One-pot Synthesis of Contra-Electronic Phenol Attained by Ir CHB

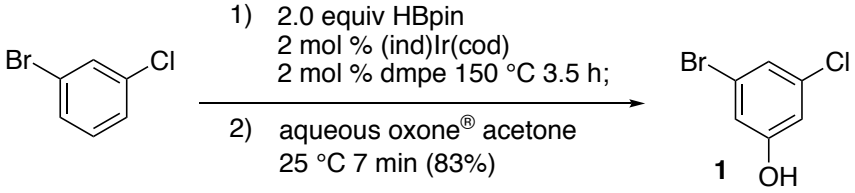

Scheme 1.15. The one-pot synthesis of 3-bromo-5-chlorophenol was reported in 2003 by Maleczka and Smith, thus sparking intense interest and development in aromatic functionalization by Ir CHB.

In this paper, 3-bromo-5-chlorophenol was prepared in 83% yield in a single day, employing the one-pot process shown in Scheme 1.15.

In 2005, Boller and Hartwig published a kinetic study with isolated intermediates of the catalytic cycle in agreement with the Ir(III) to Ir(V) mechanism published by Maleczka and Smith in 2002.[30] The isolated intermediates helped to better define the cycle in what came to be widely accepted as the mechanism of Ir CHB.

Scheme 1.16. Accepted Mechanism for Ir CHB

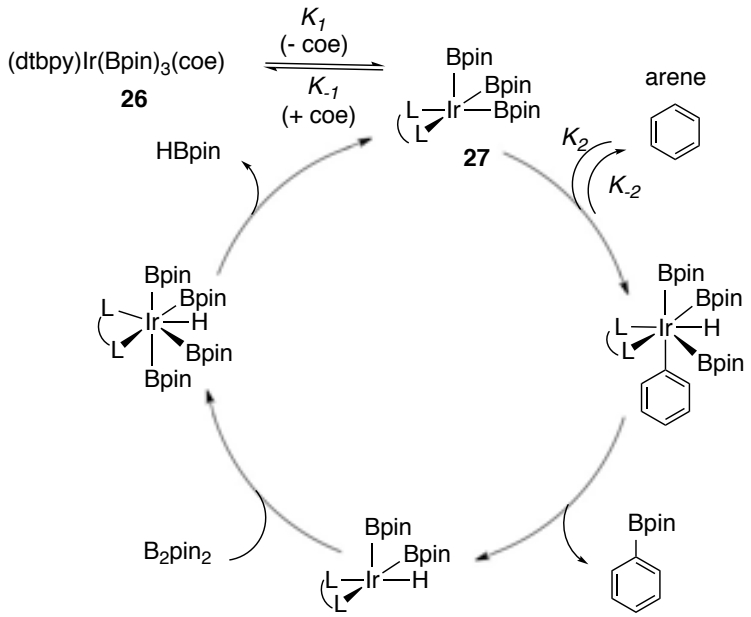

Scheme 1.16. The accepted mechanism of the catalytic manifold of Ir catalyzed CH borylation runs through Ir(III) to Ir(V) and involves a 5-coordinate trisboryl intermediate.

The kinetics of this system will be discussed more in Chapter 2.

By 2005, Ir CHB had just begun to be utilized as a synthetic method in organic chemistry for the functionalization of arenes outside the organometallic community. By this time, it was apparent that there were limitations to steric selectivities when substituents were not sufficiently large to block ortho-borylation, resulting in mixtures that were difficult to separate. Smith and Chotana embarked on an investigation of the steric and electronic properties of 1,4-benzonitriles,

due to the inherent difficulty functionalizing ortho to deactivating nitrile groups.[35] In this study, they sought to differentiate between steric and electronic effects, and, although it is not possible to completely disentangle the two properties, the borylation of 4-substituted benzonitriles presented a unique opportunity to quantify the influence of EAS-based electronic properties vs the "size" of a substituent. According to EAS selectivities, nitrile groups are deactivating meta directors, but in steric terms, nitriles are relatively small substituents. In order to quantify what constitutes a substituent as "small" or "large," Smith and Chotana established a measure of steric "size" that can be compared widely among different groups, which they termed "steric enthalpies." The concept of competing steric and electronic substituent effects is illustrated in Figure 1.1.

Figure 1.1. The Interaction of Steric and Electronic Directing Effects

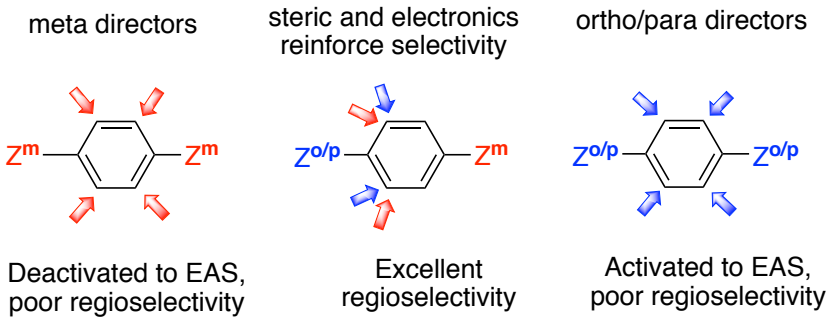

Figure 1.1. The selectivity study of 4-substituted benzonitriles presented the opportunity to evaluate the effects of electronics on the steric selectivity of Ir CHB as seen above. Isomer ratios were indicative of the competition between steric and electronic influence.

The concept of steric enthalpy is based on computational work by Fujita and coworkers for the acid catalyzed hydration of *o*-benzamides.[36-37] The parameter is based on calculations of the difference in enthalpies between 2-substituted benzamides and unsubstituted benzamide, and the difference between enthalpies of 2-substituted toluene and unsubstituted toluene. The parameter is denoted $\Delta\Delta H_s(Z)$, where H_s is called the steric enthalpy and Z refers to the substituent.

Smith postulates that since the transition states for ortho C-H borylation and ortho hydration of benzamides are similar, as illustrated in Figure 1.2, the $\Delta\Delta H_s(Z)$ values should predict calculated ortho:para ratios of the borylation of 4-substituted benzonitriles. After borylation of several 4-benzonitriles, the calculated ratios are in good agreement with experimental ratios for most substituents except for methoxy and thiol, as seen in Table 1.1.

Figure 1.2. Calculation of Steric Parameters are Based on Benzamide Model

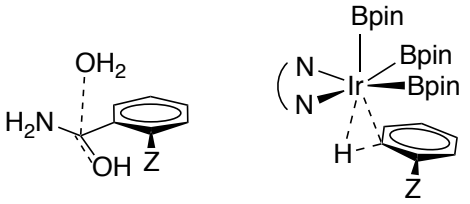

Figure 1.2. The transition state of Ir CHB is similar in structure to the acid catalyzed hydration of benzamides, thus modified calculated steric parameters used for their study provides a good model for the prediction of isomer distribution in Ir CHB.

Table 1.1. Experimental Regioisomer Ratios vs Ratios Calculated with $\Delta\Delta H_s(Z)$

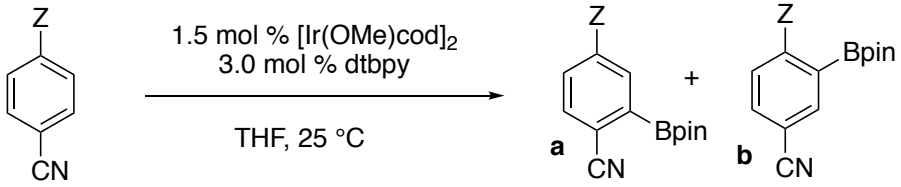

Z	$\Delta\Delta H_s(Z)$ kcal · mol^{-1}	%**a** : %**b** calc'd	%**a** : %**b** observed
H	0	—	—
CN	3.211	—	—
F	1.535	6:94	8:92
Cl	4.133	83:17	81:19
Br	5.405	98:2	97:3
I	7.759	>99:1	>99:1
CH_3	5.532	98:2	92:8
OMe	2.013	31:69	67:33
SMe	3.682	66:34	87:13
NMe_2	5.039	96:4	>99:1
CO_2Me	4.856	94:6	>99:1
NHAc	5.166	96:4	>99:1
CF_3	8.845	>99:1	>99:1

Erosion of steric selectivity was recognized as a serious limitation of Ir CHB and many groups have sought to improve selectivity and eliminate mixtures with innovations that can be categorized into three main strategies; Chelate direction, relay direction and outer-sphere direction.[7, 38-39] Of the three strategies, chelate and relay direction are inner-sphere processes, taking place through a chemical bridge from ligand to substrate. Outer sphere direction, in contrast, makes use of a ligand on the catalyst to recognize functionality in the substrate and position the substrate by H-bonding. The borylation takes place between two distinct chemical entities rather than two species chemically linked by a bond.

Ortho C-H Borylation by Chelate Direction. This strategy involves substrates with DMG groups that coordinate to the metal to form 16 electron (e^-) intermediates. Heterogeneous catalysis of surface supported ligands uses a variation of this type of chelate direction that supports 14 e^- intermediates. Chelate directed borylation with hemilabile ligands are also able to access the 14 e^- intermediate by dissociation of the weakly coordinating half of the ligand to leave two vacant sites, as shown in Scheme 1.17, where the boxes represent vacant coordination sites.

Scheme 1.17. Chelate Directed Mechanism Employing Hemilabile Ligand

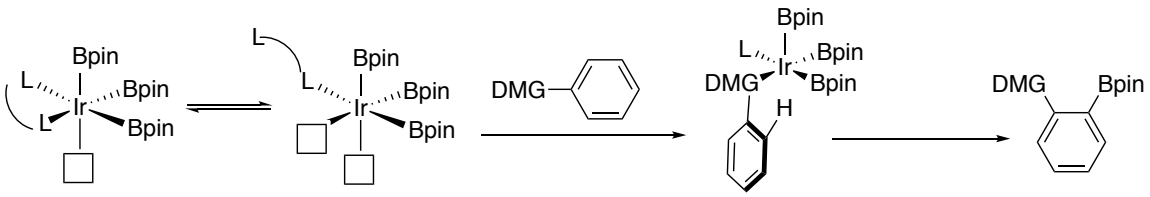

Scheme 1.17. Chelate directed C-H borylation generates a 14 e^- intermediate with a hemilabile bidentate ligand that dissociates one side to accommodate a DMG. The squares in the figure represent vacant coordination sites.

The first example of chelate direction in a borylation reaction was reported by Smith and Cho in the year 2000 for the borylation of Benzamide while using the catalyst system of Cp*Rh(η^4C$_6$Me$_6$). A statistical ratio of meta:para borylated isomers was not observed, and instead

the ortho isomer was the major product with a ratio of 4:2:1.[28] In 2010, Smith, Maleczka and Vanchura described the electronics of the chelate effect with striking examples of the borylations of veratrole and benzodioxole, as seen in Scheme 1.18. The constrained benzodioxole gave only the conventional borylation products while veratrole gave only ortho borylated product.[40]

Scheme 1.18. Chelate Directed Borylation vs Undirected Borylation

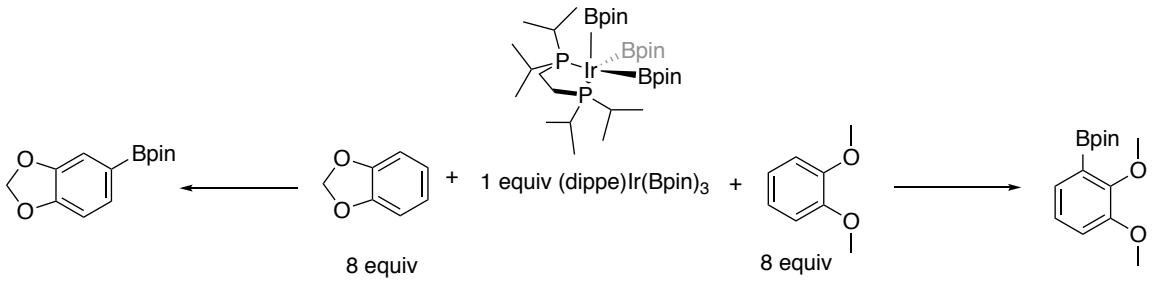

Scheme 1.18. In 2000 Smith and Vanchura provided insight into the mechanism of chelate directed borylation.

Around this time, several chelate directed ortho borylations were discovered. Ishiyama and Miyaura described ortho borylation of esters by use of bulky, monodentate phosphine ligands,[41] followed by Ito and Ishiyama's report of the ortho borylation of ketones,[42] and Lassaletta's observation of N-directed ortho borylations of 2-phenylpyridines using hemilabile ligands.[43] Clark soon reported N-directed ortho borylation of benzylamines and phosphines.[44-45]

Scheme 1.19. Heterogeneous Chelate Directed Mechanism

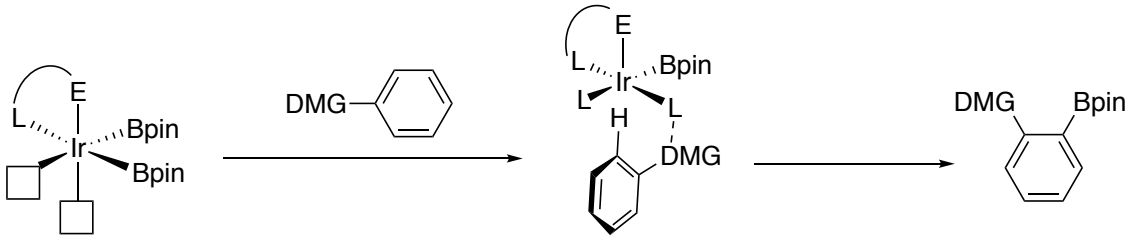

Scheme 1.19. Heterogeneous chelate directed C-H borylation operates through by a 14 e^- intermediate with 2 open coordination sites, which are represented by empty squares.

In 2009, Sawamura reported a surface supported system of phosphines for heterogeneous Rh catalysis that was highly active and ortho-selective with a much wider substrate scope,[46] using N heteroatoms as directing groups. The general mechanism for heterogeneous catalysis is shown in Scheme 1.19, where L is the siloxane linker, and E is an electrophilic P donor group on the ligand. A general depiction of how the tethered catalyst operates is shown in Scheme 1.20. The synthesis of the supported medium, called silica SMAP proved to be challenging to synthesize, thus limiting attempts to modify the system in order to engineer selectivity.

Scheme 1.20. Ortho Borylation by Silica SMAP

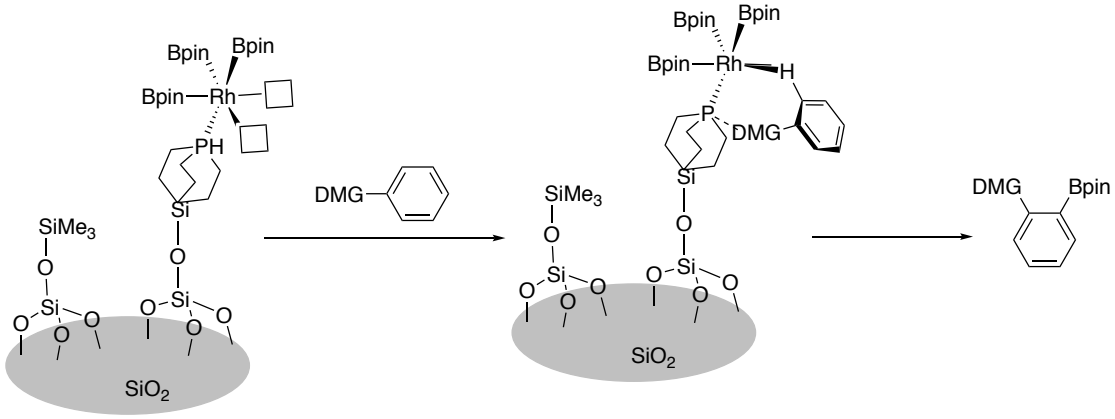

Scheme 1.20. Sawamura's solid supported Silica SMAP tethers the catalyst to a solid surface to block coordination of the tris boryl intermediate, and thus leaves two vacant coordination sites, stabilizing a 14 e^- intermediate. The vacant coordination sites are shown as boxes in the scheme.

In 2014, Ghaffari and Smith reported ortho borylation by the use of silyl N or silyl P donor ligands which can access the 14 e^- intermediate without hemilabile ligands as shown in Scheme 1.21. The substrate scope is broad, and many arenes with typical directed metalation (DMG) groups such as tertiary amides, esters, methoxy and 2-pyridines, were successfully ortho-borylated with high selectivity and yields. This system operates with a 14 e^- intermediate analogous to silica SMAP, however it is a much more flexible system where the ligands can be modified easily to tune

selectivity or to change directing effects to work with a with a different DMG. For example, Scheme 1.21 shows how meta or ortho selectivity can be accessed depending on reaction conditions.

Scheme 1.21. Donor Chelates Achieve 14 e^- Intermediates under Homogeneous Conditions

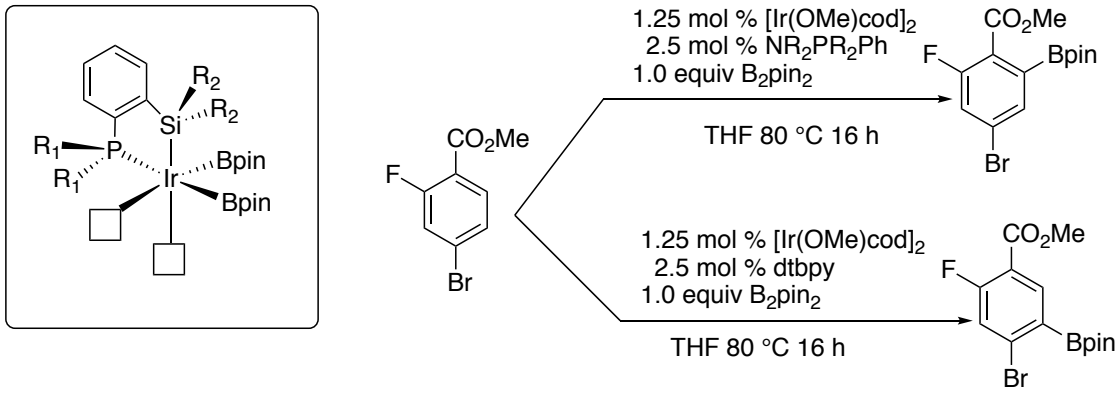

Scheme 1.21. In 2014 Ghaffari and Smith developed easily-synthesized and modified donor chelates in order to access 14 e^- intermediates without hemilabile ligands or supported media that is impractical and inconvenient synthesize. The open coordination sites are shown as empty squares.

This method meets the test for achieving a switch in selectivity under identical conditions by just changing the ligand used. The ligand synthesis is simple, and can be easily modified. The use of directing groups is necessary for this chemistry, but it is not limited to just one kind of directing group, so this method is more general than many of the directed borylation methods produced so far.

Ortho C-H Borylation by Relay Direction. This type of directed borylation relies on a substituent on the substrate to reversibly bind to the metal by σ bond metathesis. Substrates that exhibit relay directed borylation have pendant Si-H bonds. The first reported ortho C-H borylation using a silyl directing group was reported by Hartwig and Boebel in 2008,[47] as seen in Scheme 1.22.

Scheme 1.22. Relay Directed Mechanism

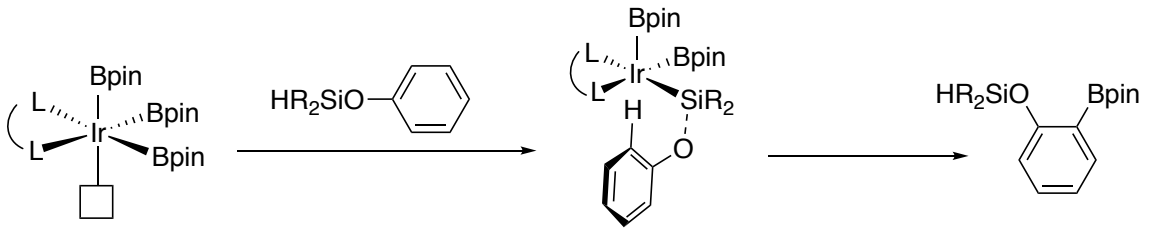

Scheme 1.22. Relay directed borylation relies on sigma bond metathesis between a pendant silyl group and the metal in order to form a chemical linker to direct borylation. Since the relay links to the ligand, a second open coordination site (depicted as an empty square) is not necessary,

The strategy involves the protection of a phenol with a silyl protecting group, R_2SiH. After the borylation the protecting group can be removed.

***Ortho C-H Borylation by Outer Sphere Direction*.** The transition state of this reaction resembles relay direction, but there is a distinction that this reaction is directed by H-bond interactions of the substrate with the ligand, and the mechanism is considered in light of descriptions of hydrogen transfer.[48] Also distinct from relay direction, the substrate and ligand remain separate chemical entities and are not linked by a formal bond. Maleczka, Smith and Singleton have used H-bond direction of boc protected anilines to selectively borylate ortho to the bulky N-H boc group.[49] Boc groups have been known to function as steric blocking groups in the borylation of pyrrole and indoles, so H-bond directed borylation ortho to N-H boc is intriguing. When a second boc group is put onto the aniline, thus removing the possibility for H-bonding, ortho borylation is not seen, and the only product is borylated meta to the boc group. The general mechanism of outer-sphere directed borylation is illustrated in Scheme 1.23.

Scheme 1.23. Outer Sphere Directed Mechanism

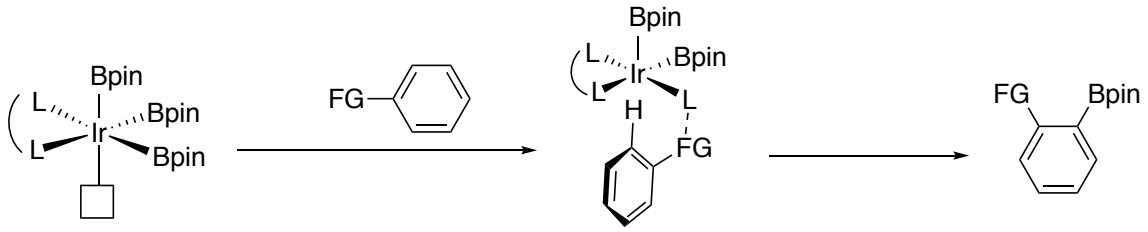

Scheme 1.23. Outer sphere direction is guided by recognition of functionality by a ligand. The ligand and substrate are chemically distinct, unlike relay direction. Here the substrate contains a FG that coordinates to a ligand, thus only requires one open coordination site (depicted as an empty square).

Examples of Directed Meta C-H Borylation. In the early development of C-H borylation, it became clear that Ir CHB of mono-substituted arenes gave statistical mixtures of meta and para isomers, and the only truly meta selective C-H borylations were of 1,3 di-substituted arenes with large substituents. In 2015, however, the first Ir catalyzed meta selective borylation of a mono-substituted arene was reported by Kanai and coworkers.[8] The borylation is directed by a bpy ligand with a pendant urea substituent that "recognizes" carbonyl groups on the substrate. The substrate is guided by H-bonding from the pendant urea, as pictured in Scheme 1.24. A large substrate scope of heterocyclic and aryl compounds and tolerance for wide variety of functional groups was demonstrated. Selectivity was generally good although some mixtures were obtained.

Scheme 1.24. Outer Sphere Borylation Achieved by Recognition of Carbonyl Functionality

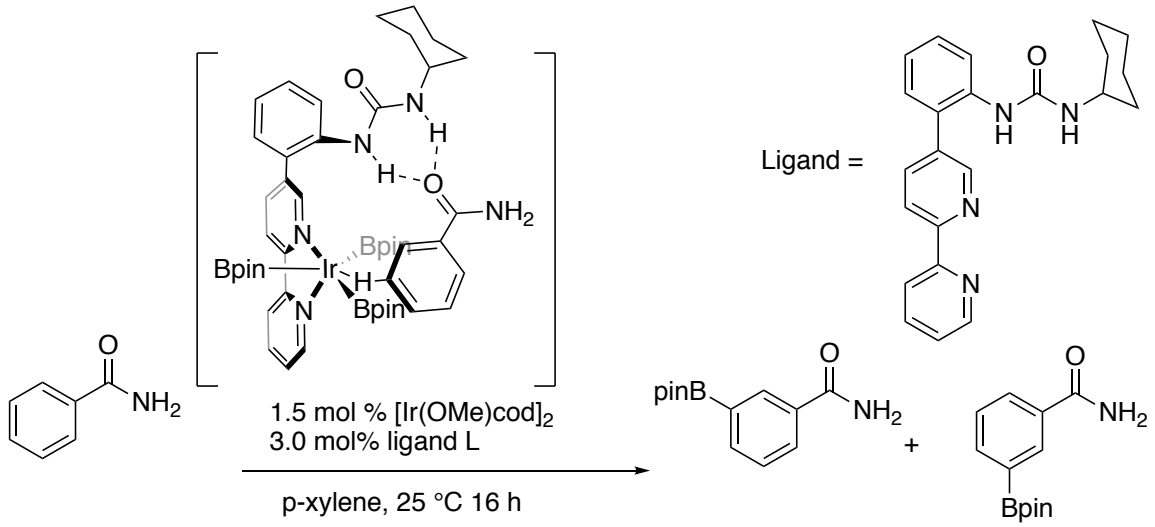

Scheme 1.24. Kanai reported Ir meta CHB by use of a pendant urea group to direct from the ligand rather than the substrate, sometimes called molecular recognition.

The synthesis of a complicated ligand and the requirement of xylene as a solvent is a significant drawback, since xylene is expensive and difficult to remove. This is an important step in the quest for selective chemistry based molecular recognition, but the need for a carbonyl directing groups and very specific ligands render this methodology not general or practical for most applications.

In 2016, Chattopadhyay reported a simpler, more general system using commercially available ligands for directed meta selective borylation of benzaldehydes, protected with tert-butyl amine. When tetramethylphenanthroline (tmp) was used as the ligand, aldehydes underwent ortho-selective borylation. When 8-aminoquinoline was used as the ligand, reminiscent of Ghaffari and Smith's N donor ligands published in 2014,[39] the reaction gave meta borylation as the major product.[50]

This approach is simple, and meets the criteria of ligand based selectivity where, under identical reaction conditions, changing the ligand leads to a switch in the major product. The

reagents are widely available and the methodology is convenient and accessible to most organic chemistry labs. The only drawback is the need to install a protected aldehyde director in order to facilitate the selectivity. If the aldehyde is already in place and part of a larger synthetic strategy, this is a very good strategy to achieve selective meta borylation. This ligand based approach and examples of substrate scope is shown in Scheme 1.25.

Scheme 1.25. Directed Meta or Ortho Borylation by Ligand-Based Selectivity

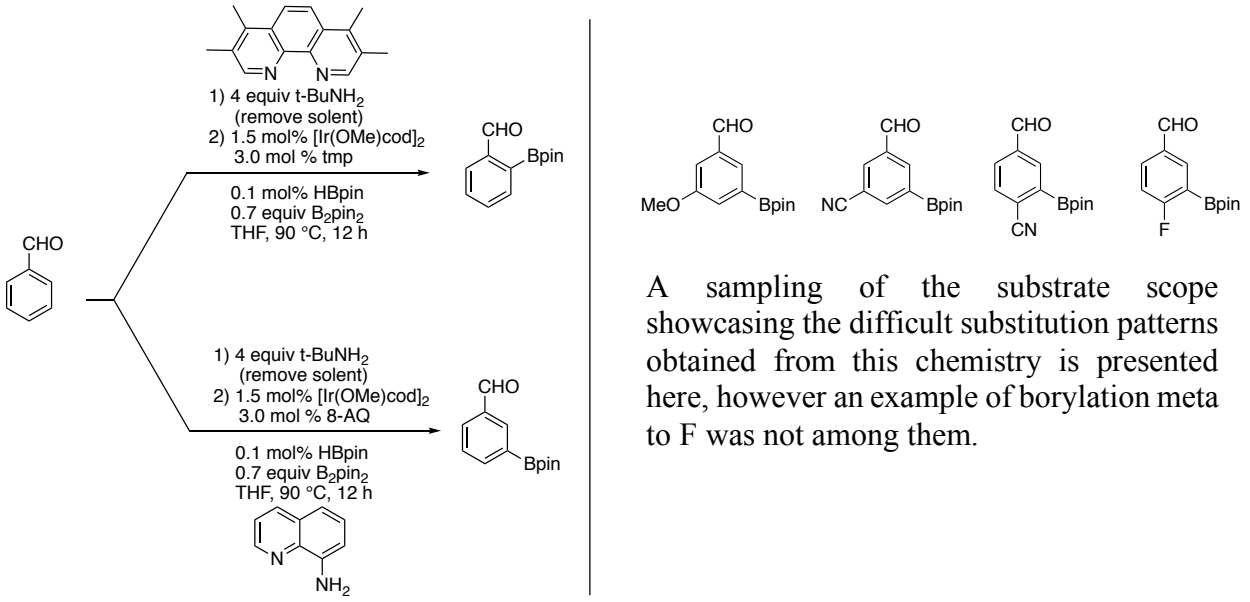

Scheme 1.25. Chattopadhyay discovered a directed borylation strategy to achieve either ortho or meta selective borylation using commercially available ligands.

With an eye towards meta borylation to small electronegative substrates like F and CN, an excellent range of borylated products are accessed, including borylation both meta and ortho to CN, but meta borylation to F is missing from the substrate scope, as seen in Scheme 1.25.

Meta Selective Borylation by Ion Pair Direction. In 2016, Phipps achieved meta-selective borylation of a variety of arenes including fluoarenes by installation of a quaternary amine group on the substrate.[51] A complimentary negatively charged sulfonate tether was installed on a bpy ligand to produce a productive ion-pairing effect which would impose a desired interaction

between the substrate and the active catalyst complex. In 4-fold improvement in meta selectivity over dtbpy was realized with this approach.

Scheme 1.26. Meta Borylation by Ion Pair Direction

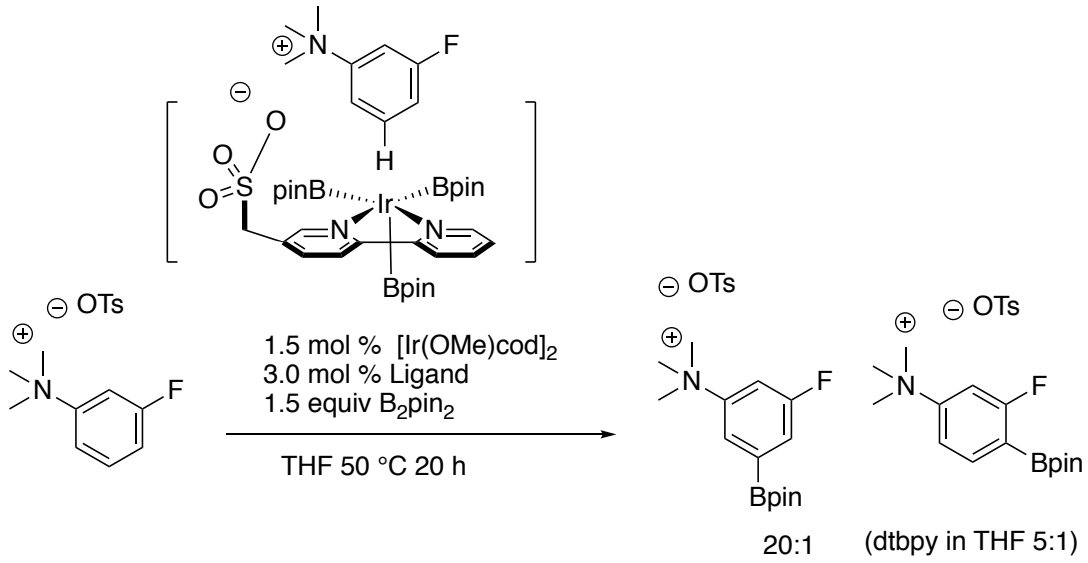

Scheme 1.26. Use of modified ligands and substrates to produce an ionic pair facilitates selective borylation meta to many substituents, including F. A drawback to this technology is that there is no easy was to remove the quaternary directing group, although it successfully participates in cross-coupling reactions, and can be left in place for that purpose.

Although this approach has achieved good meta selectivity for arenes, it does not produce selectivity for pyridines or indoles, and is prone to over-borylation resulting in mixtures of diborylated heterocycles. Fluoroarenes without the ortho position blocked were also prone to diborylation. The anionic substituent is left in place to use as a Suzuki coupling partner, but no way to remove the substituent is offered. While this is an important innovation in borylation of arenes, it is not good for general functionalization of library compounds or small molecule building blocks unless the anionic group is desired in the final product. In addition, the installation requires the presence of a methyl or ethyl group already in place on the molecule. For bulk haloarenes, there is no quick or simple way to install the directing group. Many borylation strategies to achieve

selective borylation of pyridines and indoles already exist, and this strategy offers no improvement for that application. This strategy is useful primarily to functionalize arenes that are slated for cross coupling, and will likely develop into a useful specialized application of C-H borylation.

Borylation Ortho to Fluorine by Sacrificial Blocking Group. During ongoing ligand studies, the Maleczka and Smith groups investigated the borylation of poly-halogenated substrates in collaboration with Dow Chemical Company.[52] Chathurika Jayasundara of the Maleczka group and Dr. Jossian Oppenheimer of Dow explored borylation of 3-fluoro-substituted arenes with a halogen blocking group (Br or Cl) para to F, with later removal of the halogen. The selective borylation ortho to F was achieved with a para-Br blocking group and subsequent removal of Br by Pd catalyzed reduction with polymethylhydrosiloxane (PMHS). A wide variety of difficult substitution patterns was achieved, as illustrated in Scheme 1.27.

Scheme 1.27. Selective Borylation by Steric Blocking Group

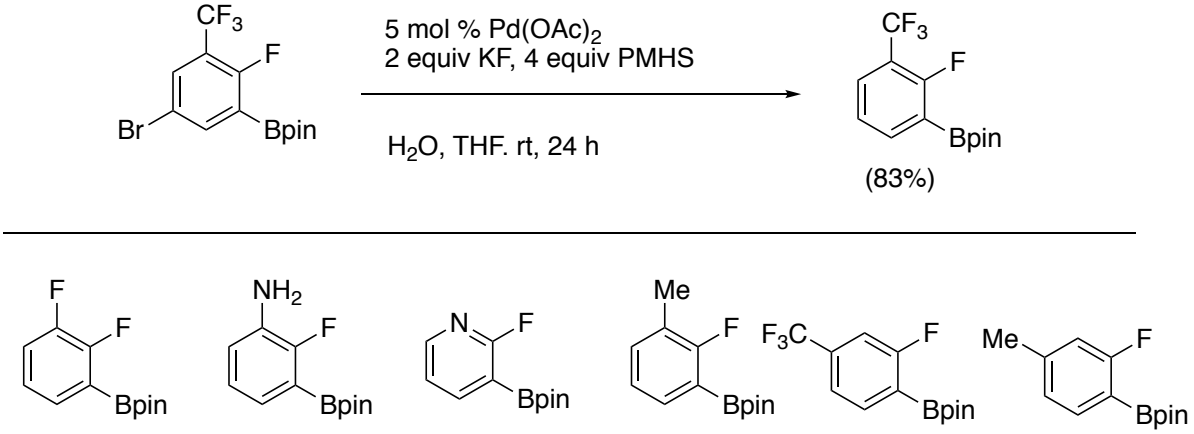

Scheme 1.27. Obtaining difficult substitution patterns for fluoroarenes has been accomplished by use of Br as a blocking group with subsequent removal of the blocking group by polymethylhydroxysiloxane (PMHS) reduction.

Diborylation followed by Selective Monodeborylation. While working on selective deutero-deborylation,[53] a method was developed to prepare single isomer batches of 3-cyano

substituted arenes and heterocycles which gave 1:1 mixtures of ortho and meta borylated products under standard borylation conditions with $[Ir(OMe)cod]_2$ and dtbpy. Substrates were diborylated then subjected to selective mono-deborylation conditions to achieve single isomer products. This method, while not atom economical, greatly simplifies the preparations of the surviving product by destroying the unwanted isomer, thus, making isolation by a short silica plug possible.

In work published while the selective deborylation work was ongoing, Movassaghi and coworkers independently published a 2,7-diborylation, selective 2-deborylation procedure on indoles using two different conditions of trifluoroacetic acid in CH_2Cl_2 (TFA) and 5% Palladium acetate in acetic acid.[54] Also, in 2016 another selective deborylation of indoles was published by Shen and coworkers using bismuth acetate.[55] These strategies are highlighted for the selective functionalization of indoles in Scheme 1.28.

Scheme 1.28. Alternate Functionalization by Poly-borylation / Selective Deborylation

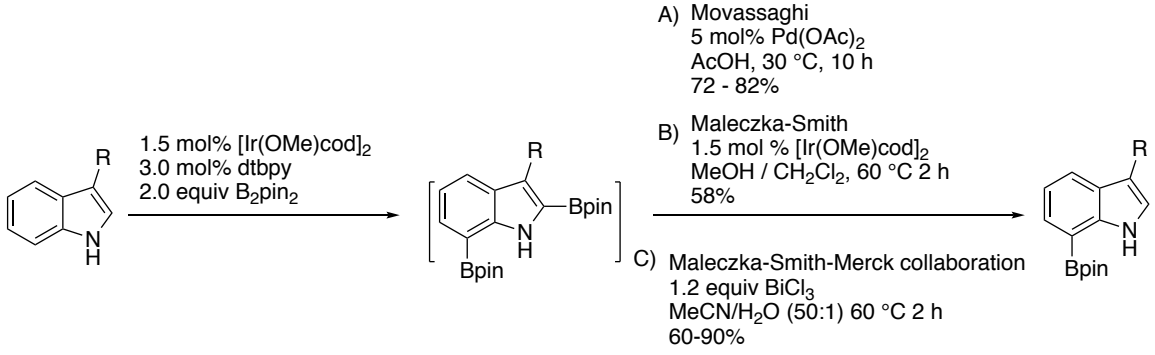

Scheme 1.28. Several methods have been reported for the selective deborylation of diborylated substrates.

Para Selective Borylation by Direction of Bulky Phosphine Ligand. In 2015 use of a bulky phosphate ligand enabled para borylation of mono-substituted substrates with very bulky substituents. While selectivity and yields for the substrates featured are generally very good, all substrates have a very bulky substituent, the smallest being a tert-butyl group. This method likely

does not work for smaller substrates or haloarenes. It also makes use of a specialized complex ligand not useful for other borylations. This is an innovative synthetic technique that will be useful for very specialized applications, but will not be useful for general purpose borylations.

Scheme 1.29. Para Borylation by Bulky Ligands that Mimic Enzyme Sites

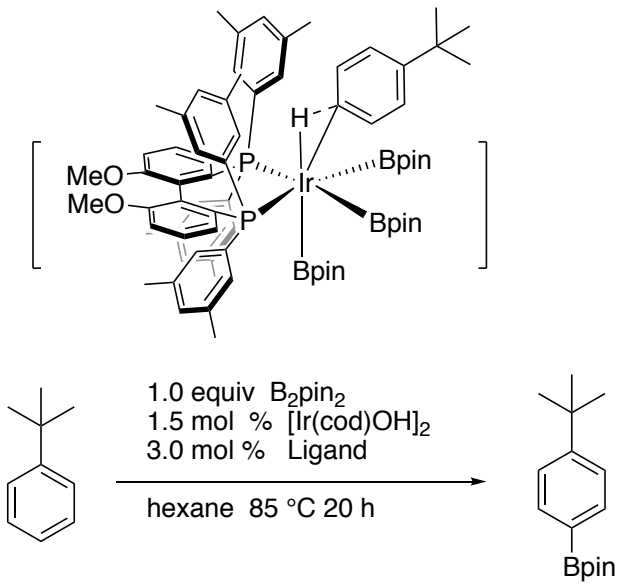

Scheme 1.29. Bulky ligands have been used to selectively functionalize bulky substrates at the para position. The inspiration for this model is based on the binding pocket of enzymes.

New strategies for selective C-H functionalization are being published rapidly, and Ir catalyzed CH borylation is not the only method that shows promise. Many strategies for Zn,[56] Co,[57-58] Cu[59-60] and Pd[61] catalyzed meta selective functionalizations have also been developed, which will not be discussed here, but nonetheless, remain as vital additions in the chemical tool box.

REFERENCES

REFERENCES

1. Commercial chemicals are divided into three classes: Commodity, Specialty and Fine. Fine chemicals are single chemicals of high purity and high value, typically >$10 per kilo. Fine chemicals have limited use, and are made in limited quantities in multi-purpose reactors, in contrast to commodity chemicals which are made in high volume in dedicated reactors. Fine chemicals are made by functionalization of commodity petrochemicals obtained from the petrolem industry. For a good description, see the following reference.

2. Pollak, P., What Fine Chemicals are. In *Fine Chemicals*, John Wiley & Sons, Inc.: 2011; pp 1-7.

3. Folkins, H. O., Benzene. In *Ullmann's Encyclopedia of Industrial Chemistry*, Wiley-VCH Verlag GmbH & Co. KGaA: 2000.

4. Mkhalid, I. A. I.; Barnard, J. H.; Marder, T. B.; Murphy, J. M.; Hartwig, J. F., C−H Activation for the Construction of C−B Bonds. *Chemical Reviews* **2010,** *110* (2), 890-931.

5. Pollak, P., Products. In *Fine Chemicals*, John Wiley & Sons, Inc.: 2011; pp 26-31.

6. Hartwig, J. F.; Larsen, M. A., Undirected, Homogeneous C–H Bond Functionalization: Challenges and Opportunities. *ACS Central Science* **2016,** *2* (5), 281-292.

7. Ros, A.; Fernandez, R.; Lassaletta, J. M., Functional group directed C-H borylation. *Chemical Society Reviews* **2014,** *43* (10), 3229-3243.

8. Kuninobu, Y.; Ida, H.; Nishi, M.; Kanai, M., A meta-selective C–H borylation directed by a secondary interaction between ligand and substrate. *Nat Chem* **2015,** *7* (9), 712-717.

9. Faraday, M., On New Compounds of Carbon and Hydrogen, and on Certain Other Products Obtained during the Decomposition of Oil by Heat. *Phil. Trans. R. Soc. Lond.* **1825,** *115*, 467-496.

10. Mallan, J. M.; Bebb, R. L., Metalations by organolithium compounds. *Chemical Reviews* **1969,** *69* (5), 693-755.

11. Schlenk, W.; Bergmann, E., Forschungen auf dem Gebiete der alkaliorganischen Verbindungen. I. Über Produkte der Addition von Alkalimetal an mehrfache Kohlenstoff-Kohlenstoff-Bindungen. *Justus Liebigs Annalen der Chemie* **1928,** *463* (1), 1-97.

12. Ziegler, K.; Colonius, H., Untersuchungen über alkali-organische Verbindungen. V. Eine bequeme Synthese einfacher Lithiumalkyle. *Justus Liebigs Annalen der Chemie* **1930,** *479* (1), 135-149.

13. Gilman, H.; Bradley, C. W., Dehydrogenation by Organometallic Compounds. *Journal of the American Chemical Society* **1938,** *60* (10), 2333-2336.

14. Wittig, G.; Pockels, U.; Dröge, H., Über die Austauschbarkeit von aromatisch gebundenem Wasserstoff gegen Lithium mittels Phenyl-lithiums. *Berichte der deutschen chemischen Gesellschaft (A and B Series)* **1938,** *71* (9), 1903-1912.

15. Snieckus, V., Directed ortho metalation. Tertiary amide and O-carbamate directors in synthetic strategies for polysubstituted aromatics. *Chemical Reviews* **1990,** *90* (6), 879-933.

16. Nair, S. K.; Rocke, B. N.; Sutton, S., Chapter 11 Lithium, Magnesium, and Copper: Contemporary Applications of Organometallic Chemistry in the Pharmaceutical Industry. In *Synthetic Methods in Drug Discovery: Volume 2*, The Royal Society of Chemistry: 2016; Vol. 2, pp 1-74.

17. Gillis, E. P.; Eastman, K. J.; Hill, M. D.; Donnelly, D. J.; Meanwell, N. A., Applications of Fluorine in Medicinal Chemistry. *Journal of Medicinal Chemistry* **2015,** *58* (21), 8315-8359.

18. Vaska, L., Reversible activation of covalent molecules by transition-metal complexes. The role of the covalent molecule. *Accounts of Chemical Research* **1968,** *1* (11), 335-344.

19. Jones, W. D.; Feher, F. J., Mechanism of arene carbon-hydrogen bond activation by (C5Me5)Rh(PMe3)(H)Ph. Evidence for arene precoordination. *Journal of the American Chemical Society* **1982,** *104* (15), 4240-4242.

20. Chatt, J.; Davidson, J. M., 154. The tautomerism of arene and ditertiary phosphine complexes of ruthenium(0), and the preparation of new types of hydrido-complexes of ruthenium(II). *Journal of the Chemical Society (Resumed)* **1965,** (0), 843-855.

21. Ittel, S. D.; Tolman, C. A.; English, A. D.; Jesson, J. P., Novel carbon-hydrogen bond cleavage by bis(dimethylphosphino)ethane complexes of iron, ruthenium, and osmium. *Journal of the American Chemical Society* **1976,** *98* (19), 6073-6075.

22. Jones, W. D.; Kosar, W. P., Carbon-hydrogen bond activation by ruthenium for the catalytic synthesis of indoles. *Journal of the American Chemical Society* **1986,** *108* (18), 5640-5641.

23. Waltz, K. M.; He, X.; Muhoro, C.; Hartwig, J. F., Hydrocarbon Functionalization by Transition Metal Boryls. *Journal of the American Chemical Society* **1995,** *117* (45), 11357-11358.

24. Iverson, C. N.; Smith, M. R., Stoichiometric and Catalytic B-C Bond Formation from Unactivated Hydrocarbons and Boranes. *Journal of the American Chemical Society* **1999,** *121* (33), 7696-7697.

25. Waltz, K. M.; Muhoro, C. N.; Hartwig, J. F., C-H Activation and Functionalization of Unsaturated Hydrocarbons by Transition-Metal Boryl Complexes. *Organometallics* **1999,** *18* (17), 3383-3393.

26. Chen, H.; Hartwig, J. F., Catalytic, Regiospecific End-Functionalization of Alkanes: Rhenium-Catalyzed Borylation under Photochemical Conditions. *Angewandte Chemie International Edition* **1999,** *38* (22), 3391-3393.

27. Chen, H.; Schlecht, S.; Semple, T. C.; Hartwig, J. F., Thermal, Catalytic, Regiospecific Functionalization of Alkanes. *Science* **2000,** *287* (5460), 1995-1997.

28. Cho, J.-Y.; Iverson, C. N.; Smith, M. R., Steric and Chelate Directing Effects in Aromatic Borylation. *Journal of the American Chemical Society* **2000,** *122* (51), 12868-12869.

29. Tse, M. K.; Cho, J.-Y.; Smith, M. R., Regioselective Aromatic Borylation in an Inert Solvent,. *Organic Letters* **2001,** *3* (18), 2831-2833.

30. Cho, J.-Y.; Tse, M. K.; Holmes, D.; Maleczka, R. E.; Smith, M. R., Remarkably Selective Iridium Catalysts for the Elaboration of Aromatic C-H Bonds. *Science* **2002,** *295* (5553), 305-308.

31. Ishiyama, T.; Takagi, J.; Ishida, K.; Miyaura, N.; Anastasi, N. R.; Hartwig, J. F., Mild Iridium-Catalyzed Borylation of Arenes. High Turnover Numbers, Room Temperature Reactions, and Isolation of a Potential Intermediate. *Journal of the American Chemical Society* **2001,** *124* (3), 390-391.

32. Maleczka, R. E.; Shi, F.; Holmes, D.; Smith, M. R., C−H Activation/Borylation/Oxidation: A One-Pot Unified Route To Meta-Substituted Phenols Bearing Ortho-/Para-Directing Groups. *Journal of the American Chemical Society* **2003,** *125* (26), 7792-7793.

33. Hodgson, H. H.; Wignall, J. S., CCLXXVIII.-Preparation of 3 : 5-dihalogenophenols. *Journal of the Chemical Society (Resumed)* **1926,** *129* (0), 2077-2079.

34. Soffers, A. E. M. F.; Veeger, C.; Rietjens, I. M. C. M., Influence of the type of halogen substituent on in vivo and in vitro phase II metabolism of 2-fluoro-4-halophenol metabolites formed from 3-halo-fluorobenzenes. *Xenobiotica* **1994,** *24* (8), 759-774.

35. Chotana, G. A.; Rak, M. A.; Smith, M. R., Sterically Directed Functionalization of Aromatic C-H Bonds: Selective Borylation Ortho to Cyano Groups in Arenes and Heterocycles. *Journal of the American Chemical Society* **2005,** *127* (30), 10539-10544.

36. Sotomatsu, T.; Murata, Y.; Fujita, T., Theoretical calculation of the steric effects of ortho substituents by the AM1 method. *Journal of Computational Chemistry* **1991,** *12* (1), 135-138.

37. Sotomatsu, T.; Fujita, T., The steric effect of ortho substituents on the acidic hydrolysis of benzamides. *The Journal of Organic Chemistry* **1989,** *54* (18), 4443-4448.

38. Roosen, P. C.; Kallepalli, V. A.; Chattopadhyay, B.; Singleton, D. A.; Maleczka, R. E.; Smith, M. R., Outer-Sphere Direction in Iridium C–H Borylation. *Journal of the American Chemical Society* **2012,** *134* (28), 11350-11353.

39. Ghaffari, B.; Preshlock, S. M.; Plattner, D. L.; Staples, R. J.; Maligres, P. E.; Krska, S. W.; Maleczka, R. E.; Smith, M. R., Silyl Phosphorus and Nitrogen Donor Chelates for Homogeneous Ortho Borylation Catalysis. *Journal of the American Chemical Society* **2014,** *136* (41), 14345-14348.

40. Vanchura, I. I. B. A.; Preshlock, S. M.; Roosen, P. C.; Kallepalli, V. A.; Staples, R. J.; Maleczka, J. R. E.; Singleton, D. A.; Smith, I. I. I. M. R., Electronic effects in iridium C-H borylations: insights from unencumbered substrates and variation of boryl ligand substituents. *Chemical Communications* **2010,** *46* (41), 7724-7726.

41. Ishiyama, T.; Isou, H.; Kikuchi, T.; Miyaura, N., Ortho-C-H borylation of benzoate esters with bis(pinacolato)diboron catalyzed by iridium-phosphine complexes. *Chemical Communications* **2010,** *46* (1), 159-161.

42. Hiroshi, I.; Takao, K.; Tatsuo, I.; Norio, M., Iridium-catalyzed ortho-C–H Borylation of Aryl Ketones with Bis(pinacolato)diboron. *Chemistry Letters* **2011,** *40* (9), 1007-1008.

43. Ros, A.; Estepa, B.; López-Rodríguez, R.; Álvarez, E.; Fernández, R.; Lassaletta, J. M., Use of Hemilabile N,N Ligands in Nitrogen-Directed Iridium-Catalyzed Borylations of Arenes. *Angewandte Chemie International Edition* **2011,** *50* (49), 11724-11728.

44. Roering, A. J.; Hale, L. V. A.; Squier, P. A.; Ringgold, M. A.; Wiederspan, E. R.; Clark, T. B., Iridium-Catalyzed, Substrate-Directed C–H Borylation Reactions of Benzylic Amines. *Organic Letters* **2012,** *14* (13), 3558-3561.

45. Crawford, K. M.; Ramseyer, T. R.; Daley, C. J. A.; Clark, T. B., Phosphine-Directed C-H Borylation Reactions: Facile and Selective Access to Ambiphilic Phosphine Boronate Esters. *Angewandte Chemie International Edition* **2014,** *53* (29), 7589-7593.

46. Kawamorita, S.; Ohmiya, H.; Hara, K.; Fukuoka, A.; Sawamura, M., Directed Ortho Borylation of Functionalized Arenes Catalyzed by a Silica-Supported Compact Phosphine−Iridium System. *Journal of the American Chemical Society* **2009,** *131* (14), 5058-5059.

47. Boebel, T. A.; Hartwig, J. F., Silyl-Directed, Iridium-Catalyzed ortho-Borylation of Arenes. A One-Pot ortho-Borylation of Phenols, Arylamines, and Alkylarenes. *Journal of the American Chemical Society* **2008,** *130* (24), 7534-7535.

48. Samec, J. S. M.; Backvall, J.-E.; Andersson, P. G.; Brandt, P., Mechanistic aspects of transition metal-catalyzed hydrogen transfer reactions. *Chemical Society Reviews* **2006,** *35* (3), 237-248.

49. Kallepalli, V. A.; Shi, F.; Paul, S.; Onyeozili, E. N.; Maleczka, R. E.; Smith, M. R., Boc Groups as Protectors and Directors for Ir-Catalyzed C-H Borylation of Heterocycles. *The Journal of Organic Chemistry* **2009,** *74* (23), 9199-9201.

50. Bisht, R.; Chattopadhyay, B., Formal Ir-Catalyzed Ligand-Enabled Ortho and Meta Borylation of Aromatic Aldehydes via in Situ-Generated Imines. *Journal of the American Chemical Society* **2016,** *138* (1), 84-87.

51. Davis, H. J.; Mihai, M. T.; Phipps, R. J., Ion Pair-Directed Regiocontrol in Transition-Metal Catalysis: A Meta-Selective C–H Borylation of Aromatic Quaternary Ammonium Salts. *Journal of the American Chemical Society* **2016,** *138* (39), 12759-12762.

52. Jayasundara, C. R. K.; Unold, J. M.; Oppenheimer, J.; Smith, M. R.; Maleczka, R. E., A Catalytic Borylation/Dehalogenation Route to o-Fluoro Arylboronates. *Organic Letters* **2014,** *16* (23), 6072-6075.

53. Kallepalli, V. A.; Gore, K. A.; Shi, F.; Sanchez, L.; Chotana, G. A.; Miller, S. L.; Maleczka, R. E.; Smith, M. R., Harnessing C-H Borylation/Deborylation for Selective Deuteration, Synthesis of Boronate Esters, and Late Stage Functionalization. *The Journal of Organic Chemistry* **2015,** *80* (16), 8341-8353.

54. Loach, R. P.; Fenton, O. S.; Amaike, K.; Siegel, D. S.; Ozkal, E.; Movassaghi, M., C7-Derivatization of C3-Alkylindoles Including Tryptophans and Tryptamines. *The Journal of Organic Chemistry* **2014,** *79* (22), 11254-11263.

55. Shen, F.; Tyagarajan, S.; Perera, D.; Krska, S. W.; Maligres, P. E., Bismuth Acetate as a Catalyst for the Sequential Protodeboronation of Di- and Triborylated Indoles. *Organic letters* **2016,** *18* (7), 1554-1557.

56. Armstrong, D. R.; Clegg, W.; Dale, S. H.; Hevia, E.; Hogg, L. M.; Honeyman, G. W.; Mulvey, R. E., Directed meta-Metalation Using Alkali-Metal-Mediated Zincation. *Angewandte Chemie International Edition* **2006,** *45* (23), 3775-3778.

57. Obligacion, J. V.; Semproni, S. P.; Chirik, P. J., Cobalt-Catalyzed C–H Borylation. *Journal of the American Chemical Society* **2014,** *136* (11), 4133-4136.

58. Cui, C.; Ren, H.; Zhou, Y.-P.; Bai, Y.-P.; Driess, M., Cobalt-Catalyzed Regioselective Borylation of Arenes: N-Heterocyclic Silylene as Electron Donors in Metal-Mediated Activation of C-H Bonds. *Chemistry – A European Journal* **2017**.

59. Fan, Z.; Ni, J.; Zhang, A., Meta-Selective CAr–H Nitration of Arenes through a Ru3(CO)12-Catalyzed Ortho-Metalation Strategy. *Journal of the American Chemical Society* **2016,** *138* (27), 8470-8475.

60. Zhou, Y.; Zhao, J.; Liu, L., Meta-Selective Transition-Metal Catalyzed Arene C-H Bond Functionalization. *Angewandte Chemie International Edition* **2009,** *48* (39), 7126-7128.

61. Dey, A.; Agasti, S.; Maiti, D., Palladium catalysed meta-C-H functionalization reactions. *Organic & Biomolecular Chemistry* **2016,** *14* (24), 5440-5453.

CHAPTER TWO

ENGINEERING SELECTIVITY WITH LIGANDS AND BORANE

Steric Effects of Substrates and Regioselective Outcomes. C–H borylation has gained popularity because the direct coupling of C–H with B–H or B–B bonds is the most atom economical route to boronate esters.[1] Another appealing feature is that sterically directed regioselectivity, typically observed for aromatic substrates, complements selectivities of electrophilic aromatic substitutions (EAS) and directed ortho metalations (D*o*M).[2] Scheme 2.1 shows how steric directing effects can be utilized to achieve selective functionalizations in 1,3- and 1,4-substituted benzenes. For 1,3-substituted benzenes, high meta selectivities are found when the benzene substituents are sufficiently large to block functionalization of their ortho C–H bonds. For 1,4-substituted benzenes, selective sterically directed C–H borylation can be achieved when the sterics of the substituents differ significantly.[3]

Scheme 2.1. Sterically Directed C–H Borylation Regioselectivities

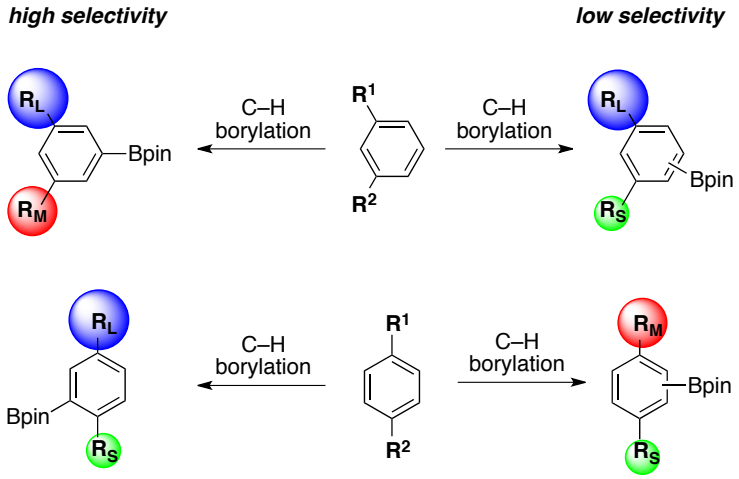

When these requirements are not met, selectivities can erode. Although recent work shows promise for borylation of C–H bonds ortho to F,[4-7] this tendency makes borylation meta to F particularly challenging when a sterically accessible ortho H is present. Some recent efforts in directed borylation have achieved success with borylation meta to F, [8-11] however simple arenes

that lack common directing groups or that have multiple C-X bonds remain problematic. Given the importance of fluorinated organic molecules, this is a serious limitation of C–H borylation. Here we show that ligand design makes it possible to achieve good selectivities for combinations of substrate classes, substituents, and substitution patterns that are daunting for C–H borylation and other C–H or C–X transformations.

The chemistry of 3-fluorochlorobenzene (**1**) illustrates some of the challenges that remain in aromatic functionalization (Chart 2.1).

Figure 2.1. C–H Functionalizations of 3-Fluorochlorobenzene

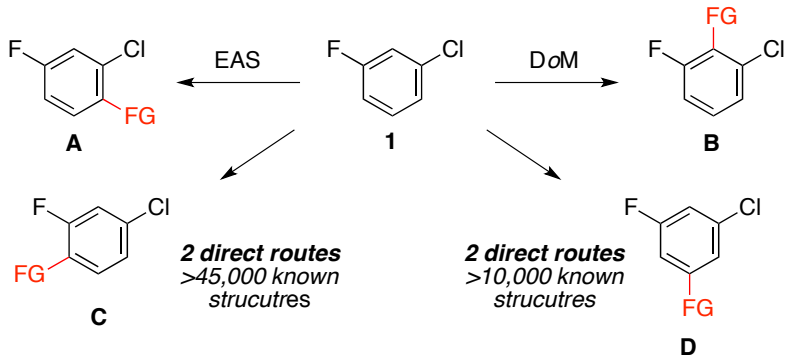

While the 2-position can be selectively transformed via D*o*M, and EAS can be used to functionalize the 6-position,[12-15] selective derivatizations at the 4-position are limited to an enzymatic hydroxylation[16,17] and the electrophilic borylation recently reported by Ingleson and co-workers.[18] Likewise only two reports, both C–H activations, describe functionalization at the 5-position.[19-20] Given that >45,000 4-substituted and >10,000 5-substituted compounds have been reported, the dearth of direct routes from **1** is remarkable.[21] Limitations in the substrate scopes of promising Co-catalyzed ortho C-H borylations reported by Cherik[7] and meta C-H borylation reported by Cui[11] likewise fails to achieve dihalogenated structures C or D by direct functionalization of **1**.

In contrast, Ir-catalyzed C–H borylation using the commonly employed dtbpy/$[Ir(OMe)(cod)]_2$ ligand/precatalyst combination gives a mixture of 4 and 5-borylated products as shown in Scheme 2.2.

Scheme 2.2. C–H Borylation of 3-Fluorochlorobenzene

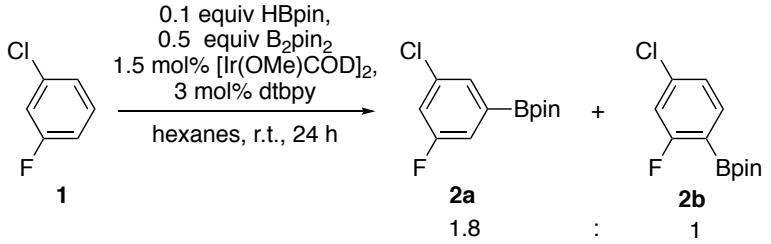

Electronic Effects of Ligands on Borylation. Despite low selectivity, C–H borylations clearly provide opportunities for these challenging transformations. Since electronic effects can influence C–H borylation regioselectivities,[22-23] Ir catalyzed C-H borylations of **1** were performed using 4,4'-disubstuted-2,2'-dipyridyl (bpy) ligands. The remote 4'-substitution site on the bpy ligand ensures that selectivities will be electronically determined. Although the changes in selectivities are modest, Table 2.1 shows that **2a** is favored for the most electron-rich ligand while **2b** is the major isomer for the most electron- poor ligand. Based on calculated pK_as of halogenated benzenes,[22] the C–H bond at the 4-position should be more acidic than the C–H at the 5-position.

Table 2.1. Electronic Effects on Borylation Regioselectivity[a]

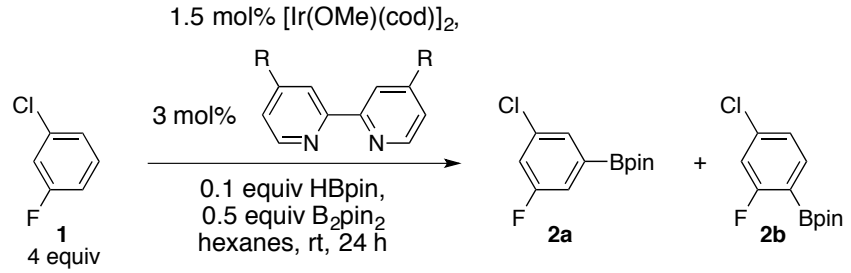

entry	R	**2a**:**2b**
1	*t*-Bu	1.8:1
2	NMe_2	2.2:1
3	CF_3	1:1.6

[a]1 equiv reflects the number of transferable Bpin groups (i.e., 2 Bpin groups per B_2pin_2).

Quantification of Electronic and Steric Effects of Ligands. Using the results in Table 2.1 and estimations of ligand steric effects, the ligand design approach in Chart 2.2 was devised for selective functionalization at the 4 or 5-positions of **1**. Specifically, hindered, electron rich ligands should favor isomer **2a**, while less encumbered electron poor ligands should select for isomer **2b**. Chart 2.2 shows a palette of chelating ligands ordered by their steric and electronic properties.

Figure 2.2. Variation of Ligand Steric and Electronic Effects

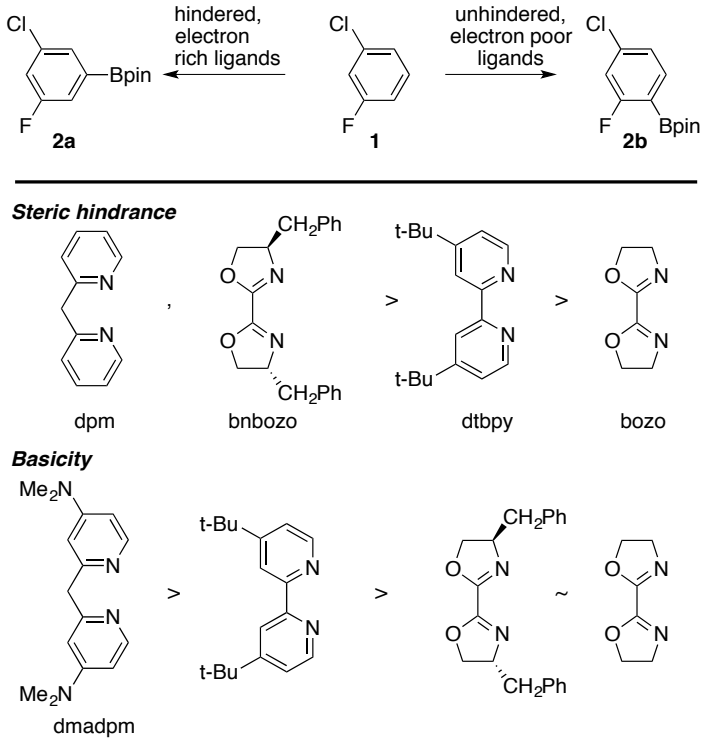

The ligands with a methylene spacer between the pyridine rings, denoted as dipyridyl methane, (dpm) and dimethylaminodipyridyl methane (dmadpm), will form puckered six-membered metalacyclic rings when chelated to the Ir, as opposed to the 5-membered planar metalacycles that result from 4,4'-di-tertbutyl-2,2'-bipyridine (dtbpy) or 2,2'-bisoxazoline (bozo) coordination to Ir.[23] Therefore dpm and dmapm will be the most sterically demanding ligands. The bozo ligand will be less sterically hindered than dtbpy because the five-membered oxazoline rings of bozo are smaller than the pyridine rings in dtbpy. When ligated to the Ir center, the benzyl

substituted bisoxazoline ligand, 2,2′-bis[(4*S*)-4-benzyl]-2-oxazoline (bnbozo) projects a benzyl group below the ligand plane into the region where the substrate approaches during borylation. Thus it should be more hindered than dtbpy and bozo.

Table 2.2: Brønsted Basicities of Related Oxazoles and Pyridines:

2-methyl oxazolium	2-methyl pyridinium	2,4-dimethyl pyridinium	N,N'-(dimethyl)-4-aminopyridinium
		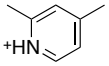	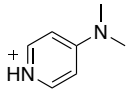
pK_a 5.52 ref. 26	pK_a 5.97 ref. 28	pK_a 6.71 ref. 27	pK_a 9.86 ref. 29

Table 2.2. Ranking of the bacisity is based on calculated pK_as of analogous monomers of the ligands. Calculations for the 2-methyl analogue of 4-dimethylamino pyridinium were not found in the literature, so the unsubstituted pyridinium is included to illustrate the significant increase in bacicity imparted by the NMe_2 substituent. Scifinder predicted properties estimates 4-(dimethylamino)-2-methyl pyridinium pK_a = 10.71.

Ligand Selectivities of 3-Fluorochlorbenzene. From the Brønsted basicities of related oxazoles and pyridines, (Table 2.2) the ligand's capacities for sigma donation should increase in the order bozo[24] < dtbpy[25] ~ dpm[26] < dmadpm.[27] If the steric and electronic effects on selectivity for borylations of **1** map as predicted, preference for **2a** should increase in the order bozo < dtbpy < dpm < dmadpm, with the positioning of bnbozo being difficult to predict a priori. The results for borylations with these ligands are shown in Table 2.3.

The selectivities follow the order predicted from the model, validating the notion that steric and electronic effects can work in concert. When bnbozo is compared to less hindered dtbpy, electronic effects for bnbozo trump sterics and the electronic product **2b** is favored. The electronically similar and less hindered bozo ligand is even more selective for **2b**.

Table 2.3. Boron Reagent Effects on the Borylation Regioselectivity of 1

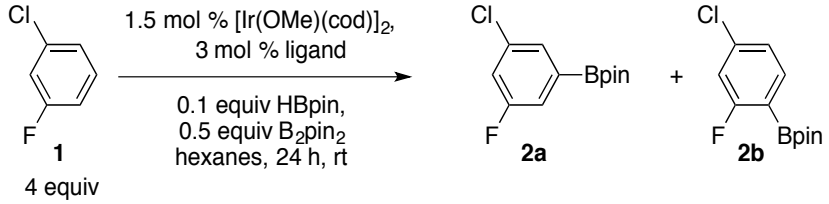

entry	ligand	% conversion[a]	**2a**:**2b**
1	bozo	74	1:3.3
2	bnbozo	79	1:2.4
3	dtbpy	>99	1.8:1
4	dpm	86	2.3:1
5	dmadpm	>99	2.9:1

[a]% conversion was determined by integrating the ^{19}F NMR resonances for **1**, **2a**, and **2b** of aliquots from the reaction mixture.

Regioselective Effects of Borane Source on 3-Fluorchlorobenzene. It has previously been documented that B_2pin_2 is more reactive than HBpin in borylations.[28] Thus, borylation with 0.5 equiv of B_2pin_2 results in a rapid borylation of arene with production of HBpin. Once the B_2pin_2 is consumed, the second stage of borylation proceeds. In the case of dpm and dmadpm, the selectivity for isomer **2a** improves as the reaction with 0.5 equiv of B_2pin_2 proceeds, suggesting that the selectivities with B_2pin_2 and HBpin differ (Scheme 2.3).

Scheme 2.3. Boron Reagent Effects on the Borylation Regioselectivity of 1

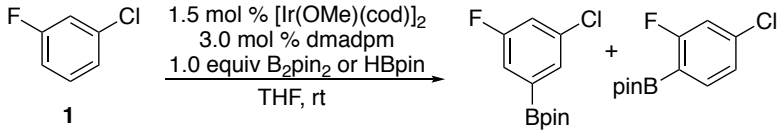

Boron reagent	**2a**	**2b**
1.0 equiv B_2pin_2	2.5	1
2.0 equiv HBpin	11	1

This was confirmed by examining HBpin and B_2pin_2 as the borylating agents in THF, where the selectivity for **2a** is slightly higher. Remarkably, the isomer ratio for dmadpm / HBpin improves

to 11:1. *This is the first time a significant difference in selectivity between B_2pin_2 and HBpin has been observed.* Selectivities with B_2pin_2 and HBpin were essentially identical for other ligands in Chart 2.2. The disparity between B_2pin_2 and HBpin with dpm and dmadpm must result from a change in catalyst resting state and/or mechanism—the details of which will be discussed later in the chapter.

Ultimately, ligand design makes the synthesis of **2a** or **2b** from **1** possible and demonstrates that Ir-catalyzed borylations can be tuned to complement EAS and D*o*M in Chart 2.1. Isomerically pure **2a** and **2b** can be economically prepared by Miyaura borylation of the commercially available bromides,[29] or by addition of boron electrophiles in the case of **2b**.[18] Nevertheless, the design principles that emerge from studying borylation of **1** can be applied to synthesize compounds where the requisite halides for Miyaura borylation are prohibitively expensive or unknown, or desired regioisomers are not accessible by Ingleson borylation.

Regioselective Outcomes for 5 and 6-Memebered Arenes and Heterocycles. A selection of 5 and 6-membered ring compounds that give isomer mixtures in borylations with dtbpy were screened against the ligands, dpm, bnbozo, and bozo, and the results are shown in Tables 2.4 and 2.5.

The ligand study was designed so that each parent substrate gave two primary products denoted as **a** and **b** regioisomers with **a** isomers (red) being sterically favored, and **b** isomers (blue) being electronically favored. Results are split between two tables, 6-membered arenes and heteroarenes in Table 2.4, and 5-membered heterocycles in Table 2.5. The products in the first entry of Table 2.4 are derived from the test substrate, 3-fluorochlorobenzene, **1**. Even with the modest selectivities gained from changing ligands, it is enough to isolate pure **2a** by use of dpm

or **2b** by use of bozo, albeit in low yields. **2a** an oil, can be eluted off a silica column with hexane and **2b**, a crystalline solid can be crystalized from the isomeric mixture dissolved in hexanes.

Table 2.4. Ligand Selectivities of C-H Borylation of 6-Membered Arenes and Heterocycles

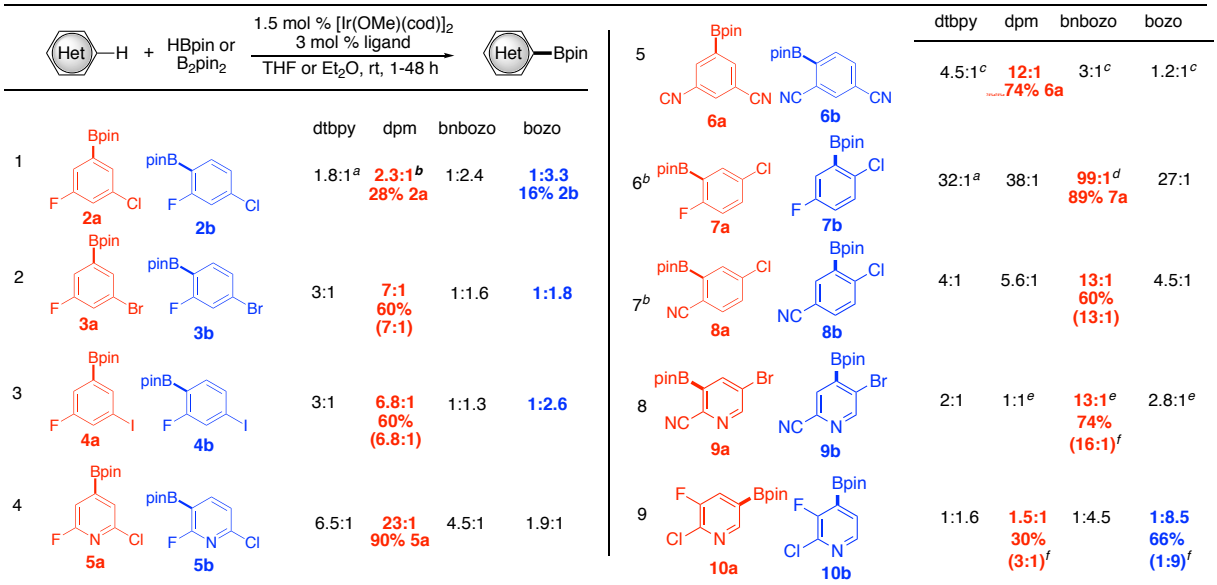

Standard conditions: 1 mmol substrate, 1.5 mol% $[Ir(OMe)cod]_2$, 3 mol% ligand, 1.5-2 equiv HBpin, 3 mL THF, reaction times vary from 1-48 h as detailed in SI. Isomer ratios (GC-FID) or single isomer isolated material in parenthesis where applicable. Yields without ratios are single isomer. [a]Hexane as solvent. [b]Ether as solvent. [c]Catalyst pregenerated in neat HBpin with 6 mol% Ir. No reaction was observed without catalyst pregeneration. [d]Stoichiometric conversion (6%). [e]Low conversion, 40-50%. [f]6 mol% Ir. [g][GC ratio] in brackets from10-fold excess substrate to eliminate diborylation. [h]Practical conditions use 2-fold excess substrate to minimize diborylation to <2%. [i]Practical conditions use 1 equiv substrate resulting in 12-19% diborylation. [j]Diborlation changes a:b ratio. [k]Ratio improved by silica plug. [l]Recrystallized form hexane. [m]a:b ratio determined by NMR. [n]5 mmol scale. [o]1 equiv B_2pin_2

Since many recent C-H borylation methods are prone to competing C-X activation, and many dihalo-substituted arenes, particularly fluoroarenes, are either incompatible or suffer from intrusive dehalogenation, we also tested the bromo and iodo analogues to **1**, shown in Entries 2 and 3 of Table 2.4. These substrates are of interest because the iodo and bromo substituents would render attempts to synthesize **3a,b** and **4a,b** by Miyaura coupling problematic. Borylation of substrates **3** and **4** by dpm proceeds smoothly to 85 – 95% completion in 24 hours and a significant

improvement in steric selectivity is seen over dtbpy. Dehalogenation is not observed in the reactions.

Boronate products **5a**,**b** and **6a**,**b** (Entries 4 and 5) are derived from parent substrates that most closely resemble **1** in that the least hindered site is flanked by two Hs, and the second site of reactivity has a more acidic C–H bond juxtaposed between H and a relatively small substituent, F or CN. As was the case for borylations of **1**, dpm selects for the less sterically hindered site favoring **5a** and **6a**. In the borylation of 6-chloro-2-fluoropyridine, the bozo ligand shifts selectivity towards **5b**, but **5a** is still the major isomer. While bozo increases borylation ortho to CN in 1,3-dicyanobenzene (Entry 5), conversions for bozo (and bnbozo) are very poor.

Entry 6 (compounds **7a**,**b**) is illustrative of a combination of steric and electronic factors working in concert to enhance selectivity of a single isomer. The parent substrate, p-chlorofluorobenzene, presents a competition between a more acidic H ortho to a smaller substituent (resulting in product **7a**) and a slightly less acidic H ortho to a larger substituent (resulting in product **7b**). All the ligands greatly favor isomer **7a** with bnbozo exhibiting essentially single isomer selectivity.

Entries 7 and 8 (**8a**,**b** and **9a**,**b**) assess selectivities for borylations ortho to CN vs. heavier halogens, Cl and Br, in six-membered ring systems.

With dtbpy, selectivity for borylation ortho to CN in Entry 7 is modest and drops significantly for the pyridine in Entry 8. The diminished selectivity in Entry 8 is due to electronic differences between arene and pyridine substrates, as borylation ortho to CN in 4-bromobenzonitrile has previously been shown to be favored relative to 4-chlorobenzonitrile.[3] The electronics of the pyridine in Entry 8 render the 4-position electronically activated, although it is ortho to a bulky Br group. Consequently, the ligands only modestly favor **9a**, surprisingly with the

most sterically demanding ligand, dpm, resulting in a 1:1 mixture. Bnbozo provides the highest selectivity despite presenting a high steric demand. In contrast, the aryl substrate of Entry 7 has a smaller chloro-substituent, yet exerts greater steric direction in the absence of competing electronic influence, and all ligands favor steric isomer **8a**.

The pyridine in Entry 9 (**10a,b**) presents a competition between the activated 4-position ortho to a small F substituent, and illustrates the consequence of decreasing the steric bulk of a pyridyl 3-substituent. Interestingly, dpm modestly favors the steric isomer **10a** while the other ligands favor **10b** borylated at the electronically enhanced 4-position, with bozo giving synthetically useful selectivity of 9:1.

For the 6 membered ring systems, these ligands produce some useful sterically driven shifts in selectivity when electronic factors are either working in concert or largely absent. For 5-membered ring heterocycles, steric effects from neighboring substituents are mitigated, hence selectivities with dtbpy diminish. Results for the borylation of several 5-membered heterocycles are shown in Table 2.5. The first three entries are 2,5-disubstituted heterocyclic substrates where borylation is favored ortho to the smaller CN group. For bnbozo, selectivity is high for **11b**, **12b**, and **13b**.

It is important to note, that for Entry 2, 2-bromo-5-cyanothiophene, bnbozo is the only ligand that can efficiently borylate this substrate under the standard conditions.

The dtbpy reaction for Entry 2 turns black and exhibits only stoichiometric borylation of 2-bromo-5-cyanothiophenene. For dpm and bozo, catalyst loading is increased to 6 mol % Ir, and the catalyst must be generated in HBpin before diluting with solvent, or no reaction occurs. Even though catalytic turnover is achieved, conversion is low at 40 – 50%.

Entry 4 is another 2,5-disubstituted thiophene where borylation competes between a large iodo substituent and a medium-sized chloro substituent. Again, bnbozo displays high Steric selectivity for product **14a**, though the substrate is less active towards borylation and higher catalyst loading is needed.

Table 2.5. Ligand Selectivities of C-H Borylation of 6-Membered Arenes and Heterocycles

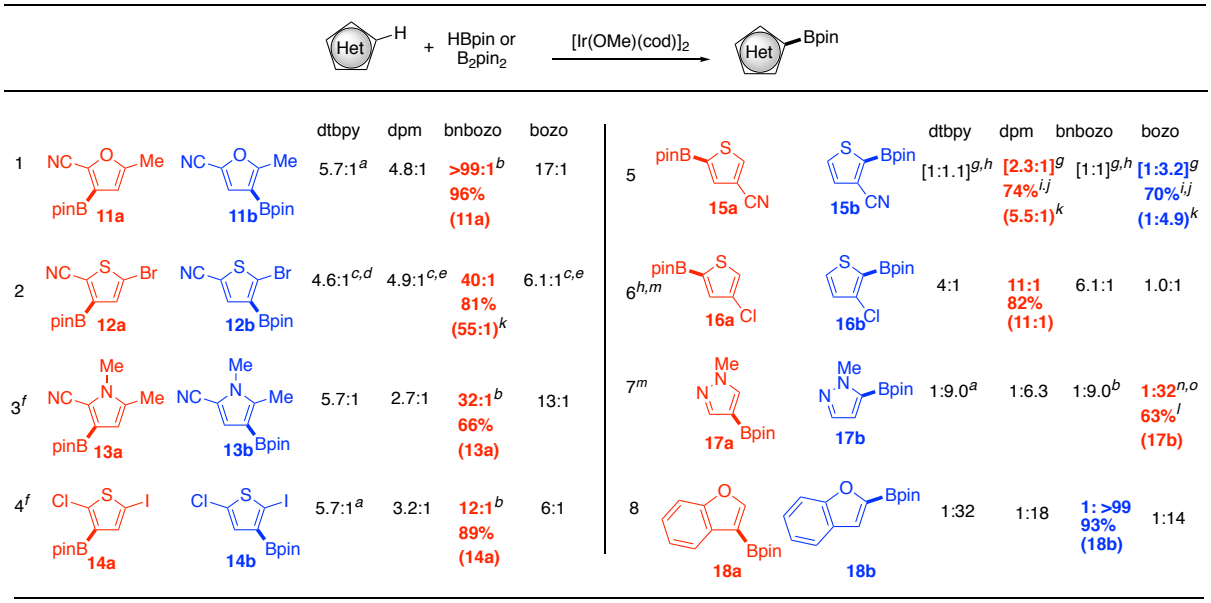

			dtbpy	dpm	bnbozo	bozo
1	**11a**	**11b**	5.7:1[a]	4.8:1	**>99:1[b] 96% (11a)**	17:1
2	**12a**	**12b**	4.6:1[c,d]	4.9:1[c,e]	**40:1 81% (55:1)[k]**	6.1:1[c,e]
3[f]	**13a**	**13b**	5.7:1	2.7:1	**32:1[b] 66% (13a)**	13:1
4[f]	**14a**	**14b**	5.7:1[a]	3.2:1	**12:1[b] 89% (14a)**	6:1
5	**15a**	**15b**	[1:1.1][g,h]	**[2.3:1][g] 74%[i,j] (5.5:1)[k]**	[1:1][g,h]	**[1:3.2][g] 70%[i,j] (1:4.9)[k]**
6[h,m]	**16a**	**16b**	4:1	**11:1 82% (11:1)**	6.1:1	1.0:1
7[m]	**17a**	**17b**	1:9.0[a]	1:6.3	1:9.0[b]	**1:32[n,o] 63%[l] (17b)**
8	**18a**	**18b**	1:32	1:18	**1: >99 93% (18b)**	1:14

Standard conditions: 1 mmol substrate, 1.5 mol% $[Ir(OMe)cod]_2$, 3 mol% ligand, 1.5-2 equiv HBpin, 3 mL THF, reaction times vary from 1-48 h as detailed in SI. Isomer ratios (GC-FID) or single isomer isolated material in parenthesis where applicable. Yields without ratios are single isomer. [a]Hexane as solvent. [b]Ether as solvent. [c]Catalyst pregenerated in neat HBpin with 6 mol% Ir. No reaction was observed without catalyst pregeneration. [d]Stoichiometric conversion (6%). [e]Low conversion, 40-50%. [f]6 mol% Ir. [g][GC ratio] in brackets from10-fold excess substrate to eliminate diborylation. [h]Practical conditions use 2-fold excess substrate to minimize diborylation to <2%. [i]Practical conditions use 1 equiv substrate resulting in 12-19% diborylation. [j]Diborlation changes a:b ratio. [k]Ratio improved by silica plug. [l]Recrystallized form hexane. [m]a:b ratio determined by NMR. [n]5 mmol scale. [o]1 equiv B_2pin_2

Entries 5 and 6 are 3-substituted thiophenes where borylation at the 2 and 5 positions compete. In both cases, dpm favors borylation at the less hindered 5 position, although with the small CN substituent of Entry 5, significant amounts of 2-borylation occurs. Entry 6 has a Cl substituent, which is larger than CN, and consequently dpm selectivity for **16a** is greater than **15a**.

Bozo, on the other hand favors borylation at the electronically more activated 2-position. With 3-cyanothiophene (Entry 5), pure **15a** is isolated by crystallization from the dpm reaction, and pure **15b** is isolated by crystallization form the bozo reaction, both in moderate yields. The interesting feature of Entry 5 is that the selectivity advantage is modest when all diborylation is prevented by running the reaction with a 10-fold excess of substrate, as the ratios in brackets show. However, when diborylation occurs, the ratio is enhanced for **15a** to 5.5:1 in the dpm system, thus making crystallization easy after separating diborylated material with a short silica plug in a 1:1 dichloromethane : hexane solvent mixture.

A good illustration of the contrasting effects of sterically driven regioselectivity between bnbozo and bozo is seen when Entries 5 and 6 are compared. For Entry 5, which has a small 3-CN substituent, bnbozo gives 1:1 selectivity for **15a**:**15b** (borylation at the 5 vs 2 position), while bozo is selective for 2-borylation. For the larger 3-Cl substituent in Entry 6, bnbozo gives good selectivity for **16a**, (6.1:1) while bozo gives poor 1:1 selectivity.

For Entry 7, N-methylpyrazine, the steric position is substantially less acidic than the electronic position, but the electronic positon is ortho to a bulky methyl group.

All ligands favor 2-borylation, **17b**, with the smallest ligand, bozo, giving the best selectivity. Dpm, while still favoring **17b**, produces more of isomer **17a** than the other ligands. For the last entry, benzofuran, all ligands greatly favor borylation at the more activated 2-position, **18b**, with bnbozo essentially displaying single isomer selectivity. The intriguing result, however, is bozo, the smallest of the ligands, shows the lowest ratio for **18b** when the only steric demand presented is the electron pairs of the O atom. Even though bozo produces the lowest ratio at 14:1, it is still highly selective for **18b**.

Improving Regioselective Outcomes by Ligand Design. For each substrate in Tables 2.4 and 2.5, the entries with the highest selectivities are highlighted for products that are major isomers, and isolated yields are given, most resulting in moderate to excellent single isomer products. Significantly, there is no example where dtbpy, the most commonly used ligand in Ir-catalyzed C-H borylation gives superior selectivity.

For the cases where dpm favored the sterically preferred product, comparisons were made with the more electron rich ligand, dmadpm. The comparisons are shown in Table 2.6. Improvement in selectivity was seen for products **2a**, **3a**, **4a**, **5a**, and **13a**, whereas dmadpm selectivity for **6a** and **14a** was worse.

Table 2.6. Comparison of dmadpm Selectivities of Selected Substrates

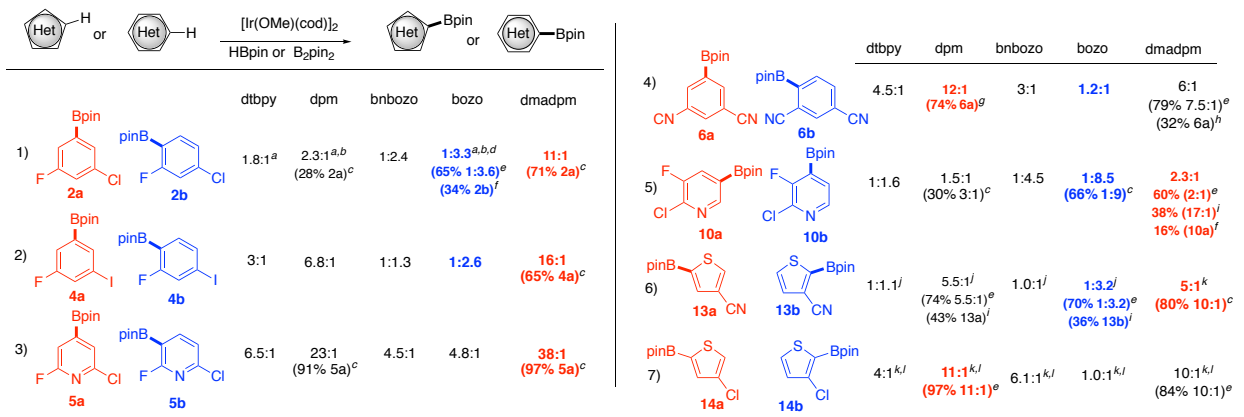

Standard conditions: 1 mmol substrate, 1.5 mol% $[Ir(OMe)cod]_2$, 3 mol% ligand, 2 equiv HBpin, 3 mL THF, reaction times vary from 1-48 h as detailed in SI. Isomer ratios (GC-FID) or single isomer isolated material in parenthesis where applicable. Yields without ratios are single isomer. [a]Hexane as solvent. [b]4 equiv substrate. [c]Isolation by silica plug with hexane. [d]1 equiv B_2pin_2. [e] Isolated by silica plug with CH_2Cl_2. [f]Recrystallized twice from hexane. [g]Isolation by kugelrohr distillation. [h]Recrystallized from ethanol. [i]Recrystallized once from hexane. [j]12-15% diborylation. Ratio of **13a**:**13b** is changed significantly by diborylation when dpm is used as ligand. [k]2 equiv substrate, 2-5% diborylation. [l] Ratio a:b determined by NMR.

In the case of **5a**, the selectivity was sufficiently high that a 95% isolated yield of pure **5a** could be obtained at a low catalyst loading (Scheme 2.4).

Scheme 2.4. Highly Selective Borylation Meta to Fluorine

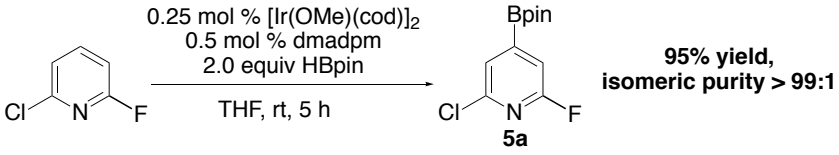

Expanding Synthetic Options for C-H vs C-X Borylation Routes. The utility of the ligand and borane reagent-modulated selectivity that we have developed is showcased in Figure 2.3. C-H borylations are compared to putative C–X borylations (X = Br or I) of the type pioneered by Miyaura. Factors that would be considered in choosing between these routes are selectivity for the desired product and the price of reagents.

Figure 2.3. Comparisons Between C–H and C–X Borylation Routes

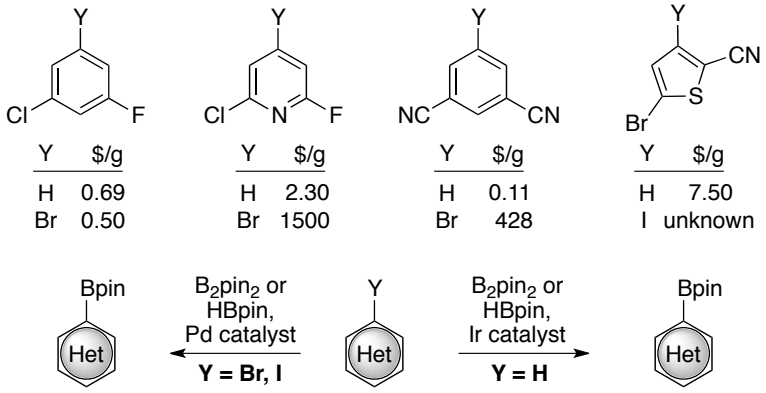

For the synthesis of **2a**, the high regio-specificity of the Miyaura borylation and the low cost of the aryl bromide substrate make it the route of choice. In contrast the aryl and heteroaryl halides that would be required for Miyaura coupling routes to **5a**, **6a**, or **12a** range from being costly to nonexistent. It is noteworthy that directed ortho metalations of substrates where Y = H followed by trapping with boron electrophiles will not give **5a** or **6a** as major isomers, and bromo-thiophenes are known for halogen dance rearrangements. Therefore, Ir-catalyzed C–H borylation is the best option for the synthesis of isomers **5a**, **6a**, and **12a**.

Variation of Regioisomer Ratios with Borane Concentration. These Studies show that ligand modifications can dramatically improve regioselectivity in C–H borylations of substrates where the most commonly used ligand, dtbpy, gives isomer mixtures that can limit synthetic utility. In addition, we have shown for the first time that the nature of the boron reagent can significantly affect the regioselectivity in C–H borylation. Considering the dramatic effect that the borane source has on the selectivity of dpm and dmadpm borylation reactions, we decided to further probe the source of this disparate reactivity between HBpin and B_2pin_2 with the dpm-type ligands.

Table 2.7. Changes in 2a:2b GC Ratio over Time as Concentration of HBpin Changes

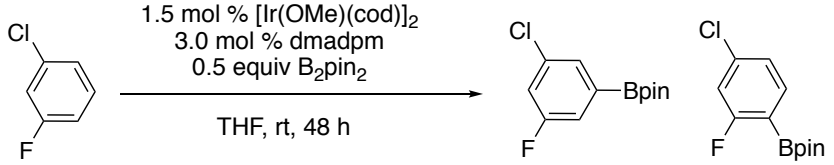

Entry	Time (h)	Conversion	Ratio **2a**:**2b**
1	1	6%	1.3:1.0
2	2	10%	1.4:1.0
3	6	16%	1.8:1.0
4	12	31%	3.7:1.0
5	20	55%	4.8:1.0
6	24	64%	4.8:1.0

This effect was first noticed when preliminary borylation tests performed on **1** with dmadpm ligand suffered a lack of consistency among various reaction conditions with varied amounts of HBpin used to pre-generate the catalyst, and the choice of 1.0 equiv B_2pin_2 or 0.5 equiv B_2pin_2. In order to eliminate the variability of dispensing HBpin, no HBpin was added to subsequent reactions, and 0.5 equiv B_2pin_2 was chosen as the borane stoichiometry for the next round of experiments. When the reactions were monitored by GC over time, the ratios of **2a**:**2b** changed as the reaction proceeded, as seen in a Table 2.7.

A summary of the range of ratios obtained based on the type and amounts of borane reagent used in the reaction is seen in Table 2.8. This result is striking in itself, but it is particularly noteworthy in context of the well-established borylation kinetics of Boller and Hartwig,[30] published in 2005. In their paper, it was established that borylation reactions of $[Ir(OMe)cod]_2$ / dtbpy with B_2pin_2 are zero order in B_2pin_2, and the reaction rates are dependent only on the concentration of arene present in the reaction. The borylation of 3-fluorochlorobenzene with the ligand dmadpm as seen in Tables 2.7 and 2.8 did not seem consistent with a reaction that is zero order in borane, so we wondered if the catalytic cycle for dmadpm and HBpin is significantly different than that of dtbpy.

Table 2.8. Selectivity of dmadpm in the Borylation of 1 Varies with Borane Reagent.

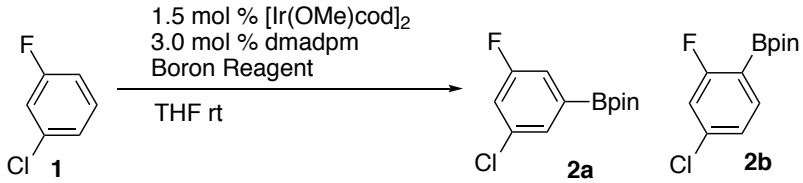

Boron source	Ratio **a** : **b**
1.0 equiv B_2pin_2	2.4 : 1.0
0.5 equiv B_2pin_2	3.6 : 1.0
1.1 equiv B_2pin_2	10.3 : 1.0
2.0 equiv HBpin	11.1 : 1.0

Kinetic Studies of Ligand and Borane Combinations. We decided to subject the ligand dmadpm to the kinetics experiments performed in the Boller-Hartwig studies to see if dmadpm adhered to the accepted catalytic cycle where C-H activation is the rate limiting step and the catalytic cycle is zero order in borane. A key difference between our studies and the work of Boller and Hartwig is that their work employed the isolated cyclooctene (coe) adduct of the dtbpy ligated Ir tris-boryl intermediate (**26**) as the catalyst instead of generating a catalytic species from $[Ir(OMe)cod]_2$ and dtbpy.

Scheme 2.5. (coe)Ir(dtbpy)Bpin$_3$, 26, does not enter the catalytic cycle or impact the order of borane.

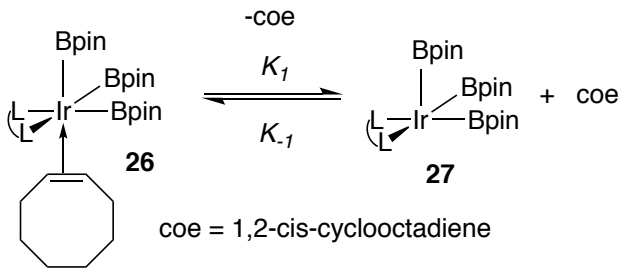

Unfortunately, the isolation of an analogous dmadpm ligated Ir trisboryl complex is ongoing, and so an isolated intermediate was not available to our kinetics study. Instead, we generated the catalyst from [Ir(OMe)cod]$_2$ and dmadpm ligand at the beginning of each kinetics experiment.

The purpose of using the preassembled dtbpy tris-boryl iridium complex in the 2005 kinetics studies was to avoid complications arising from the kinetics of catalyst assembly from [Ir(OMe)cod]$_2$ and free dtbpy. In keeping with Halpern's maxim[31] that true reaction intermediates are almost never isolable, Boller and Hartwig showed that **26** is a catalyst resting state, and there is a rapid and reversible dissociation (shown in Scheme 2.6) of coe to form a 16-electron intermediate, **27**, which is the actual participant in the proposed catalytic cycle, as shown in Scheme 2.7.[30] Since **26** does not directly react with arenes, or participate in the catalyst cycle, it cannot give us information about the order in borane. Although it may affect the rates of reactions, generation of the active catalyst species from [Ir(OMe)cod]$_2$ and free ligand instead of a dmadpm analogue of **26** should reliably provide an accurate assessment of whether borylation reactions with dmadpm are zero order in borane.

Scheme 2.6. Dissociation of 26, (coe)Ir(dtbpy)Bpin$_3$ generates the active catalyst, 27.

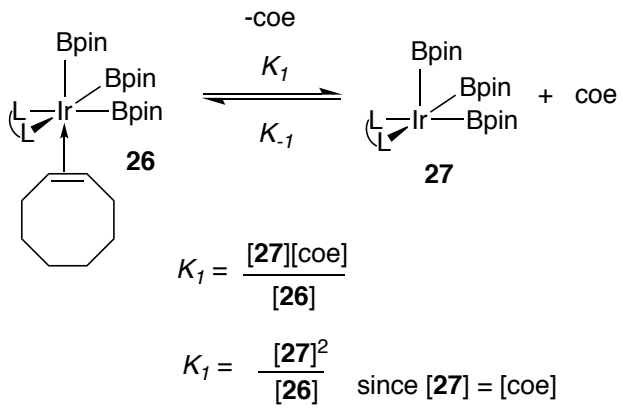

Scheme 2.7. Intermediate 27 enters the catalytic cycle after dissociation of 26.

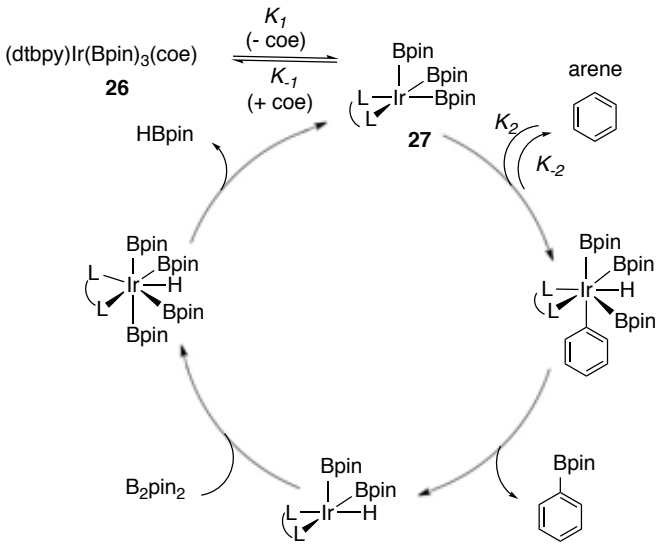

The rate equation of Ir catalyzed borylation was determined experimentally by Boller and Hartwig from stoichiometric reactions of **26** and benzene,[30] as shown below labeled as equation 1.

$$\text{rate} = K_1k_2[\text{Ir}][\text{arene}]/[\text{coe}] \qquad \textbf{(eq. 1)}$$

Although equation 1 forms the foundation for understanding the catalytic cycle of the $[Ir(OMe)cod]_2$/dtbpy system, in practice, catalytic borylation reactions do not have a direct dependence on coe concentration due to the low catalyst loadings of 1 – 3 mol % that are typically employed. Boller and Hartwig also showed that the equilibrium for the dissociation of **26** into (**27** + coe) lies far to the left, favoring the associated coe-adduct over the dissociated active species, **27**, which results in a concentration dynamic of [coe] << [**26**] << [arene].[30] The rate equation for catalytic borylation with **26** can be simplified and rearranged to equation 2.

$$\text{rate} = K_1^{1/2}\, k_2[\mathbf{26}]^{1/2}[\text{arene}] \qquad \textbf{(eq. 2)}$$

For Ir-catalyzed reactions, the rate can be expressed in terms of an experimentally observed rate constant, k_{obs}, which encompasses the pre-catalyst assembly into **26** and dissociation into **27.** After the establishment of the initial catalytic cycle, kinetic studies demonstrate the reaction depends only on how much arene is present, and exhibits rates consistent with equation 3.[30]

$$\text{rate} = k_{obs}\,[\text{arene}] \qquad \textbf{(eq. 3)}$$

$$\text{set eq. 1 = eq. 2:} \quad k_{obs} = K_1^{1/2}\, k_2\,[\mathbf{26}]^{1/2}$$

By setting equations 1 and 2 equal to each other, an expression is derived where the rate constants can be calculated if the concentration of the precatalyst **26** is known. This is another advantage to using an isolated precatalyst rather than *in situ* generation of an active species.

Detailed mechanistic and kinetics experiments by Boller and Hartwig demonstrate a clear first order dependence in arene concentration and a zero order dependence in B_2pin_2

concentration.[30] Changing the ligand of the active catalyst species from one substituted pyridyl-based ligand to another would be expected to follow a similar reaction profile, though the observed rate would vary according to the properties imparted by the ligand.

In the case of dmadpm, however, the considerable difference in rate and selectivity seen between HBpin and B_2pin_2 does not support Boller and Hartwig's observed zero order behavior in borane concentration. The effect of HBpin as the boron source was not investigated in Hartwig's paper, and the authors chose 1.6 equiv of B_2pin_2 as a standard condition in the kinetic studies, thus ensuring that B_2pin_2 was always available as a boron source. They offered the observation that *"The simplest data were obtained when the concentration of B_2pin_2 exceeded the concentration of arene."*[30]

The search for a plausible explanation behind the divergent reactivity of HBpin vs B_2pin_2 in the dmadpm ligated system led to the design of a series of experiments analogous to the kinetic studies detailed in the 2005 Boller-Hartwig paper,[30] where a series of NMR tube reactions were performed with fluorine-containing substrates, and the borylation reactions were monitored by ^{19}F NMR. This approach was adapted to the dmadpm system using the substrate of interest, 3-fluorochlorobenzene, and the boron reagents HBpin and B_2pin_2.

The starting point for this investigation was to replicate the published results in the lab and then adapt a procedure suitable to the dmadpm system. Since we did not have an isolated dmadpm tris-boryl intermediate, the first task in the investigation was to ensure that the assembly of the active catalyst from $[Ir(OMe)cod]_2$ and dmadpm did not significantly change the outcome of Boller and Hartwig's experimental observations.

We first synthesized **26** and repeated Hartwig's initial experiment of the borylation of 3-trifluomethyltoluene **17**, with 1.6 equiv (0.49 M) B_2pin_2 in cyclohexane, (Experiment 1, Scheme

2.8). The reactions were assembled in the glove box, transferred into screw cap NMR tubes, and the substrate was injected just before monitoring of the reaction by an arrayed ^{19}F NMR experiment.

Scheme 2.8. NMR Tube Conditions: Experiment 1 of Kinetics Study

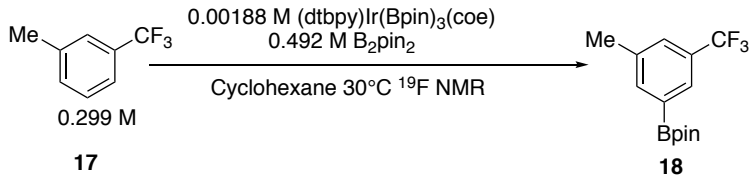

The first order plot was linear and k_{obs} was on the order of Hartwig's reported value. See the Chapter 2 appendix for all detailed information regarding the kinetics experiments, including concentrations of reagents and graphs and k_{obs} values.

Next, **17** was borylated under pseudo-first order conditions with **26** and 4.5 equiv (1.3 M) B_2pin_2 in cyclohexane (Experiment 2). The k_{obs} was slightly lower than Experiment 1, but matched Hartwig's reported values. Although they were not the same, the k_{obs} values of Experiments 1 and 2 were on the same order of magnitude, within a multiple of 3, and the first order plots for both were linear over 4 half–lives.

Next, the catalyst was generated from $[Ir(OMe)cod]_2$ and dtbpy (Ir/dtbpy) for the standard borylation of **17** with 1.6 equiv (0.49 M) B_2pin_2 (Experiment 3, Scheme 2.9 and the graph seen in Figure 2.4).

This produced a linear first order plot with the same k_{obs} that Hartwig reported, so it seemed that catalyst generation did not affect the behavior of the reaction. The substrate of interest for the dmadpm system is 3-fluorochlorobenzene, **1**, and so the next step required the borylation of **1** using complex **26** and 0.49 M B_2pin_2 in cyclohexane (Experiment 4).

Scheme 2.9. Borylation with B_2pin_2 by generating the catalyst from $[Ir(OMe)cod]_2$ gives the same result as catalysis from 26. (Exp. 3)

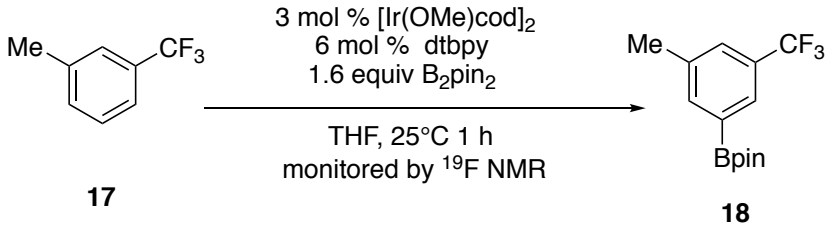

17 **18**

Figure 2.4. Borylation of 17 with B_2pin_2 by generating the catalyst from $[Ir(OMe)cod]_2$ gives the similar result as catalysis from 26. (Exp. 3)

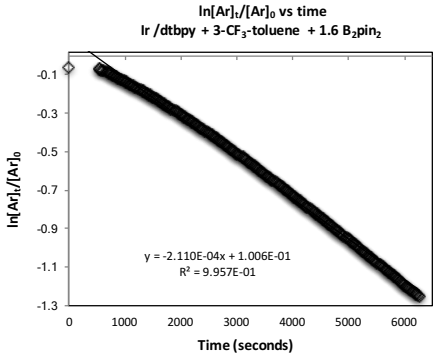

A second borylation of substrate **1** with the active catalyst generated from Ir/dtbpy with 0.49 M B_2pin_2 in a different solvent, THF, was also run (Experiment 5, as seen in Scheme 2.10).

The reactions progressed too rapidly to be followed by NMR with the same conditions as the more electron rich substrate **17**. The temperature was lowered from 30°C to 25°C and the catalyst load was halved from 0.018 M to 0.009 M (6 mol % lowered to 3 mol %). The k_{obs} values of the reactions catalyzed by **26** in cyclohexane and the reaction of Ir/dtbpy in THF were within 5% of each other, with the THF reaction slightly faster.

Both first order plots were linear, both with R^2 values of 0.997. The ratios of **2a**:**2b** for Experiment 4 (catalyzed by **26** in cyclohexane) was 1.5:1, compared to Experiment 5 (Ir/dtbpy reaction in THF) **2a**:**2b** ratio of 1.9:1. This solvent effect is consistent with observed ratio differences of **2a**:**2b** in the borylation reactions of **1** run in THF compared to hexane.

Scheme 2.10. Borylation of 3-Fluorochlorobenzene, 1, with B_2pin_2 by generating the catalyst from $[Ir(OMe)cod]_2$ gives the same result as catalysis from 26. (Exp. 5)

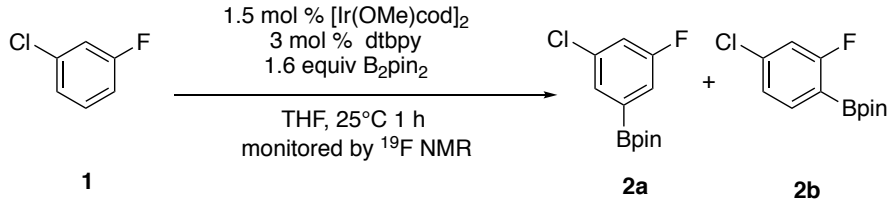

Figure 2.5. Borylation of 1 with generated catalyst gives comparable data. (Exp. 5)

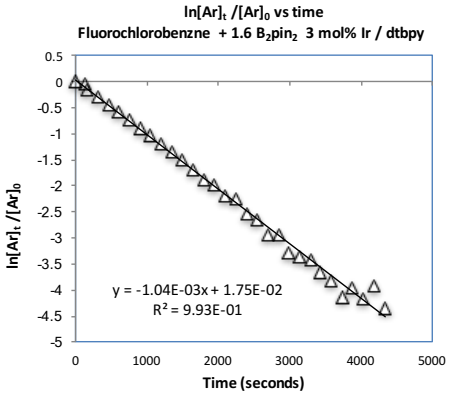

Next, **1** was borylated with Ir/dmadpm, and 0.49 M B_2pin_2 in THF (Experiment 6). The reaction was too slow to provide useful kinetic data, so the temperature was increased from 25 °C to 50 °C, while the catalyst concentration was kept 0.009 M. The reaction was much slower than dtbpy ligated reaction, with a k_{obs} of 6.5 x 10^{-5} s^{-1}. In 5 hours, 57% conversion was observed with a **2a**:**2b** ratio of 2.5:1. The first order plot was linear with an R^2 of 0.990.

The fact that the first order plots were linear, the k_{obs} values were repeatable, the data was reasonable and in line with reported values, it was determined that these kinetics conditions were suitable to study the dmadpm system of the borylation of **1** in THF. After confirmation that dmadpm provided useful kinetic data, and was zero order in B_2pin_2 for the prescribed B_2pin_2 concentrations, the next step was to test whether HBpin likewise exhibits zero order behavior in borylation reactions.

Experiment 7 was a repeat of Experiment 1 (catalyzed by **26** with B_2pin_2 and substrate **17** in cyclohexane) except using 2 equivalents of HBpin (0.64 M) instead of B_2pin_2. (2 equiv is the stoichiometry where the **2a**:**2b** ratio is the greatest, 11:1). Even though **17** will not form mixtures, the borane was kept at the same stoichiometry as the reaction of interest. Experiment 7 was carried out at 30 °C and 0.018 M in **26**. The reaction was very slow and in 2.5 hours, only 30% conversion was realized. The first order graph was not linear. This reaction was not zero order in borane.

Experiment 7 conditions were repeated with substrate **1** in cyclohexane with 0.64 M HBpin at 50 °C (Experiment 8, shown in Scheme 2.11). In 2 h, 88% conversion was realized with a **2a**:**2b** ratio of 2:1. The first order plot was not linear. The second order plot, however, appeared linear with an R^2 of 0.999. The second order k_{obs} was 0.04 $M^{-1}s^{-1}$. To compare the effect of HBpin to B_2pin_2 on selectivity, the ratios of reactions 4 and 8 are compared, Reaction 4 (**26**-catalyzed borylation of **1** with B_2pin_2 in cyclohexane) gave a ratio of 1.5 :1. The same reaction conditions with HBpin in experiment 8 gave a 2:1 ratio.

Scheme 2.11. 26-catalyzed Borylation of 1 with HBpin is not zero order in borane. (Exp. 8)

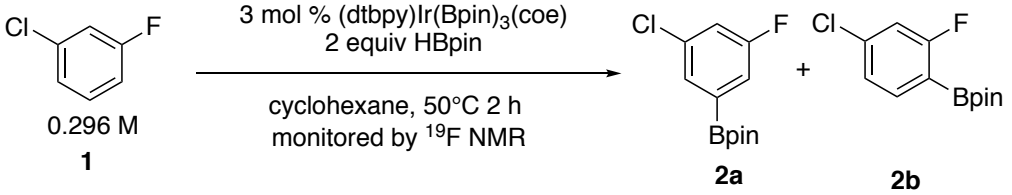

Figure 2.6. Borylation reactions with HBpin appear to be second order in arene. (Exp. 8)

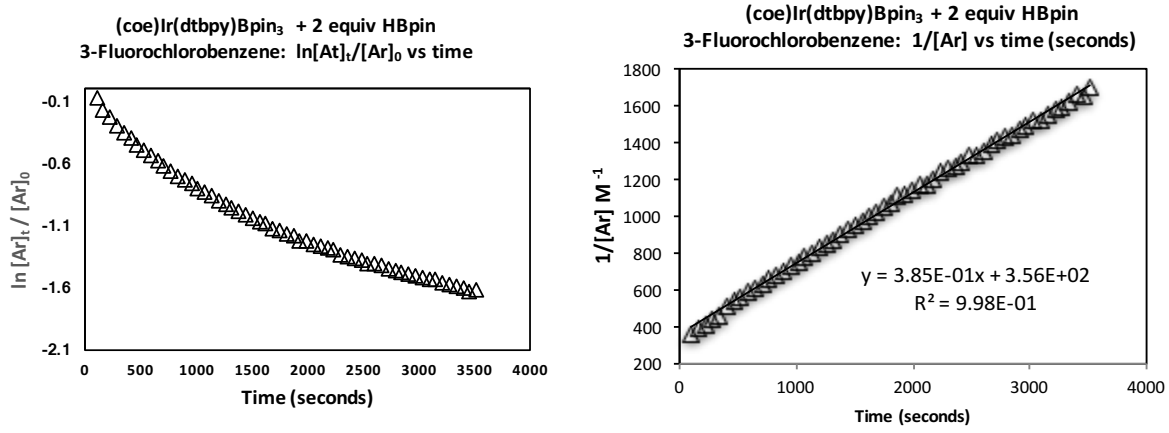

It was confirmed that borylation reactions with 2 equiv HBpin are not zero order in borane, and this behavior holds among different substrates, ligands and solvents, not just dpm type ligands. Figure 2.2 shows the first and second order plots for the borylation of **1** with 2 equiv HBpin catalyzed by the isolated intermediate **26**. Even for with the assembled precatalyst, the order in borane depends on the boron source.

After control experiments were evaluated, borylation of **1** with HBpin and the ligand dmadpm was tested. Ir/dmadpm catalyzed borylation of **1** with 0.64 M HBpin at 30 °C was very slow and less than 50% conversion was reached in 12 h. The reaction was repeated at 40°C but it was still too slow. These two initial experiments did not provide usable kinetic data, but the ratios of **2a**:**2b** were both 11:1 as determined by integration of ^{19}F NMR.

Scheme 2.12. Comparison of 2 Equiv HBpin vs Pseudo-First Order HBpin with dmadpm (Experiments 9 and 10)

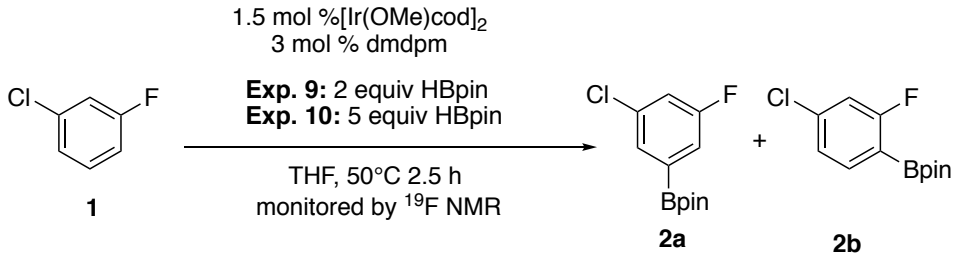

Figure 2.7. Borylation of 1 with dmadpm and HBpin. (Experiments 9 and 10)

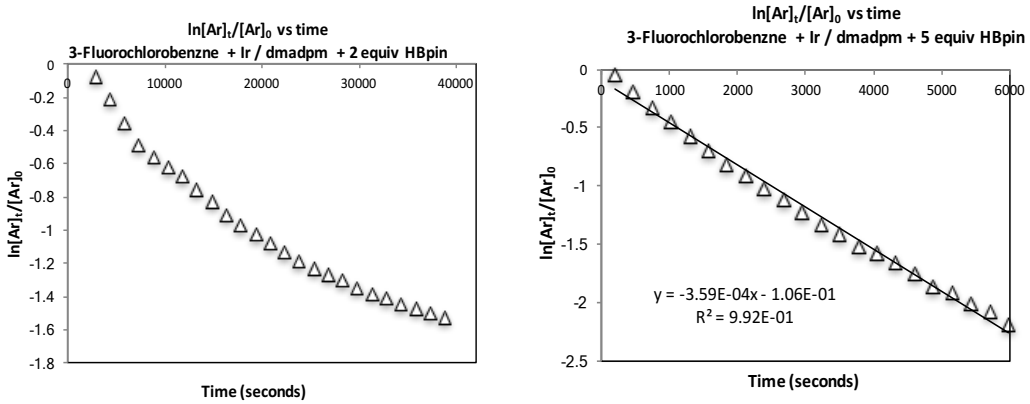

The first order plots were not linear, but there was not enough conversion to make any inference from the experiments. The experimental conditions were repeated at 50°C (Experiment

9), and 79% conversion was reached in 12 h. The first order plot was not linear, while the second order plot was linear with an R^2 of 0.998. The second order k_{obs} was 0.0029 $M^{-1}s^{-1}$. Heating the reaction to 50°C resulted in a lower **2a**:**2b** ratio of 7.5:1.

The next reaction (Experiment 10) explored the borylation of **1** under pseudo first order HBpin concentration. Ir/dmadpm catalyzed borylation of **1** with 1.6 M HBpin in THF at 50°C over 5 h resulted in 97% conversion, and a **2a**:**2b** ratio of 11:1. The first order plot was approximately linear over 3 half-lives with an R^2 value of 0.982. The k_{obs} over the reaction was 0.00029 s^{-1}. The second order plot was not linear.

It was interesting to observe that 2 equivalents of HBpin resulted in a non- zero order in borane, with a linear second order plot, but the borylation of **1** under pseudo first order concentrations of HBpin (Experiment 11) produced an approximate zero order behavior, yet also exhibited the increased **2a**:**2b** ratio of 11:1.

Since these experiments infer that concentrations of borane do matter, we wondered what effect would be seen from the **26**-catalyzed reaction of **1** in cyclohexane with exactly 1.0 equiv B_2pin_2 (0.3 M), (Experiment 12). Over 3 half-lives, the first order plot is linear with R^2 value of 0.997 and k_{obs} of 0.0017 s^{-1}. 3 half-lives are reached in 20 minutes. After that, the rate slows rapidly and the linearity is lost. Full conversion is seen over 2 h, with a **2a**:**2b** ratio of 1.6:1.

Scheme 2.13. Borylation Reactions with 1.0 equiv B_2pin_2 (Exp. 12)

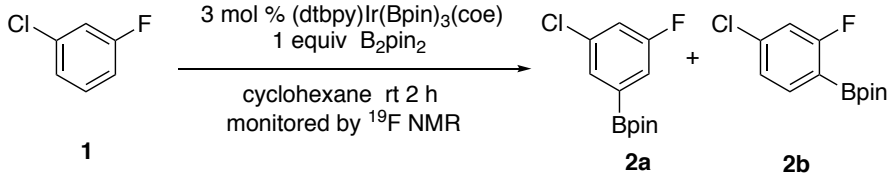

Figure 2.8. First order Plot of Borylation Reaction with 1.0 equiv B_2pin_2 (Exp. 12)

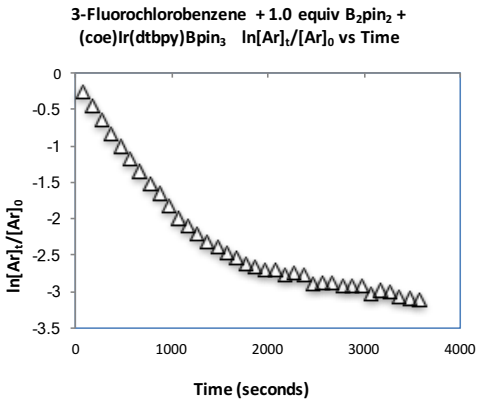

The last kinetics experiment (Experiment 13) repeated the conditions of Experiment 12 with 0.5 equiv B_2pin_2 (0.16 M). The initial rate was rapid, and 11% conversion was seen by the first spectrum about 60 s after the substrate was injected. The first half life was reached at 9 minutes, but then the reaction began to slow rapidly and over 2 h, only 67% conversion was realized, less than 2 half-lives. The first and second order plots are not linear over any part of them.

The differences in rate and the non-linear first order graphs made us wonder if the HBpin borylation went through a different catalytic cycle than B_2pin_2. We carried out competitive borylation experiments on an equimolar mixture of D_6-benzene and H_6-benzene. The results were compared to KIE studies from the Boller-Hartwig paper.[30]

KIE Studies of Ligands and Borane. The linear nature of the second order plots constructed from reactions with excess HBpin suggests that the rate depends not only on the concentration of arene but also on the concentration of another reaction species. If a large primary isotope effect is observed, it will suggest that the CH activation step is still rate limiting but has been slowed or subjected to an equilibrium involving another species somehow. If there is no large isotope effect, it will suggest the possibility, (although not the certainty), that a different catalytic cycle has been activated and C-H activation is no longer the rate limiting step.

The K_H/K_D is calculated from the ratio of protiated to deuterated products. These products can be separated by a slow ramping GC-MS method with a long isothermal plateau. The products can then be quantified by a quantitative integration program based on calibration curves of the pure H_5 and D_5 phenyl-Bpin products. Conversion was assessed by ^{11}B NMR and by use of dodecane as an internal standard for quantitative mass spec analysis.

The initial reactions were followed as written in the Boller-Hartwig paper, but significant amounts of diborylation, both protiated and deuterated resulted.

It was not clear if the investigators missed diborylated byproducts by having too short of a GC-MS method or if it was an oversight where the wrong protocol was included in the manuscript by mistake. The first task of this investigation was to determine if the published KIEs were accurate. To that end, a procedure was developed that avoided diborylation, and a quantitative GC-MS method was developed to accurately measure the amounts of D_5- and H_5-phenyl Bpin produced.

The faulty procedure is most likely an oversight in the manuscript preparation rather than missing diborylated byproducts, as the KIE values from our early attempts with significant diborylation produced K_H/K_D ratios the range of 3.0 – 3.4, lower than the reported range of 5.0 ± 0.4.

In an attempt to optimize the reaction, the ratio of the mix of benzenes was increased from a 6-fold excess (3 equiv per benzene species) to a 10-fold increase (5 equiv per benzene species). Still, intrusive amounts of diborylation (~10%) plagued the reaction. The reaction times were significantly shortened to an hour and still diborylation was not eliminated, though it was limited to about 2-5%. In the reactions with a 10-fold excess of benzenes, the diborylated products did not

contain the mass of 334 by GC-MS, indicating no deuterated diborylated phenyl-Bpin was produced.

To avoid wasting large amounts of deuterated benzene, the amount of B_2pin_2 in the reaction was decreased from 1.5 mmol to 0.1 mmol, a reduction from 200 mg to 25 mg. Under 10 mmol of benzenes per 0.1 mmol B_2pin_2, essentially at 100-fold excess, the reaction did not produce diborylation. These conditions were used for all subsequent analyses in this investigation. Also, to check for variation of KIE ratios, the reactions were sampled at various points in the reaction, from very early conversion to late conversion up to a day after completion of the reaction.

The optimized conditons under which all KIE experiments were run is shown in Scheme 2.14.

Scheme 2.14. The Modified Conditions for the Competitive Borylation Experiment of the KIE Studies

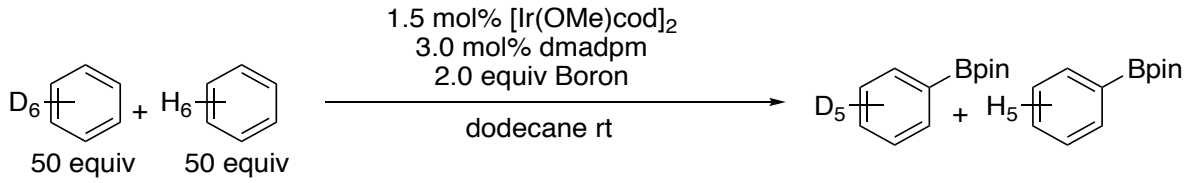

Scheme 2.14. The modified conditions used for competitive borylation in the KIE study of dmadpm. Benzene and d_6-benzene ratios were increased, and the reaction scale was reduced to 0.1 mmol B_2pin_2 to prevent diborylation. (1 equiv B_2pin_2 = 2 equiv Boron).

The reactions were carried out in 20 mL vials equipped with stir bars or put into NMR tubes to monitor conversion by ^{11}B NMR. Rate and conversion of the NMR tube reactions were much lower than the reactions in vials, but KIE ratios remained within a small range of values, and KIE values did not change significantly over the course of the reactions nor did they differ depending in which reaction vessel the reactions were run.

Reaction conversion was assessed by ^{11}B NMR and GC-MS. K_H/K_D ratios were determined by quantitative GC-MS methods using dodecane as internal standard as described in the supporting

information. The average KIE values for the ligands dtbpy and dmadpm for the competative borylation of C_6D_6 / C_6H_6 with HBpin and B_2pin_2 are summarized in Table 2.9.

Table 2.9. Results of Borylation KIE Experiments for dtbpy and dmadpm with B_2pin_2 and HBpin

Entry	ligand	Borane	Avg. KIE
1	dtbpy	B_2pin_2	5.0 ± 0.4
2	dtbpy	HBpin	5.0 ± 0.4
3	dmadpm	B_2pin_2	3.8 ± 0.3
4	dmadpm	HBpin	4.2 ± 0.3

The KIEs obtained for Ir-catalyzed C-H borylation with dmadpm as the ligand and HBpin or B_2pin_2 as the borane are on par with dtbpy KIE values for the same systems, as they are large primary isotope effects. Both dtbpy and dmadpm catalytic cycles appear to have C-H activation as the rate limiting step and that does not change when HBpin is the borane source.

In summary, the order in borane for both dtbpy and dmadpm ligands is zero order when B_2pin_2 is in excess, but deviates significantly when HBpin concentration becomes dominant. When HBpin is present in pseudo first order amounts, the order in borane is roughly zero again. The deviation in the catalytic cycle appears to be related to HBpin and not the ligand. Noteworthy, however, for dtbpy, the product ratios do not differ significantly between borylation with B_2pin_2 vs HBpin, whereas there is a considerable difference in ratios for dmadpm. The reason behind this behavior is not clear, and more kinetic studies are needed to clarify the role of HBpin, although it is clear that the reaction rates are inhibited as the concentration of HBpin becomes significant.

APPENDIX

Kinetics Experiment 1: (coe)Ir(dtbpy)Bpin$_3$ with Excess B_2pin_2 on 3-Trifluoromethyltoluene

Scheme 2.15. Experiment 1

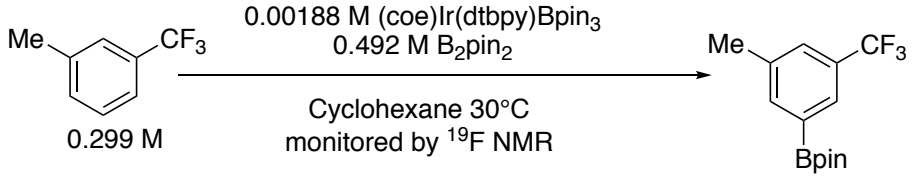

(6 mol% Ir)

Table 2.10. Experiment 1 Table of Reactants

Reagent	vol(mL)	d (g/mL)	FW (g/mol)	mass (g)	mols	rxn vol (mL)	[reagent] M	mol ratio
3-CF_3-tol	0.025	1.148	160.14	0.029	1.79E-04	0.60	2.99E-01	1.000
[(COE)Ir(dtbpy)bpin$_3$]		xxxx	886.62	0.010	1.13E-05	0.60	1.88E-02	0.063
B_2pin_2	xxxx	xxxx	253.94	0.075	2.95E-04	0.60	4.92E-01	1.648
C_6F_6	0.009	1.612	186.06	1.45E-02	7.80E-05	0.60	1.30E-01	0.435
cyclohexane	0.60						70% conversion	

Figure 2.9. Experiment 1 First Order Plot

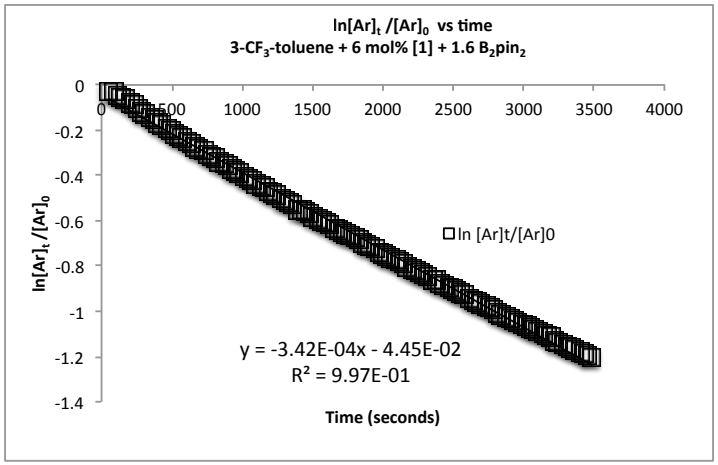

Kinetics Experiment 1 continued: (coe)Ir(dtbpy)$Bpin_3$ with Excess B_2pin_2 on 3-Trifluoromethyltoluene at One Half-Life

Scheme 2.15. Experiment 1 continued

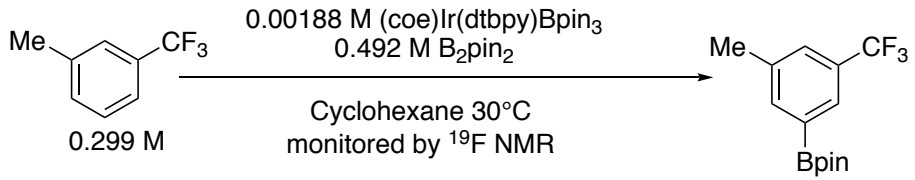

Conversion = 70%

Figure 2.10. Experiment 1 First Order Plot at First Half-Life

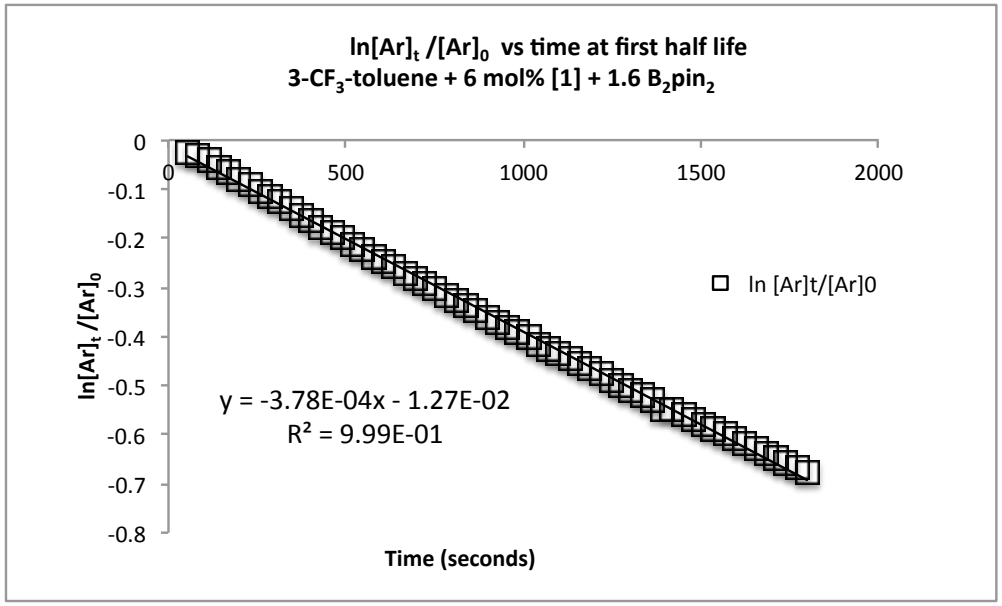

Kinetics Experiment 2: (coe)Ir(dtbpy)(Bpin)$_3$ Pseudo-First Order in B_2pin_2 on 3-Trifluoromethyltoluene

Scheme 2.16. Experiment 2

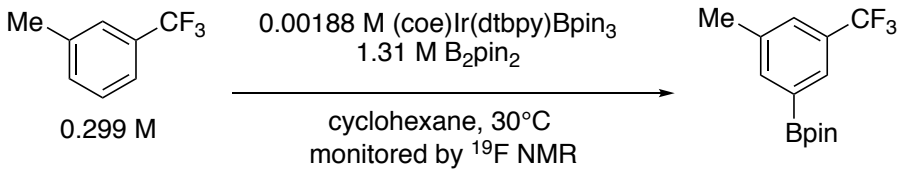

Table 2.11. Experiment 2 Table of Reactants

Reagent	vol(mL)	d (g/mL)	FW (g/mol)	mass (g)	mols	rxn vol (mL)	[reagent] M	mol ratio
3-CF_3-tol	0.025	1.148	160.14	0.029	1.79E-04	0.60	2.99E-01	1.000
[(COE)Ir(dtbpy)bpin$_3$]		xxxx	886.62	0.010	1.13E-05	0.60	1.88E-02	0.063
B_2pin_2	xxxx	xxxx	253.94	0.200	7.88E-04	0.60	1.31E+00	4.395
C_6F_6	0.009	1.612	186.06	1.45E-02	7.80E-05	0.60	1.30E-01	0.435
cyclohexane						0.60	72% conversion	

Figure 2.11. Experiment 2 First Order Plot

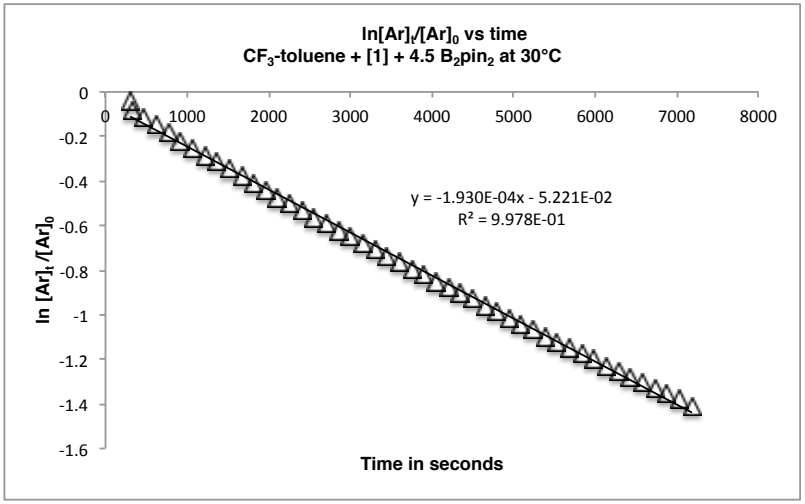

Kinetics Experiment 3: Catalyst Pre-Generated from $[Ir(OMe)cod]_2$ and dtbpy on 3-Trifluoromethyltoluene

Scheme 2.17. Experiment 3

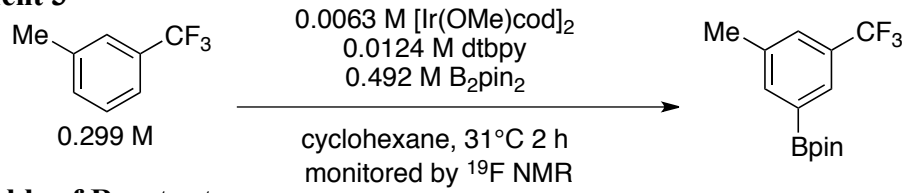

Table 2.12. Experiment 3 Table of Reactants

Reagent	vol(mL)	d (g/mL)	FW (g/mol)	mass (g)	mols	stock soln M	rxn vol (mL)	[reagent] M	mol ratio
3-CF_3-tol	0.0250	1.148	160.14	0.029	1.79E-04	xxxx	0.60	2.99E-01	1.00
$[Ir(OMe)cod]_2$	2.50E-01	xxxx	663	2.50E-03	3.78E-06	1.51E-02	0.60	6.29E-03	0.02
dtbpy	xxxx	xxxx	268.4	0.002	7.45E-06	xxxx	0.60	1.24E-01	0.04
B_2pin_2	xxxx	xxxx	253.94	0.075	2.95E-04	xxxx	0.60	4.92E-01	1.65
C_6F_6	not added							xxxx	xxxx
cyclohexane	0.600							72% conversion	

Figure 2.12. Experiment 3 First Order Plot

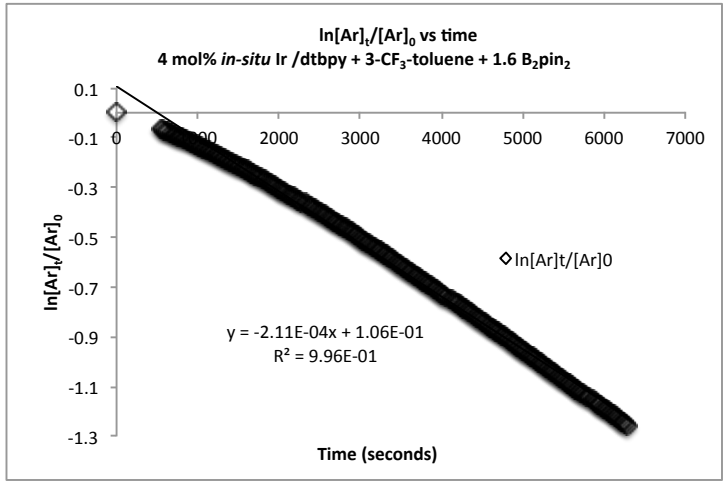

Kinetics Experiment 4: (coe)Ir(dtbpy)(Bpin)$_3$ with Excess B_2pin_2 on 3-Fluorochlorobenzene

Scheme 2.18. Experiment 4

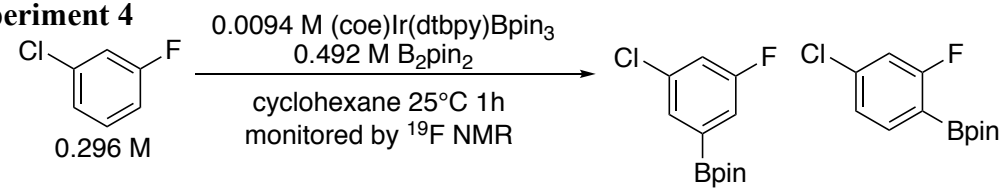

Table 2.13. Experiment 4 Table of Reactants

Reagent	vol(mL)	d (g/mL)	FW (g/mol)	mass (g)	mols	rxn vol (mL)	[reagent] M	ratio
C_6H_4ClF	0.019	1.219	130.55	0.023	1.77E-04	0.60	2.96E-01	1.000
[(COE)Ir(dtbpy)bpin$_3$]		xxxx	886.62	0.005	5.64E-06	0.60	9.40E-03	0.032
B_2pin_2	xxxx	xxxx	253.94	0.075	2.95E-04	0.60	4.92E-01	1.665
C_6F_6	0.009	1.612	186.06	1.45E-02	7.80E-05	0.60	1.30E-01	0.440
cyclohexane						0.60		

conversion = 84%
a:b ratio = 1.5 : 1

Figure 2.13. Experiment 4 First Order Plot

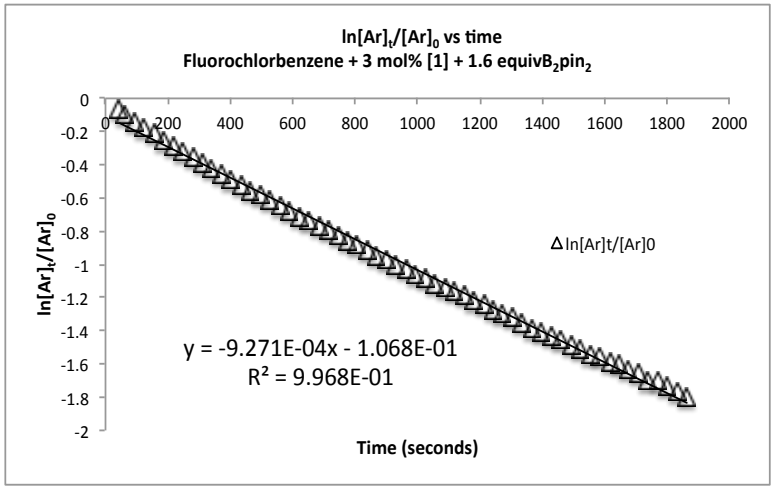

Kinetics Experiment 5: Catalyst Pre-Generated from $[Ir(OMe)cod]_2$ and dtbpy with Excess B_2pin_2 in THF on 3-Fluorochlorobenzene

Scheme 2.19. Experiment 5

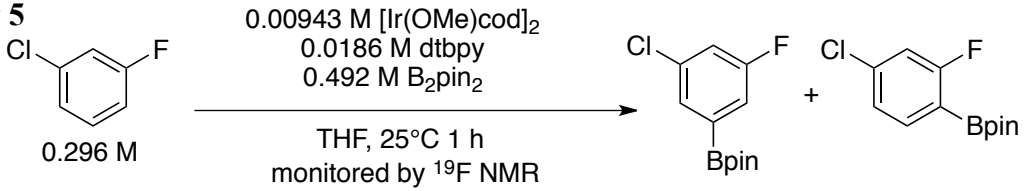

Table 2.14. Experiment 5 Table of Reactants

Reagent	vol(mL)	d (g/mL)	FW (g/mol)	mass (g)	mols	stock soln M	rxn vol (mL)	[reagent] M	mol ratio
cl-f-bz	0.019	1.219	130.55	0.023	1.77E-04	xxxx	0.600	2.96E-01	1.000
$[Ir(OMe)cod]_2$	0.150	xxxx	663	0.004	5.66E-06	3.77E-02	0.600	9.43E-03	0.032
dtbpy	0.050	xxxx	268.4	0.003	1.12E-05	2.24E-01	0.600	1.86E-02	0.063
B_2pin_2	xxxx	xxx	253.94	0.075	2.93E-04	xxxx	0.600	4.92E-01	1.651
C_6F_6	0.013	1.612	186.06	0.021	1.13E-04	xxxx	0.600	1.88E-01	0.635
THF	0.400							conversion = 100% a:b ratio = 1.9:1	

Figure 2.14. Experiment 5 First Order Plot

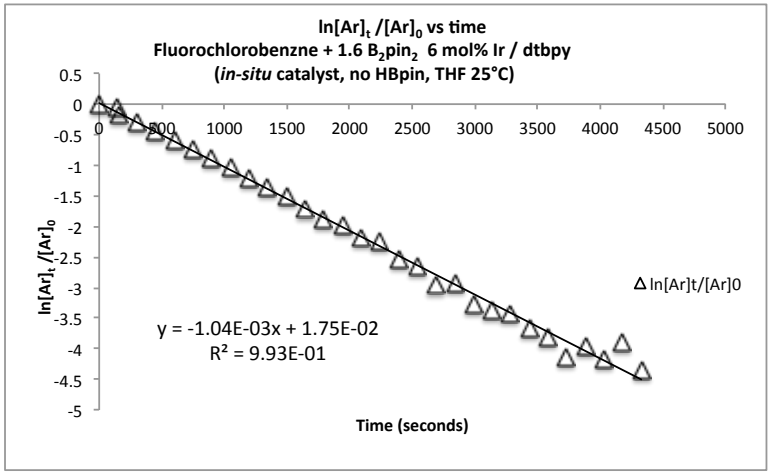

Kinetics Experiement 6: Catalyst Pre-Generated from $[Ir(OMe)cod]_2$ and dmadpm with Excess B_2pin_2 in THF on 3-Fluorochlorobenzene

Scheme 2.20. Experiment 6

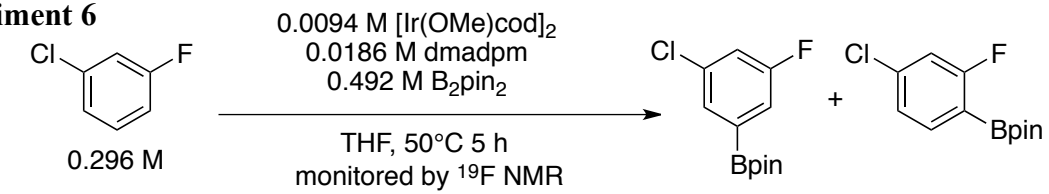

Table 2.15. Experiment 6 Table of Reactants

Reagent	vol(mL)	d (g/mL)	FW (g/mol)	mass (g)	mols	stock soln M	rxn vol (mL)	[reagent] M	mol ratio
C_6H_4ClF	0.019	1.219	130.55	0.023	1.77E-04	xxxx	0.600	2.96E-01	1.000
$[Ir(OMe)cod]_2$	0.150	xxxx	663	0.004	5.66E-06	3.77E-02	0.600	9.43E-03	0.032
dmadpm	0.050	xxxx	256.35	0.003	1.12E-05	2.24E-01	0.600	1.86E-02	0.063
B_2pin_2	xxxx	xxx	253.94	0.075	2.93E-04	xxxx	0.600	4.92E-01	1.651
C_6F_6	0.013	1.612	186.06	0.021	1.13E-04	xxxx	0.600	1.88E-01	0.635
THF	0.400						conversion = 57% a:b ratio = 2.5:1		

Figure 2.15. Experiment 6 First Order Plot

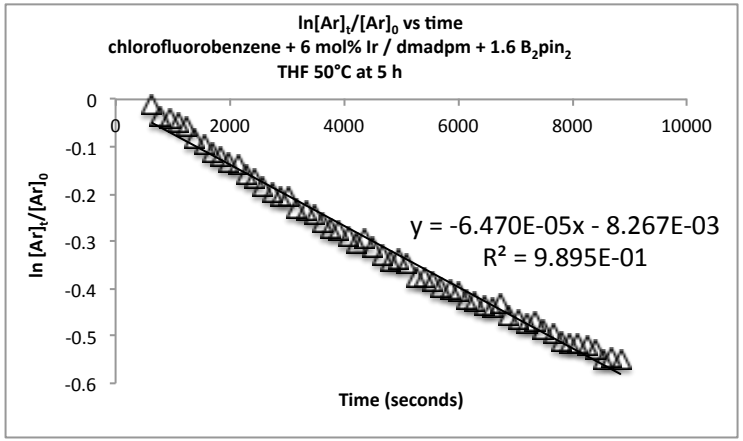

Kinetics experiment 7: (coe)Ir(dtbpy)Bpin$_3$ with 2 equiv HBpin on Trifluoromethyltoluene

Scheme 2.21. Experiment 7

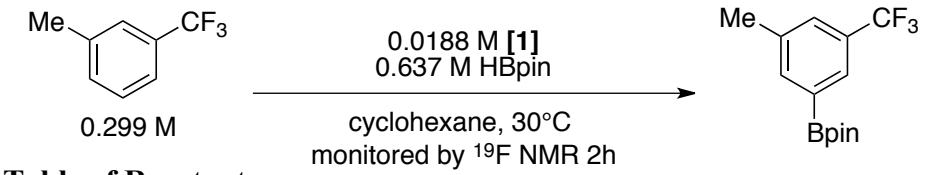

Table 2.16. Experiment 7 Table of Reactants

Reagent	vol(mL)	d (g/mL)	FW (g/mol)	mass (g)	mols	rxn vol (mL)	[reagent] M	equiv
3-CF_3-tol	0.025	1.148	160.14	0.0287	1.79E-04	0.6	0.2987	1.00
[(COE)Ir(dtbpy)bpin$_3$]		xxxx	.886.62	0.01	1.13E-05	0.6	0.0188	0.063
Hbpin	0.055	0.882	126.97	0.049	3.82E-04	0.6	0.6368	2.13
C_6F_6	0.009	1.612	186.06	0.015	7.80E-05	0.6	0.1300	0.44
cyclohexane						0.6	conversion = 30%	

Figure 2.16. Experiment 7 First Order Plot

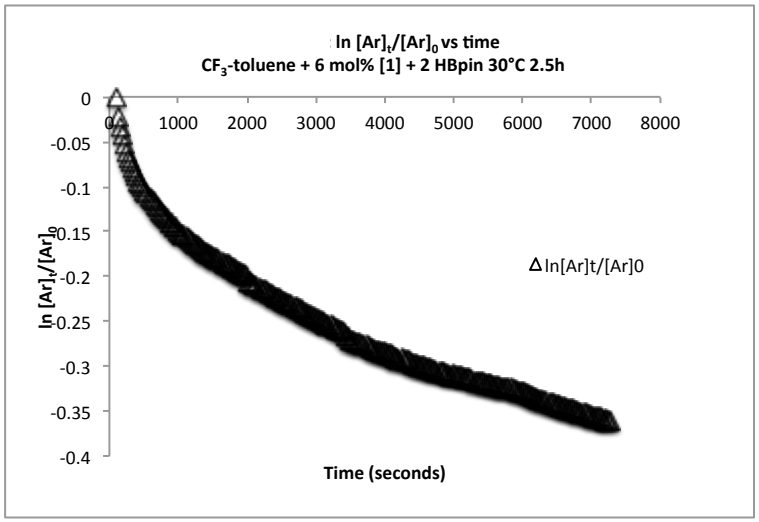

Kinetics Experiment 7 continued: (coe)Ir(dtbpy)Bpin$_3$ with 2 equiv HBpin on 3-Trifluoromethyltoluene

Scheme 2.21. Experiment 7 continued

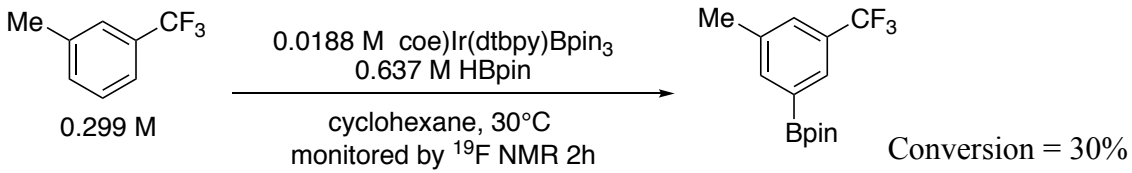

Conversion = 30%

Figure 2.17. Experiment 7 Comparison of First Order and Second Order Plots

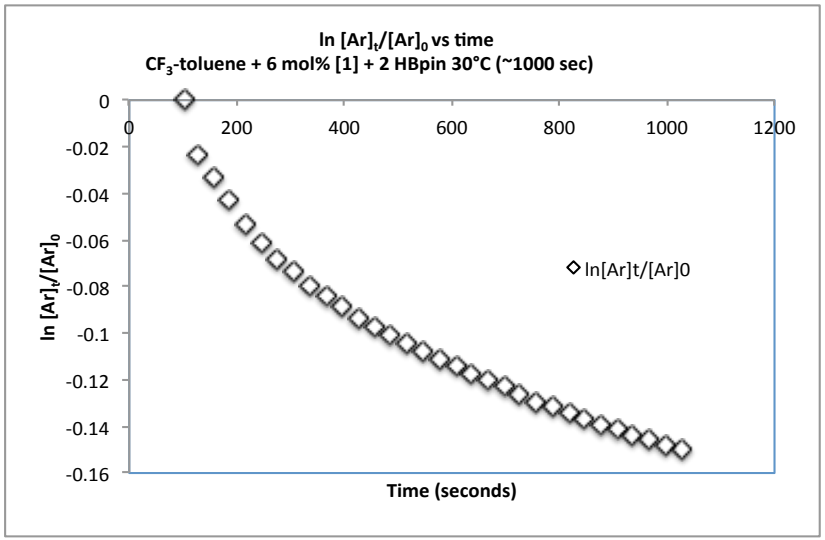

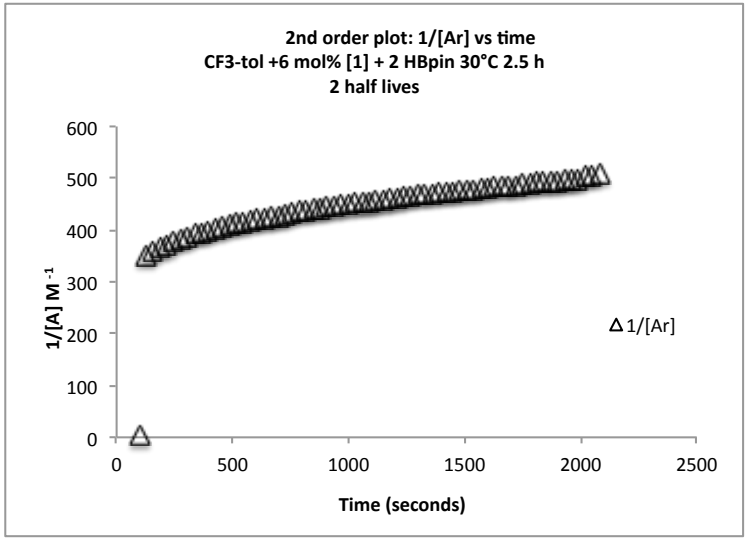

Kinetics Experiment 8: (coe)Ir(dtbpy)Bpin$_3$ with Excess HBpin on 3-Fluorochlorobenzene at 50 °C

Scheme 2.22. Experiment 8

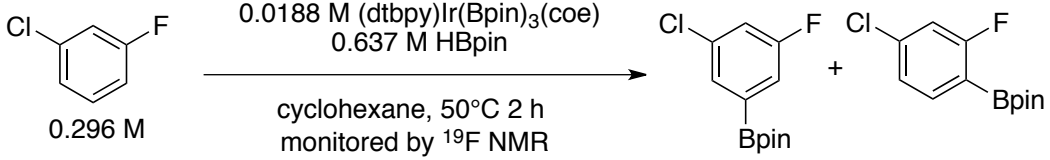

6 mol% Ir

Table 2.17. Experiment 8 Table of Reactants

Reagent	vol(mL)	d (g/mL)	FW (g/mol)	mass (g)	mols	rxn vol (mL)	[reagent] M	mol ratio
C_6H_4ClF	0.019	1.219	130.55	0.023	1.77E-04	0.60	2.96E-01	1.000
[(COE)Ir(dtbpy)bpin$_3$]		xxxx	886.62	0.010	1.13E-05	0.60	1.88E-02	0.064
Hbpin	0.055	0.882	126.97	0.049	3.82E-04	0.60	6.37E-01	2.154
C_6F_6	0.009	1.612	186.06	1.45E-02	7.80E-05	0.60	1.30E-01	0.440
cyclohexane	0.600					0.60	88% conversion a:b ratio = 2 : 1	

Figure 2.18. Experiment 8 First Order Plot

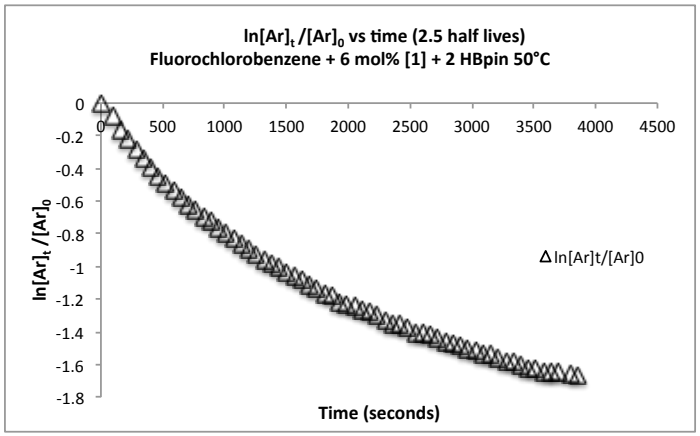

Kinetics Experiment 8 continued: (coe)Ir(dtbpy)$Bpin_3$ with Excess HBpin on 3-Fluorochlorobenzene at 50°C

Scheme 2.22. Experiment 8 continued

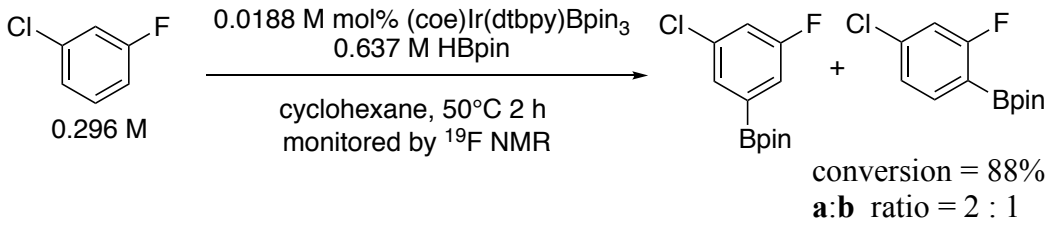

conversion = 88%
a:**b** ratio = 2 : 1

Figure 2.19. Experiment 8 Comparison of First Order and Second Order Plots at 2 Half-Lives

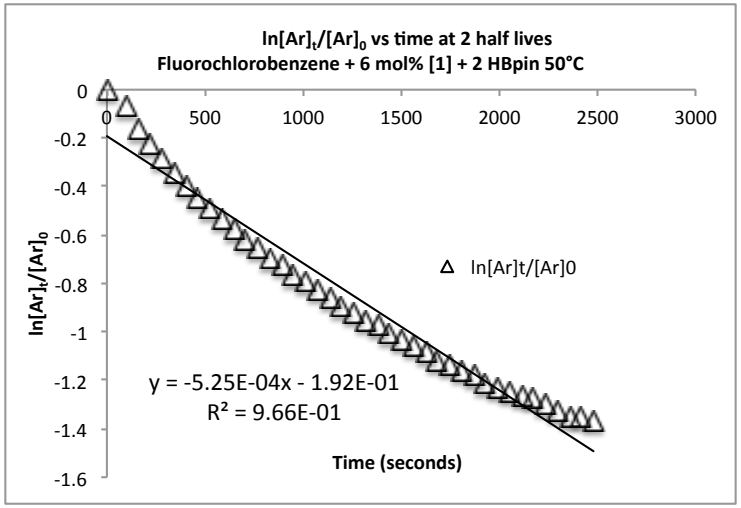

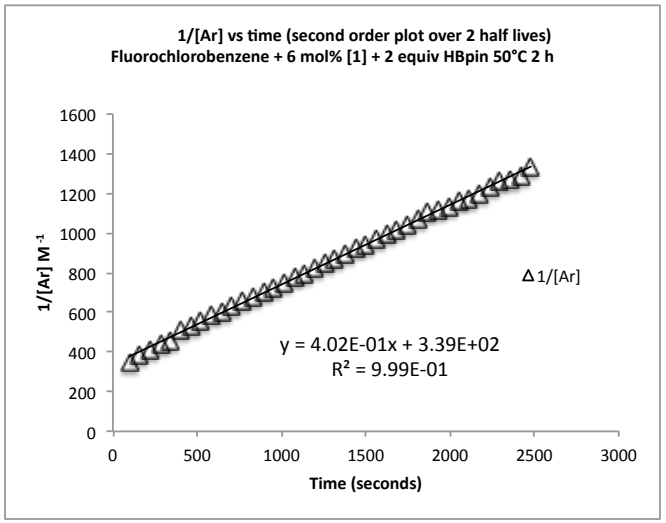

Kinetics Experiment 9: [Ir(OMe)cod]$_2$ and dmadpm with 2 equiv HBpin on 3-Fluorochlorbenzene

Scheme 2.23. Experiment 9

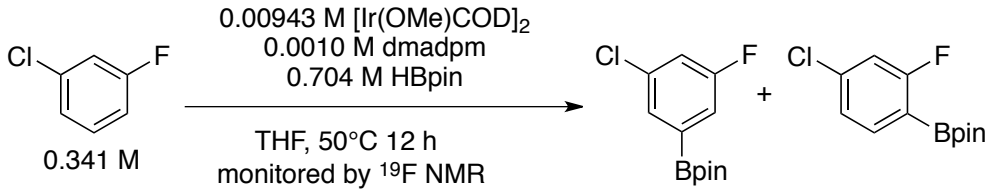

conversion = 79%
a:**b** ratio = 7.5:1

Table 2.18. Experiment 9 Table of Reactants

Reagent	vol(mL)	d (g/mL)	FW (g/mol)	mass (g)	mols	stock soln M	rxn vol (mL)	[reagent] M	ratio
C_6H_4ClF	0.027	1.219	130.55	0.033	2.52E-04	xxxx	0.740	3.41E-01	1.00E+00
[Ir(OMe)cod]$_2$	0.500	xxxx	663	xxxx	3.75E-06	7.50E-03	0.740	9.43E-03	1.49E-02
dmadpm	0.240	xxxx	256.35	xxxx	7.49E-06	3.12E-02	0.740	1.01E-02	2.97E-02
Hbpin	0.075	0.882	126.97	0.066	5.21E-04	xxxx	0.740	7.04E-01	2.05E+00
C_6F_6	0.009	1.612	186.06	0.015	7.80E-05	xxx	0.740	1.05E-01	3.09E-01
THF	0.040						0.074		

Figure 2.20. Experiment 9 First Order Plot

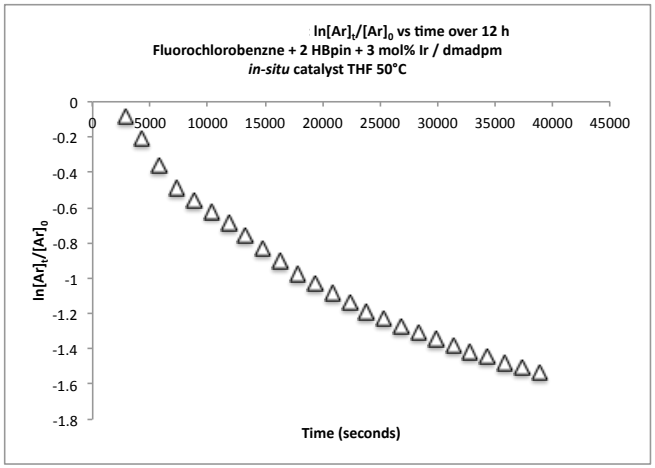

Kinetics Experiment 9 continued: $[Ir(OMe)cod]_2$ and dmadpm with 2 equiv HBpin on 3-Fluorochlorobenzene

Scheme 2.23. Experiment 9 continued

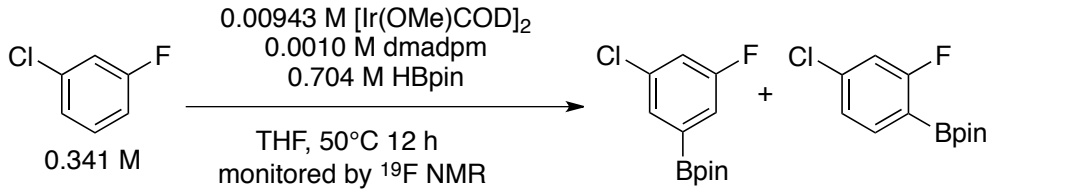

79% conversion
a:b ratio = 7.5 : 1

Figure 2.21. Experiment 9 Second Order Plot

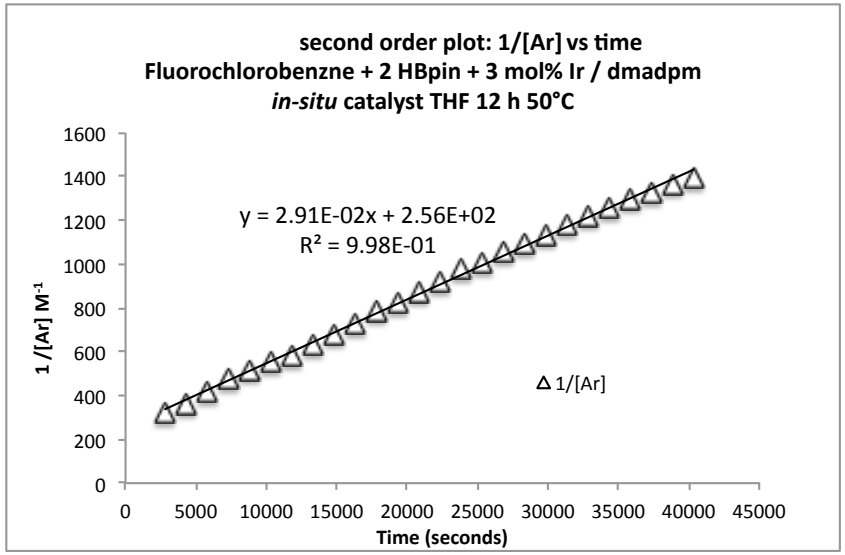

Kinetics Experiment 9 continued: [Ir(OMe)cod]$_2$ and dmadpm with 2 equiv HBpin - Previous Low-Conversion Trials (Earlier trial runs at room temperature or below 40°C had better a:b ratios)

Scheme 2.24. Experiment 9 at Room Temperature

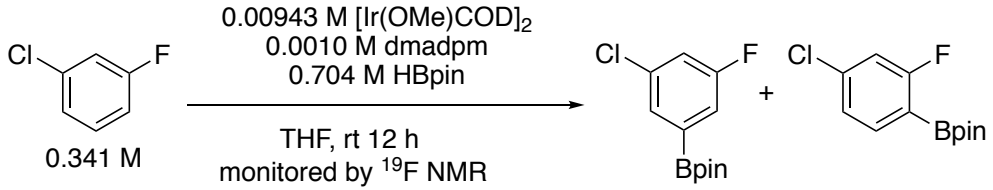

only 30 % conversion
a:b ratio = 11:1

Figure 2.22. Experiment 9 Comparison of First Order and Second Order Plots

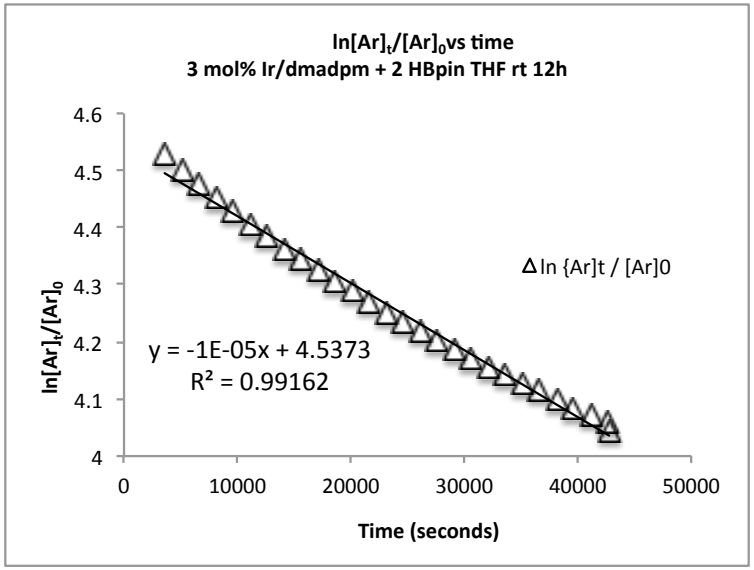

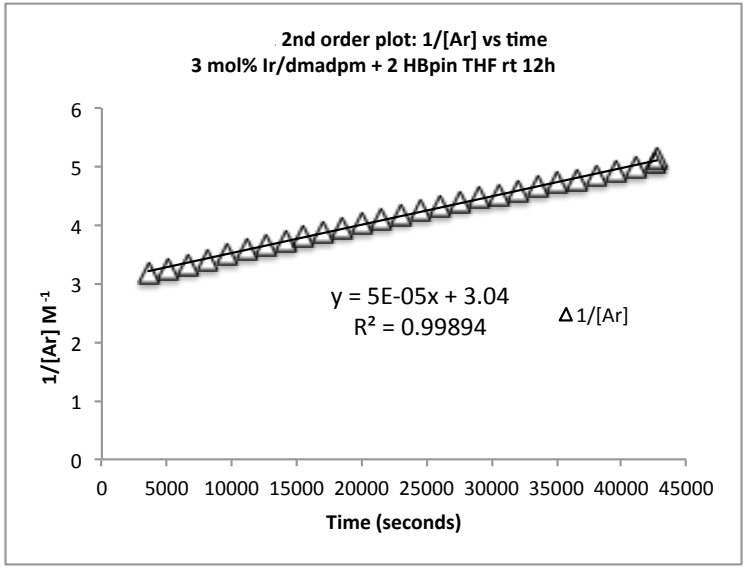

Kinetics Experiment 9 continued: $[Ir(OMe)cod]_2$ and dmadpm with 2 equiv HBpin – Ratio of a : b over time
Earlier trial run at room temperature or below 40°C had better a:b ratios

Scheme 2.24. Experiment 9 at Room Temperature

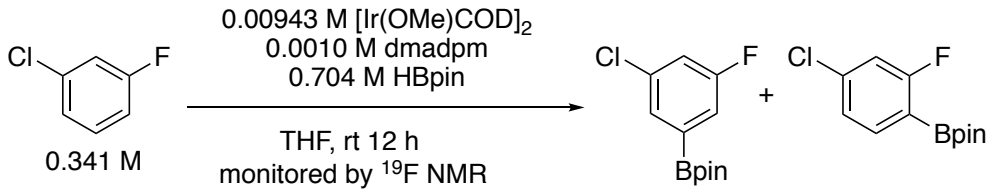

only 30 % conversion
a:b ratio = 11:1

Figure 2.23. Experiment 9 Ratio of a:b over Time

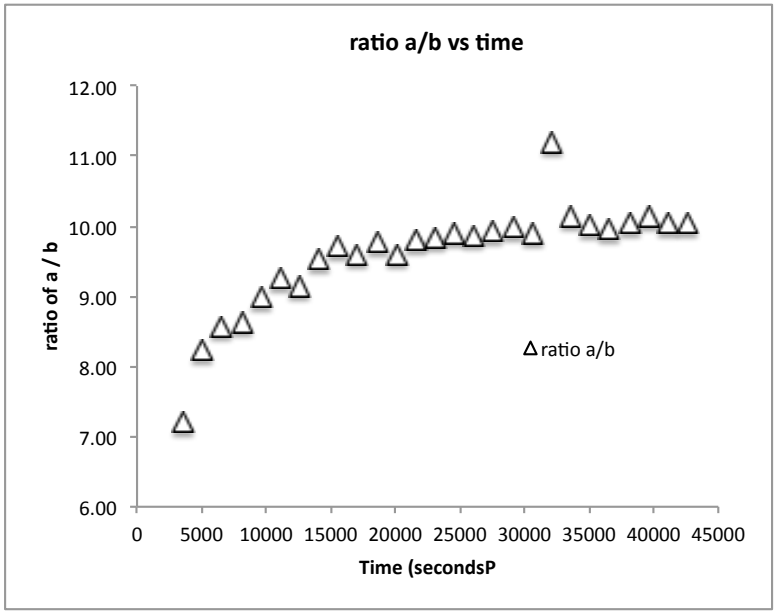

Kinetics Experiment 10: [Ir(OMe)cod]$_2$ and dmadpm Pseudo First-Order in HBpin on 3-Fluorochlorbenzene

Scheme 2.25. Experiment 10

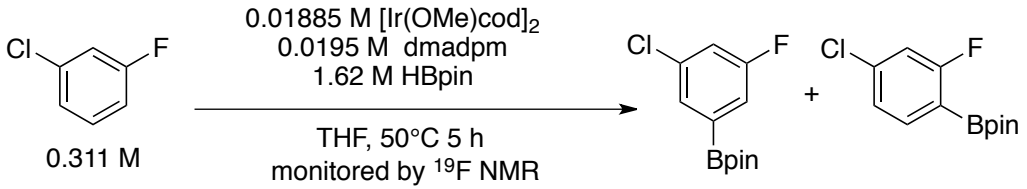

Table 2.19. Experiment 10 Table of Reactants

Reagent	vol(mL)	d (g/mL)	FW (g/mol)	mass (g)	mols	stock soln M	rxn vol (mL)	[reagent] M	mol ratio
C_6H_4ClF	0.020	1.219	130.55	0.024	1.87E-04	xxxx	0.600	3.11E-01	1.000
[Ir(OMe)cod]$_2$	0.150	xxxx	663	0.004	5.66E-06	3.77E-02	0.600	9.43E-03	0.030
dmadpm	0.150	xxxx	268.4	0.003	1.17E-05	7.80E-02	0.600	1.95E-02	0.063
Hbpin	0.140	0.882	126.97	0.123	9.73E-04	xxxx	0.600	1.62E+00	5.208
C_6F_6	0.000	1.612	186.06	0.000	0.00E+00	xxxx	0.600	0.00E+00	0.000
THF	0.200						conversion =97% a:b ratio = 11: 1		

Figure 2.24. Experiment 10 Comparison of First Order and Second Order Plots

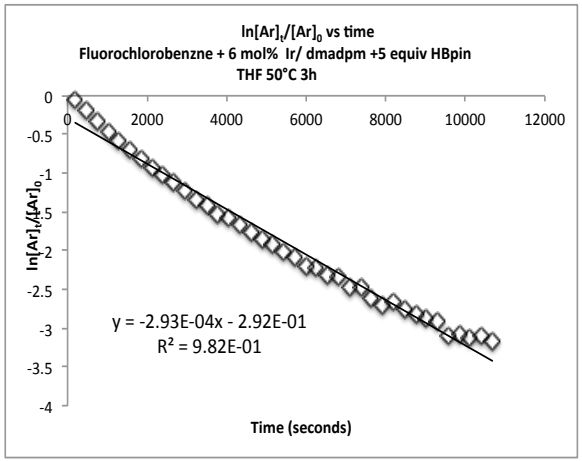

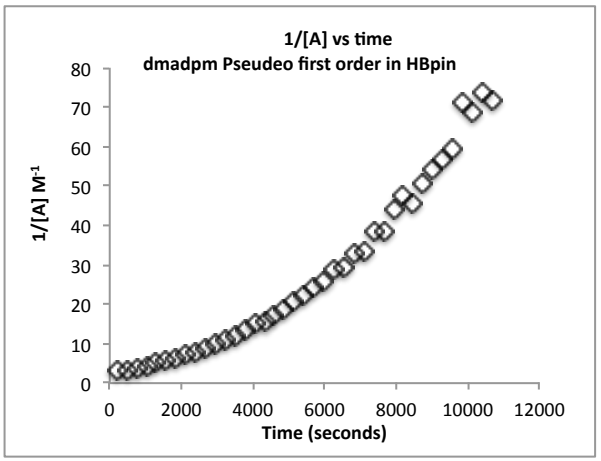

Kinetics Experiment 11: [Ir(OMe)cod]$_2$ and dtbpy Pseudo First-Order in HBpin on 3-Fluorochlorbenzene

Scheme 2.26. Experiment 11

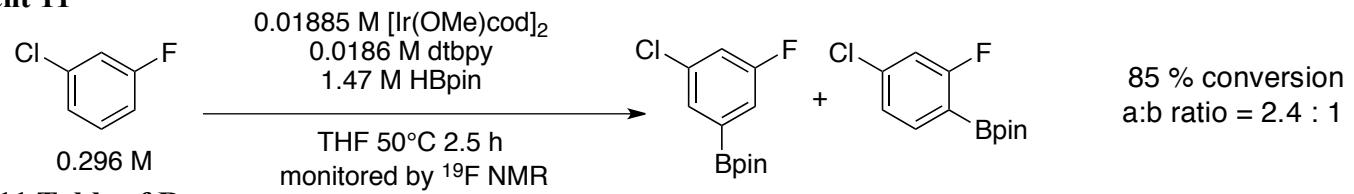

Table 2.20. Experiment 11 Table of Reactants

Reagent	vol(mL)	d (g/mL)	FW (g/mol)	mass (g)	mols	stock soln M	rxn vol (mL)	[reagent] M	mol ratio
cl-f-benzene	0.019	1.219	130.55	0.023	1.77E-04	xxxx	0.60	2.96E-01	1.000
[Ir(OMe)cod]2	0.150	xxxx	663	0.004	5.66E-06	3.77E-02	0.60	9.43E-03	0.032
dtbpy	0.050	xxxx	268.4	0.003	1.12E-05	2.24E-01	0.60	1.86E-02	0.063
Hbpin	0.128	0.882	128	0.113	8.82E-04	xxxx	0.60	1.47E+00	4.972
C6F6	0.015	1.612	186.06	0.024	1.30E-04	xxx	0.60	2.17E-01	0.733
THF	0.040						0.06		

Figure 2.25. Experiment 11 First Order Plot

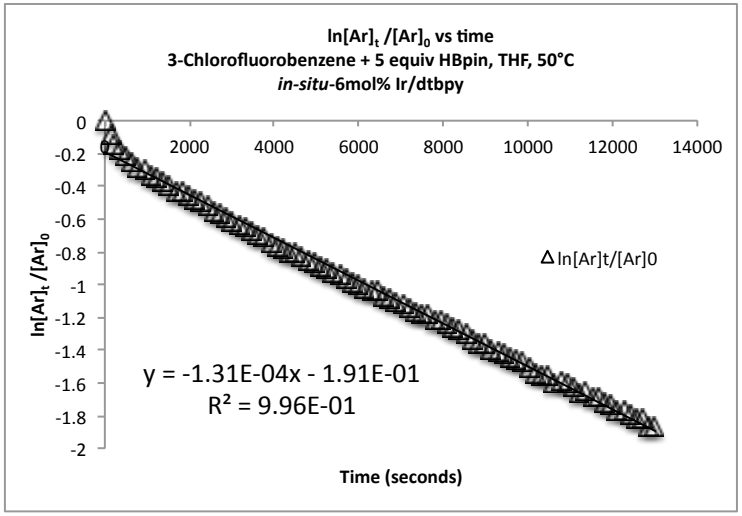

Kinetics Experiment 12: (coe)Ir(dtbpy)Bpin$_3$ and 1.0 equiv B_2pin_2 on 3-Fluorochlorobenzene

Scheme 2.27. Experiment 12

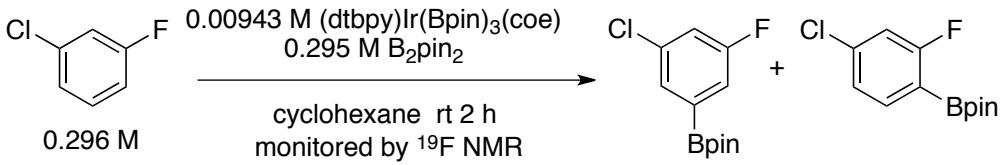

Table 2.21. Experiment 12 Table of Reactants

Reagent	vol(mL)	d (g/mL)	FW (g/mol)	mass (g)	mols	rxn vol (mL)	[reagent] M	mol ratio
C_6H_4ClF	0.019	1.219	130.55	0.023	1.77E-04	0.60	2.96E-01	1.000
[(COE)Ir(dtbpy)bpin$_3$]		xxxx	886.62	0.005	5.64E-06	0.60	9.40E-03	0.032
B_2pin_2	xxxx	xxxx	253.94	0.045	1.77E-04	0.60	2.95E-01	0.999
C_6F_6	0.009	1.612	186.06	1.45E-02	7.80E-05	0.60	1.30E-01	0.440
cyclohexane	0.60				full conversion		a:b ratio = 1.6 :1	

Figure 2.26. Experiment 12 First Order Plot

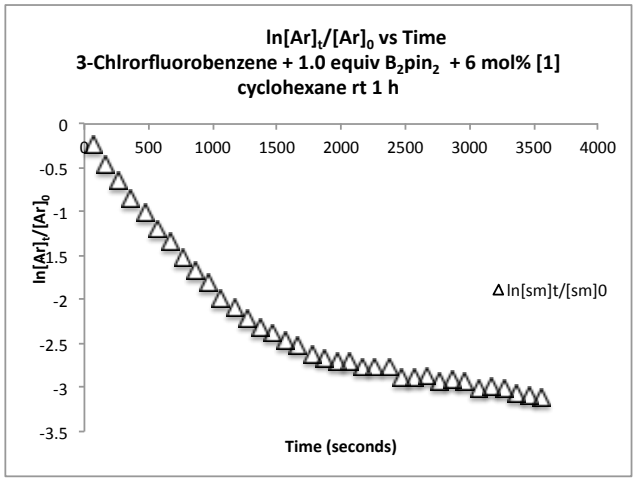

Kinetics Experiment 12 continued: (coe)Ir(dtbpy)Bpin$_3$ and 1.0 equiv B_2pin_2 on 3-Fluorochlorobenzene

Scheme 2.27. Experiment 12 continued

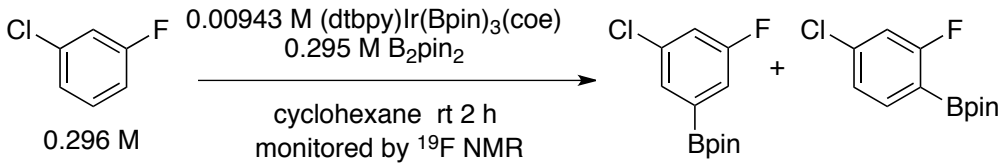

Full Conversion
a:b ratio = 1.6 : 1

Figure 2.27. Experiment 12 First Order Plot at 3 Half-Lives

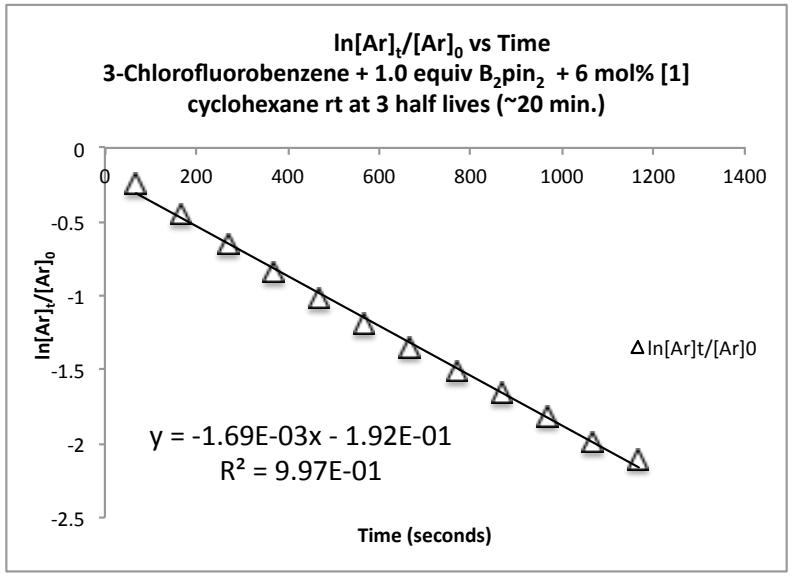

Kinetics Experiment 13: (coe)Ir(dtbpy)Bpin$_3$ and 0.5 equiv B_2pin_2 on 3-Fluorochlorobenzene

Scheme 2.28. Experiment 13

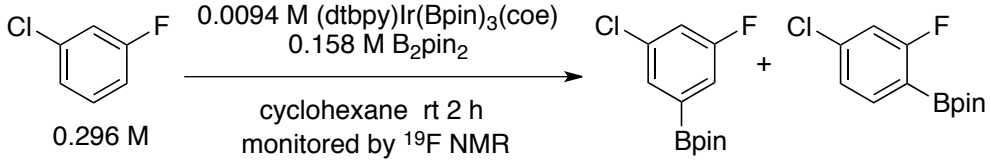

Table 2.22. Experiment 13 Table of Reactants

Reagent	vol(mL)	d (g/mL)	FW (g/mol)	mass (g)	mols	rxn vol (mL)	[reagent] M	mol ratio
Fluorochlorobenzene	0.019	1.219	130.55	0.023	1.77E-04	0.60	2.96E-01	1.000
[(COE)Ir(dtbpy)bpin$_3$]		xxxx	886.62	0.005	5.64E-06	0.60	9.40E-03	0.032
B_2pin_2	xxxx	xxxx	253.94	0.024	9.45E-05	0.60	1.58E-01	0.533
C_6F_6	0.009	1.612	186.06	1.45E-02	7.80E-05	0.60	1.30E-01	0.440
cyclohexane	0.60				conversion = 67% a:b ratio = 1.6:1			

Figure 2.28. Experiment 13 First Order Plot

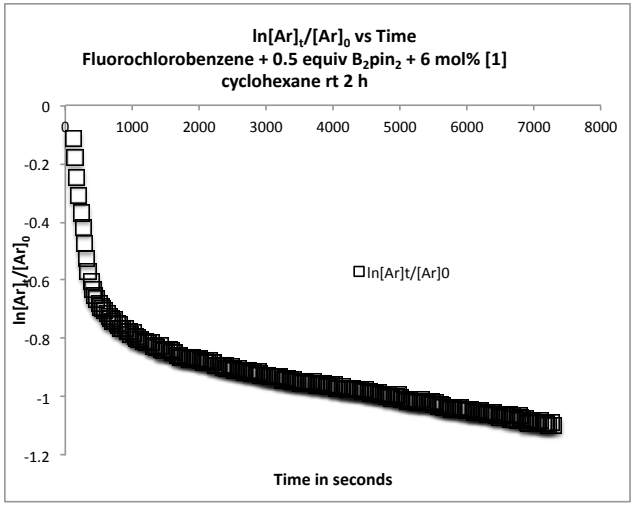

Kinetics Experiment 13 continued: (dtbpy)Ir(Bpin)$_3$(coe) and 0.5 equiv B_2pin_2 on 3-Fluorochlorobenzene

Scheme 2.28. Experiment 13 continued

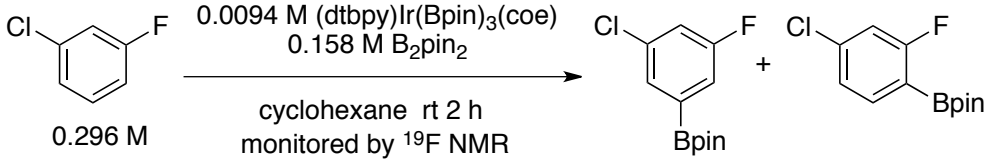

Conversion = 100%
a:b ratio = 1.6 : 1

Figure 2.29. Experiment 13 Comparison of First Order and Second Order Plots

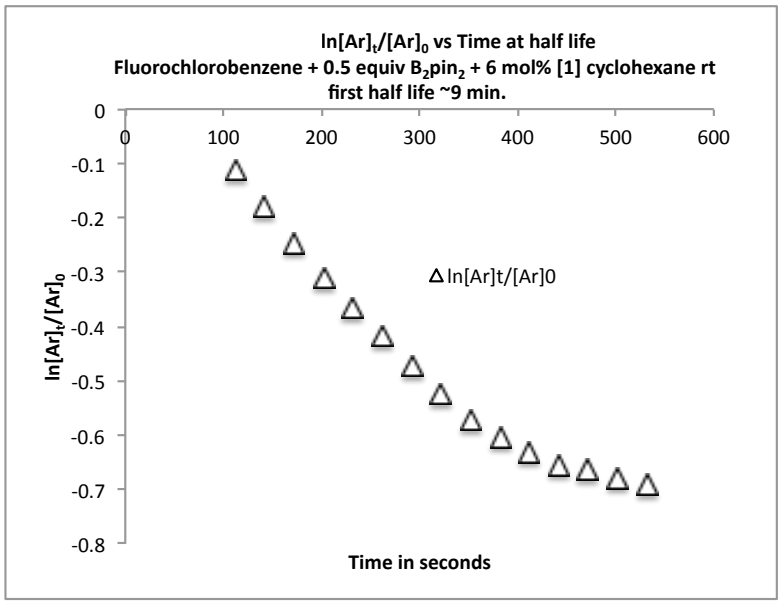

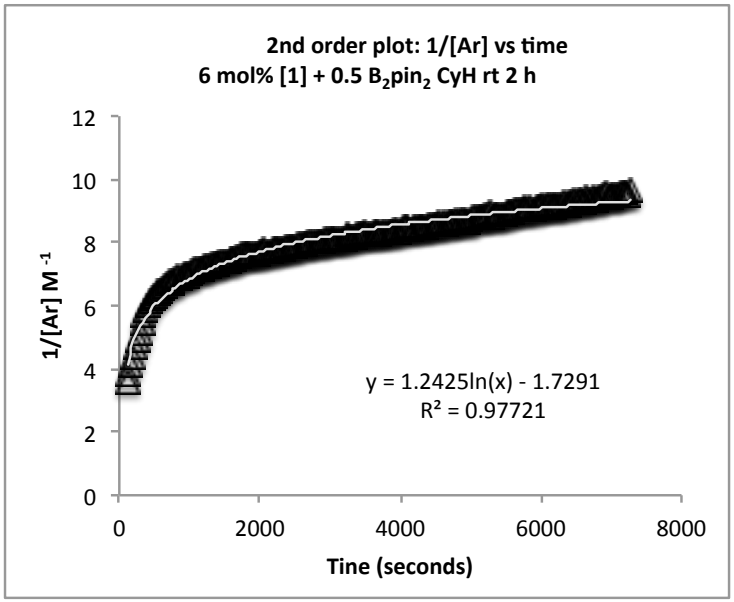

REFERENCES

REFERENCES

1. Mkhalid, I. A. I.; Barnard, J. H.; Marder, T. B.; Murphy, J. M.; Hartwig, J. F., C−H Activation for the Construction of C−B Bonds. *Chemical Reviews* **2010,** *110* (2), 890-931.

2. Ros, A.; Fernandez, R.; Lassaletta, J. M., Functional group directed C-H borylation. *Chem. Soc. Rev.* **2014,** *43*, 3229-3243.

3. Chotana, G. A.; Rak, M. A.; Smith, M. R., III, Sterically Directed Functionalization of Aromatic C-H Bonds: Selective Borylation Ortho to Cyano Groups in Arenes and Heterocycles. *J. Am. Chem. Soc.* **2005,** *127* (30), 10539-10544.

4. Obligacion, J. V.; Semproni, S. P.; Chirik, P. J., Cobalt-Catalyzed C–H Borylation. *Journal of the American Chemical Society* **2014,** *136* (11), 4133-4136.

5. Furukawa, T.; Tobisu, M.; Chatani, N., C–H Functionalization at Sterically Congested Positions by the Platinum-Catalyzed Borylation of Arenes. *Journal of the American Chemical Society* **2015,** *137* (38), 12211-12214.

6. Takaya, J.; Ito, S.; Nomoto, H.; Saito, N.; Kirai, N.; Iwasawa, N., Fluorine-controlled C-H borylation of arenes catalyzed by a PSiN-pincer platinum complex. *Chem. Commun.* **2015**.

7. Obligacion, J. V.; Bezdek, M. J.; Chirik, P. J., C(sp2)–H Borylation of Fluorinated Arenes Using an Air-Stable Cobalt Precatalyst: Electronically Enhanced Site Selectivity Enables Synthetic Opportunities. *Journal of the American Chemical Society* **2017,** *139* (7), 2825-2832.

8. Bisht, R.; Chattopadhyay, B., Formal Ir-Catalyzed Ligand-Enabled Ortho and Meta Borylation of Aromatic Aldehydes via in Situ-Generated Imines. *Journal of the American Chemical Society* **2016,** *138* (1), 84-87.

9. Kuninobu, Y.; Ida, H.; Nishi, M.; Kanai, M., A meta-selective C–H borylation directed by a secondary interaction between ligand and substrate. *Nat Chem* **2015,** *7* (9), 712-717.

10. Davis, H. J.; Mihai, M. T.; Phipps, R. J., Ion Pair-Directed Regiocontrol in Transition-Metal Catalysis: A Meta-Selective C–H Borylation of Aromatic Quaternary Ammonium Salts. *Journal of the American Chemical Society* **2016,** *138* (39), 12759-12762.

11. Cui, C.; Ren, H.; Zhou, Y.-P.; Bai, Y.-P.; Driess, M., Cobalt-Catalyzed Regioselective Borylation of Arenes: N-Heterocyclic Silylene as Electron Donors in Metal-Mediated Activation of C-H Bonds. *Chemistry – A European Journal* **2017**.

12. Schlienger, N.; Lund, B. W.; Pawlas, J.; Badalassi, F.; Bertozzi, F.; Lewinsky, R.; Fejzic, A.; Thygesen, M. B.; Olsson, R.; Tabatabaei, A.; Bradley, S. R.; Gardell, L. R.; Piu, F., Synthesis, structure-activity relationships, and characterization of novel nonsteroidal and selective androgen receptor modulators. *J. Med. Chem.* **2009,** *52* (22), 7186-7191.

13. Belsham, M. G.; et al., *J. Chem. Soc., Perk. Trans. 2* **1974**, 119-125.

14. Diep, B. K.; et al., *J. Chem. Soc.* **1963**, 2784-2787.

15. Joshi, K. C.; Dubey, K.; Dandia, A., Possible psychopharmacological agents. Part XIII: Synthesis and CNS activity of some new fluorine containing 1,2,4-triazine derivatives. *J. Indian Chem. Soc.* **1983,** *60* (Copyright (C) 2013 American Chemical Society (ACS). All Rights Reserved.), 369-372.

16. Soffers, A. E. M. F.; Veeger, C.; Rietjens, I. M. C. M., Influence of the type of halogen substituent on in vivo and in vitro phase II metabolism of 2-fluoro-4-halophenol metabolites formed from 3-halo-fluorobenzenes. *Xenobiotica* **1994,** *24* (8), 759-774.

17. Keenan, M.; Abbott, M. J.; Alexander, P. W.; Armstrong, T.; Best, W. M.; Berven, B.; Botero, A.; Chaplin, J. H.; Charman, S. A.; Chatelain, E.; von Geldern, T. W.; Kerfoot, M.; Khong, A.; Nguyen, T.; McManus, J. D.; Morizzi, J.; Ryan, E.; Scandale, I.; Thompson, R. A.; Wang, S. Z.; White, K. L., Analogues of Fenarimol Are Potent Inhibitors of Trypanosoma cruzi and Are Efficacious in a Murine Model of Chagas Disease. *J. Med. Chem.* **2012,** *55* (9), 4189-4204.

18. Del Grosso, A.; Ayuso Carrillo, J.; Ingleson, M. J., Regioselective electrophilic borylation of haloarenes. *Chemical Communications* **2015,** *51* (14), 2878-2881.

19. Shul'pin, G. B.; Kitaigorodskii, A. N., *J. Organomet. Chem.* **1981,** *212*, 275-282.

20. Wencel-Delord, J.; Nimphius, C.; Wang, H.; Glorius, F., Rhodium(III) and Hexabromobenzene-A Catalyst System for the Cross-Dehydrogenative Coupling of Simple Arenes and Heterocycles with Arenes Bearing Directing Groups. *Angew. Chem., Int. Ed.* **2012,** *51* (Copyright (C) 2013 American Chemical Society (ACS). All Rights Reserved.), 13001-13005.

21. Carey, J. S.; Laffan, D.; Thomson, C.; Williams, M. T., Analysis of the reactions used for the preparation of drug candidate molecules. *Organic & Biomolecular Chemistry* **2006,** *4* (12), 2337-2347.

22. Shen, K.; Fu, Y.; Li, J. N.; Liu, L.; Guo, Q. X., What are the pKa values of C-H bonds in aromatic heterocyclic compounds in DMSO? *Tetrahedron* **2007,** *63* (7), 1568-1576.

23. Webster-Gardiner, M. S.; Fu, R.; Fortman, G. C.; Nielsen, R. J.; Gunnoe, T. B.; Goddard, W. A., III, Arene C-H activation using Rh(i) catalysts supported by bidentate nitrogen chelates. *Catal. Sci. Technol.* **2015,** *5* (1), 96-100.

24. Porter, G. R.; Rydon, H. N.; Schofield, J. A., Transformations of 2-methyl-Δ 2-oxazoline in aqueous solution. *Journal of the Chemical Society (Resumed)* **1960,** (0), 2686-2690.

25. Soovali, L.; Rodima, T.; Kaljurand, I.; Kutt, A.; Koppel, I. A.; Leito, I., Basicity of some P1 phosphazenes in water and in aqueous surfactant solution. *Organic & Biomolecular Chemistry* **2006,** *4* (11), 2100-2105.

26. Menger, F. M.; Singh, T. D.; Bayer, F. L., Nitrogen to nitrogen proton transfer. The significance of large negative entropies of activation. *Journal of the American Chemical Society* **1976,** *98* (16), 5011-5012.

27. Rochester, C. H.; Waters, J. A., Thermodynamic study of the acid dissociation of substituted pyridinium ions in methanol. *Journal of the Chemical Society, Faraday Transactions 1: Physical Chemistry in Condensed Phases* **1982,** *78* (4), 1303-1312.

28. Ishiyama, T.; Takagi, J.; Hartwig, J. F.; Miyaura, N., A stoichiometric aromatic C-H borylation catalyzed by iridium(I)/2,2 '-bipyridine complexes at room temperature. *Angew. Chem. Int. Ed.* **2002,** *41* (16), 3056-3058.

29. Ishiyama, T.; Murata, M.; Miyaura, N., Palladium(O)-Catalyzed Cross-Coupling Reaction of Alkoxydiboron with Haloarenes - a Direct Procedure for Arylboronic Esters. *J. Org. Chem.* **1995,** *60* (23), 7508-7510.

30. Boller, T. M.; Murphy, J. M.; Hapke, M.; Ishiyama, T.; Miyaura, N.; Hartwig, J. F., Mechanism of the Mild Functionalization of Arenes by Diboron Reagents Catalyzed by Iridium Complexes. Intermediacy and Chemistry of Bipyridine-Ligated Iridium Trisboryl

31. Halpern, J., Mechanism and Stereoselectivity of Asymmetric Hydrogenation. *Science* **1982,** *217* (4558), 401-407.

CHAPTER 3

IMPROVEMENTS IN SELECTIVITY AND REACTIVITY

Reactivity vs Selectivity of Ligands. Although the design of the dpm ligand framework was successful in that it resulted in a significant shift towards steric selectivity, the dpm ligands did not exhibit a level of reactivity suitable for general, all-purpose use. Dpm and dmadpm have lower catalytic activity than dtbpy, resulting in longer reaction times and lower conversions. Although borylation studies[1] established a correlation between electron donation, (*i.e.* basicity) with better reactivity, dmadpm does not follow that trend. It is the most basic of the ligand series, yet the least active. Although far more basic than 3,4,7,8-tetramethyl-1,10-phenanthrolene (tmp) (pK_a measured at 6.0),[2] dmadpm is unsuitable for electron rich arenes, which tmp borylates with ease. Unlike tmp, dpm-type ligands do not form stable catalyst complexes at elevated temperatures, thus heating reactions does not improve conversion, and hastens catalyst decomposition.

Figure 3.1. Dpm-Ir Complexes Compared to dtbpy-Ir Complexes

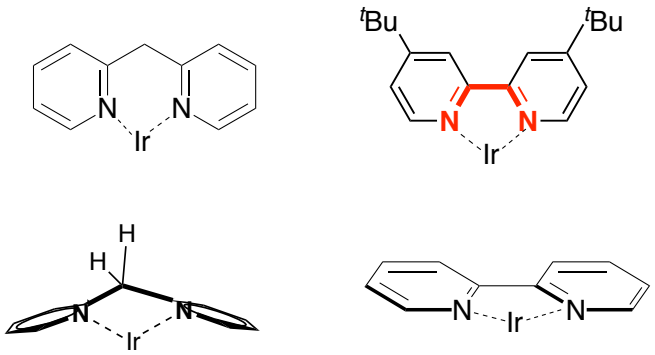

Figure 3.1. The non-planar Ir-dpm complex results in diminished electron donation to the metal compared to the planar complex of Ir-dtbpy.

The challenge of designing a more sterically selective yet sufficiently reactive catalyst remained to be solved. Although the 4,4' substitution of NMe_2 improved steric selectivity of dmadpm over dpm and introduced an interesting kinetic effect with HBpin that may provide a path

to engineer greater selectivity through shifting catalytic cycles, the general reactivity remained low with long reaction times and the same thermal instability that plagued dpm.

The Pyridyl-Imine Ligand Framework. The source of decreased reactivity, as depicted in Figure 3.1, is likely the flexible 6-membered transition structure diminishing the electron donation to the metal, and stability may also be affected by the disruption of aromaticity by the methylene spacer between the pyridyl rings. Active pyridyl ligands such as dtbpy and tmp are rigid and planar, thus locking electron donation in place. The objective to construct a pyridyl based ligand with bulk near the metal, yet having a planar coordination with the metal, turned our attention away from dpm and shifted focus towards pyridyl-imine ligands.

Figure 3.2. Ligands with Diimine and Pyridyl Imine Backbones in the Literature

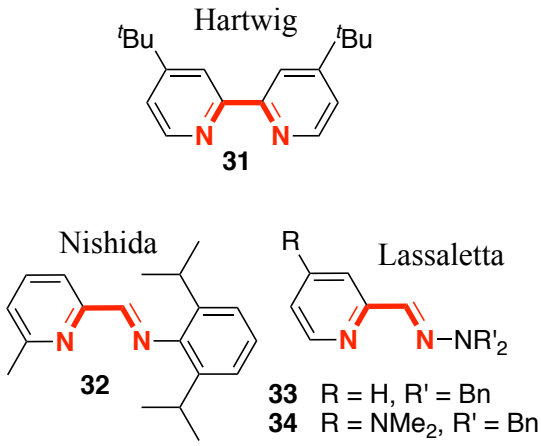

Figure 3.2. Ligands with imine backbones that have been reported in the literature.

The first reported use of pyridyl imine ligands for C-H borylation was made by Nishida in 2004[3] from the recognition of the bpy framework as a diimine system. Nishida substituted the imine arm of his ligands with bulky R groups. Substrates were symmetric arenes and pyridines and indoles unsubstituted at the 2-position, so selectivity was not addressed. Later Lassaletta and others developed similar pyridyl imine ligands for use as hemilabile directing groups in borylation,[4-5] resulting in another method for ortho borylation. Some diimine ligands that have been reported in the literature are seen in Figure 3.2 on the previous page..

As part of the project to design a meta selective ligand, Smith and Maleczka began a collaboration to investigate several ligand frameworks, notably imine, 2,2'-bisoxazoline (box) and bipyridyl (bpy) ligands. This collaboration was instructive in the recognition and classification of a useful imine ligand that was fortuitously discovered during the dpm project.

Synthesis of a Reactive Pyridyl-Imine Ligand. When dmadpm became a ligand design target, the chosen synthetic route required reduction of the corresponding dipyridyl ketone, **28**, in order to install the methylene spacer. The ketone was converted to the hydrazone, **29**, and reduced according to a Wolf-Kischner protocol, as seen in Scheme 3.1. During the conversion to dmadpm, **30**, it was noted that the intermediate hydrazone was unusually stable and not easily reduced. In preliminary ligand tests, early batches of dmadpm contained traces of the intermediate hydrazone **29**.

Scheme 3.1. Synthesis of the Dipyridyl Methane Ligand

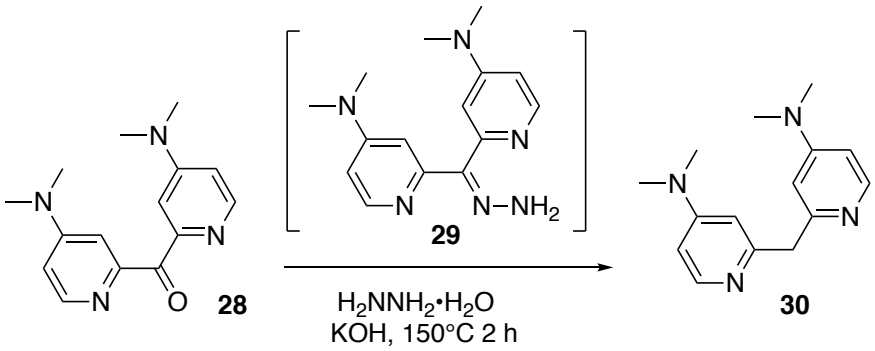

Scheme 3.1. Pyridyl imine ligands were synthesized in the Smith and Maleczka labs for ligand selectivity studies**. 29** features a 4-dimethylaminopyridine (4-DMAP) substituted at the imine carbon.

Although dmadpm is easily purified by sublimation, as a precaution, **29** was synthesized and isolated to test whether its trace presence influenced catalytic activity. The catalytic activity of dmadpm remained the same in the absence of **29**. When **29** was tested as a ligand, however, the initial catalytic reactivity was far greater than dpm-type ligands, and on par with dtbpy. Furthermore, the steric selectivity was superior to both dtbpy and the dpm ligands for several

substrates. The similarity of **29** to ligands possessing imine backbones reported by Nishida and Lassaletta was noticed. It is interesting to consider, that although **29** is similar to **33** and **34**, Lassaletta's ligands are only used for chelate-directed borylation, in stark contrast to the steric selectivity observed from ligand **29**.

Scheme 3.2. Lassaletta's Substituted Hydrazone Ligands Exhibit Directed Borylation

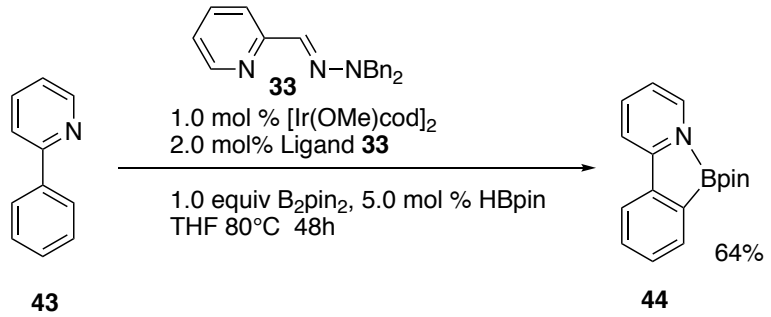

Scheme 3.2. Lassaletta's directed borylation with ligand **33** results in borylation directed to the 2-phenyl position.

In order to test whether **29** would react according to a chelate directed mechanism, 2-phenyl pyridine (**43**) was subjected to borylation under Lassaletta's conditions. As seen in Scheme 3.2, the Ir-catalyzed borylation of **43** with **33** as the ligand produces only borylation at the 2-poition of the phenyl group as directed by the N atom of the pyridine ring.

Scheme 3.3. DMAP-Imine Substituted Ligand does not Exhibit Directed Borylation

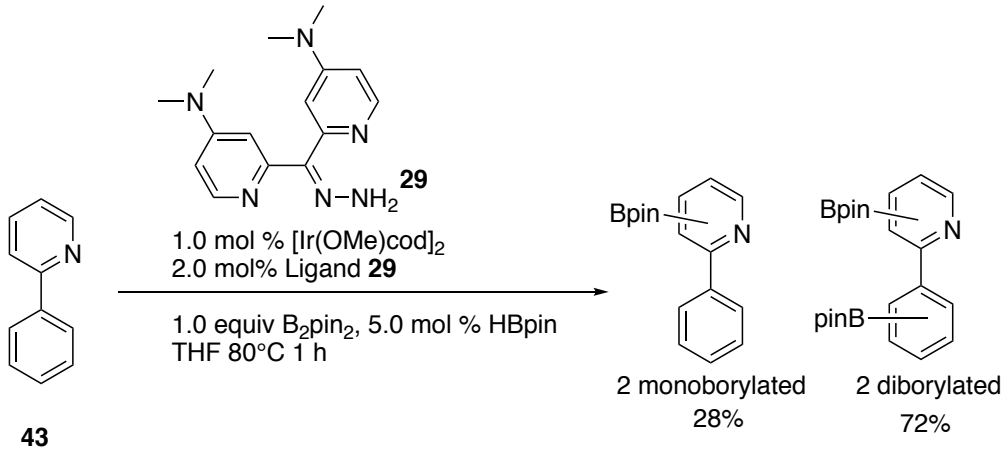

Scheme 3.3. Ligand **29** does not exhibit directed borylation under Lassaletta's conditions.

When **29** was used as the ligand with B_2pin_2 under Lassaletta's conditions, over-borylation of the pyridine and phenyl rings was observed, as shown in Scheme 3.3, resulting in two mono-borylated isomers and two diborylated isomers. When 2-phenylpyridine was borylated at room temperature with **29** as ligand and 2 equiv HBpin, according to the standard conditions previously established for dpm-type ligands, over-borylation of substrate also occurred within 12 h, resulting in another mixture of mono and diborylated products. When HBpin was limited to 1 equiv, the result was a 1:3 mixture of **45:46.**

To compare the effect of N-benzyl substitution on the function of the ligand, an unsubstituted hydrazone analog (**35**) of the dibenzyl ligand **34** was synthesized.

Scheme 3.4. Substituted vs. Unsubstituted Hydrazone Ligands

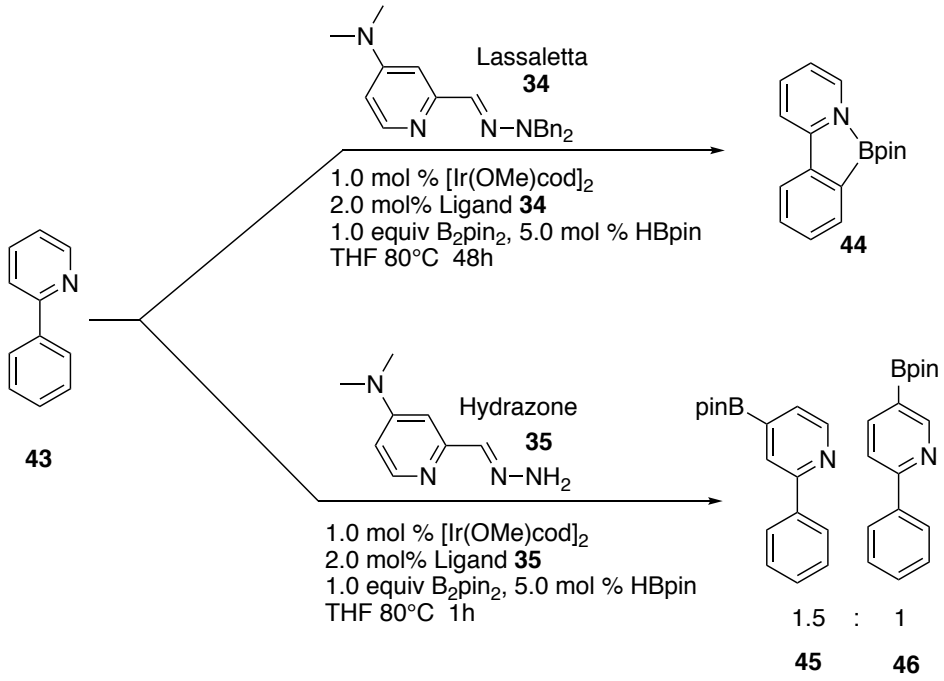

Scheme 3.4. N,N-dibenzyl substitution of the hydrazone in ligand **33** leads to directed borylation. The bare NH_2 of ligand **35** does not facilitate directed borylation.

Testing Ligands for Reactivity. Borylations of **43** were carried out under Lassaletta's conditions with ligands **34** and **35** to observe if directed borylation resulted with the bare hydrazone, as seen in Scheme 3.4. Dibenzyl ligand **34** gave only directed borylation product **44**.

The free hydrazone **35** gave only monoborylated **45** and **46**, and no directed product **44** was observed in the reaction mixture.

Table 3.1. Reactivity Test by Borylation of 1,3-Dicyanobenzene

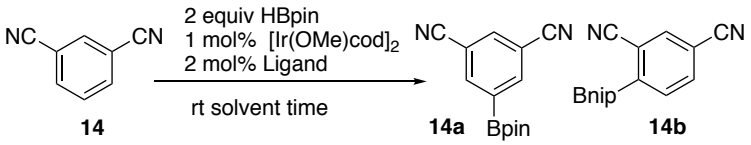

Ligand	entry	Ligand #	conversion		14a : 14b
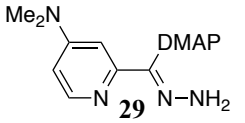	1.	**29**	THF rt 1h	>99%	16:1
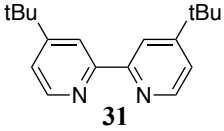	2.	**31**	THF rt 1h	>99%	4:1
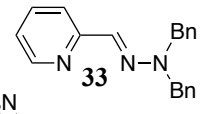	3.	**33**	THF rt 24h	38%	3:1
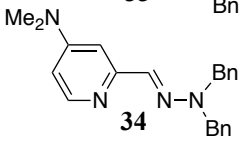	4.	**34**	THF rt 24h	68%	5:1
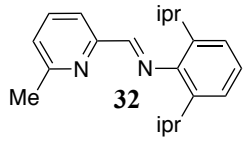	5.	**32**	Cy rt 24h	40%	1.6:1

Table 3.1. The hydrazone ligand **29** is compared to known imine ligands from the literature in the borylation of 1,3-dicyanobenzene.

In order to gauge the reactivity of **29**, a borylation test of 1,3-dicyanobenzene (**14**) was devised, a substrate that had proven difficult and slow for dpm-type ligands Also included in the test were ligands **31** (dtbpy), Nishida's bulky ligand **32** and Lassaletta's ligands, **33** and **34.**

The results are summarized in Table 3.1. Of the ligands featured in Table 3.1, Entries 1 (**29)**, and 2 (**31**) demonstrate significant reactivity, completing the borylation reaction in just 1 hour. Entries 3 (**33**) and 5 (**35)** exhibit low reactivity.

Moderate reactivity of 68% is shown by **34** in Entry 4. Ligands **31**, **33**, and **34**, dtbpy and Lassaletta's ligands, all have similar selectivity producing a range of about 3-5 :1 **14a**:**14b** borylation. Nishida's **32** has the least selectivity at 1.6:1. The two most reactive ligands, **29** and **31**, show equal reactivity, however **29** produces four times more meta borylation with a ratio of 16:1.

Table 3.2. Comparison of NNH_2 Substitution on Reactivity

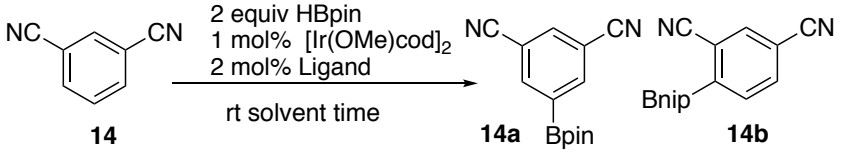

	entry	Ligand	conversion		14a : 14b
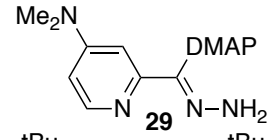	1.	**29**	THF rt 1h	>99%	16:1
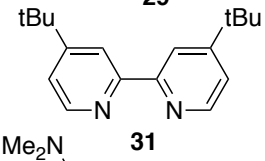	2.	**31**	THF rt 1h	>99%	4:1
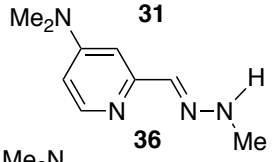	3.	**36**	THF rt 15h	63%	4:1
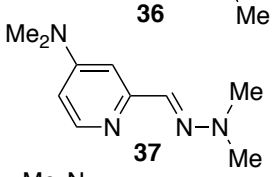	4.	**37**	THF rt 24h	13%	not integrable
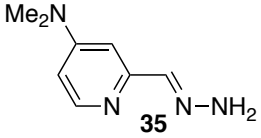	5.	**35**	THF rt 1h	96%	4.6:1

Table 3.2. Reactivity and selectivity decrease with N-substitution of the hydrazone.

With the recognition that only ligand **29** contained a free NH_2 functional group, the effect of substitution of the N atom was tested next. The N-methyl hydrazone substituted ligand, **36**, and N,N-dimethyl hydrazone substituted ligand, **37**, and free, hydrazone with unsubstituted NH_2, **35**,

were synthesized. Borylation reactions of dicyanobenzene with **35**, **36**, and **37** were performed and compared to **29** and **31**, as seen in Table 3.2.

Entry 5 of Table 3.2 indicates that free hydrazone **35**, is almost as active as **29** and **31,** with 93% conversion in 1 hour. The meta selectivity of **35** is better than **31**, but at 16:1, **29** remains the most meta-selective ligand tested. The N-methyl **36**, shows moderate reactivity with 63% conversion in 15 hours, but the N,N-dimethyl **34**, shows poor reactivity. The GC-FID for Entry 4 is messy, and does not integrate well. These results indicate that the high reactivity exhibited by **29** and **35** is diminished when the N atom is substituted with non-H groups. Counterintuitively, the free NH_2 of **29** and **35** gives higher steric selectivity than the more hindered ligands **32**, **33**, **34**, **36**, and **37**.

Although the **36** and **37** show diminished reactivity, the bulky N,N- dibenzyl **34**, exhibits moderately better reactivity than N-methyl **36**. This likely due to the benzyl groups being farther away and more flexible, and ultimately creating less steric pressure close to the metal, in contrast to methyl groups.

Hydrazone Interaction with HBpin. In order to probe the high reactivity imparted by the free NH_2 of hydrazone ligands, an NMR experiment was devised to monitor the interaction between **29** and HBpin. **29** was dissolved in $CDCl_3$ and 2 equiv HBpin were added. The mixture was stirred then transferred to an NMR tube, and ^{11}B and ^{1}H NMR spectra were taken immediately. The mixture was monitored at 3, 24 and 48 hours.

The first NMR showed HBpin as a large doublet at 27 ppmin the ^{11}B spectrum. There was a small sharp peak at 2.9 ppm. The ^{1}H NMR integrated properly with the NH peak integrating to 2 protons. The NMR at 3 h showed the sharp peak at 2.9 ppm growing slowly in the ^{11}B spectrum, and the NH peak in the ^{1}H spectrum was integrating as less than 2 protons. At 24 h the NH peak

integrated to 1 proton and the aromatic peaks had shifted. The ^{11}B spectrum showed the doublet of HBpin and a large sharp peak at 2.9 ppm, and the two peaks integrated 1:1. The sharp peak is consistent with boron in a tetrahedral environment. After 48 h, the NMR did not change. The NH peak remained at the same integration.

Figure 3.3. DMAP-Imine Substituted Ligand forms a Hydrazone-HBpin Complex

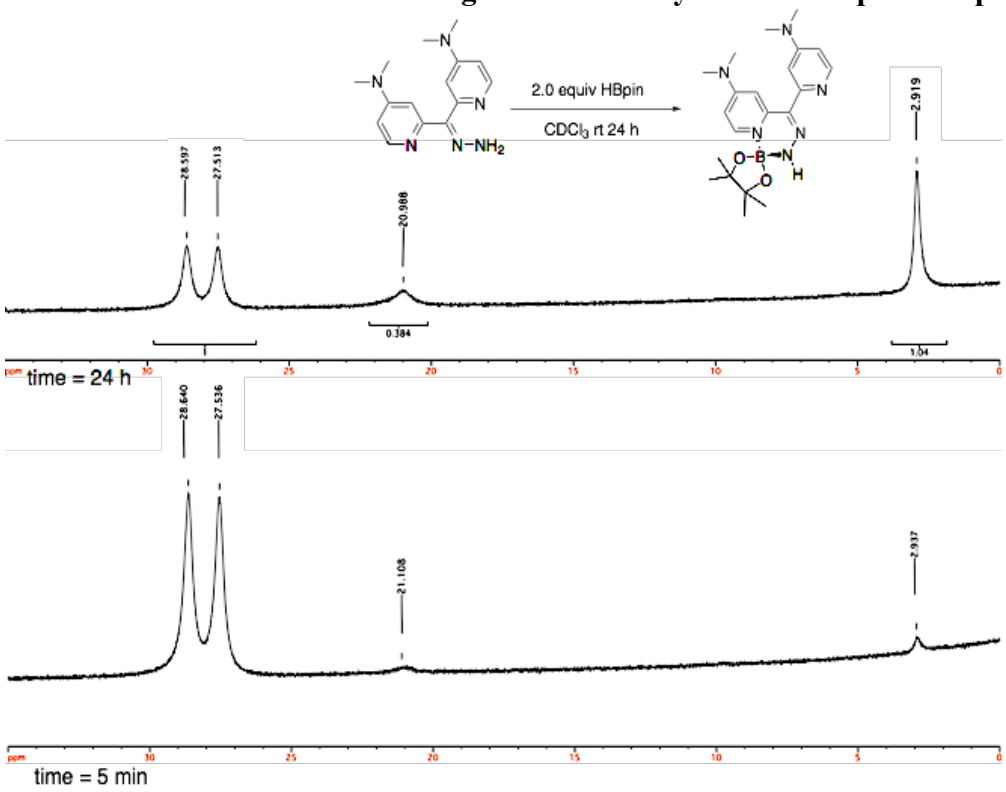

Figure 3.3. Ligand **29** reacts with 1 equivalent of HBpin to form a complex. The sharp peak at 2.9 in the ^{11}B NMR indicates a boron in a tetrahedral environment.

This NMR study was compared to a study that was previously conducted on the methyl imine substituted ligand **38** (shown in Table 3.2). To investigate if the unsubstituted pyridine ring of the ligand was likely undergo borylation during a reaction, ligand **38** was subjected to borylation conditions with 5 mol % $[Ir(OMe)cod]_2$ and 2 equiv HBpin in THF and monitored by ^{11}B NMR. After 1 hour, the ^{11}B spectrum showed the large doublet of HBpin at 27 ppm and a large, broad peak at 24.2 ppm, signifying N-B bond formation. No sharp peak was present at 2.9 ppm. After

24 h, a broad peak at 30 ppm was apparent, evidence that borylation on the pyridine ring had occurred.

Figure 3.4. Methyl-Imine Substituted Ligand does not form a Hydrazone-HBpin Complex

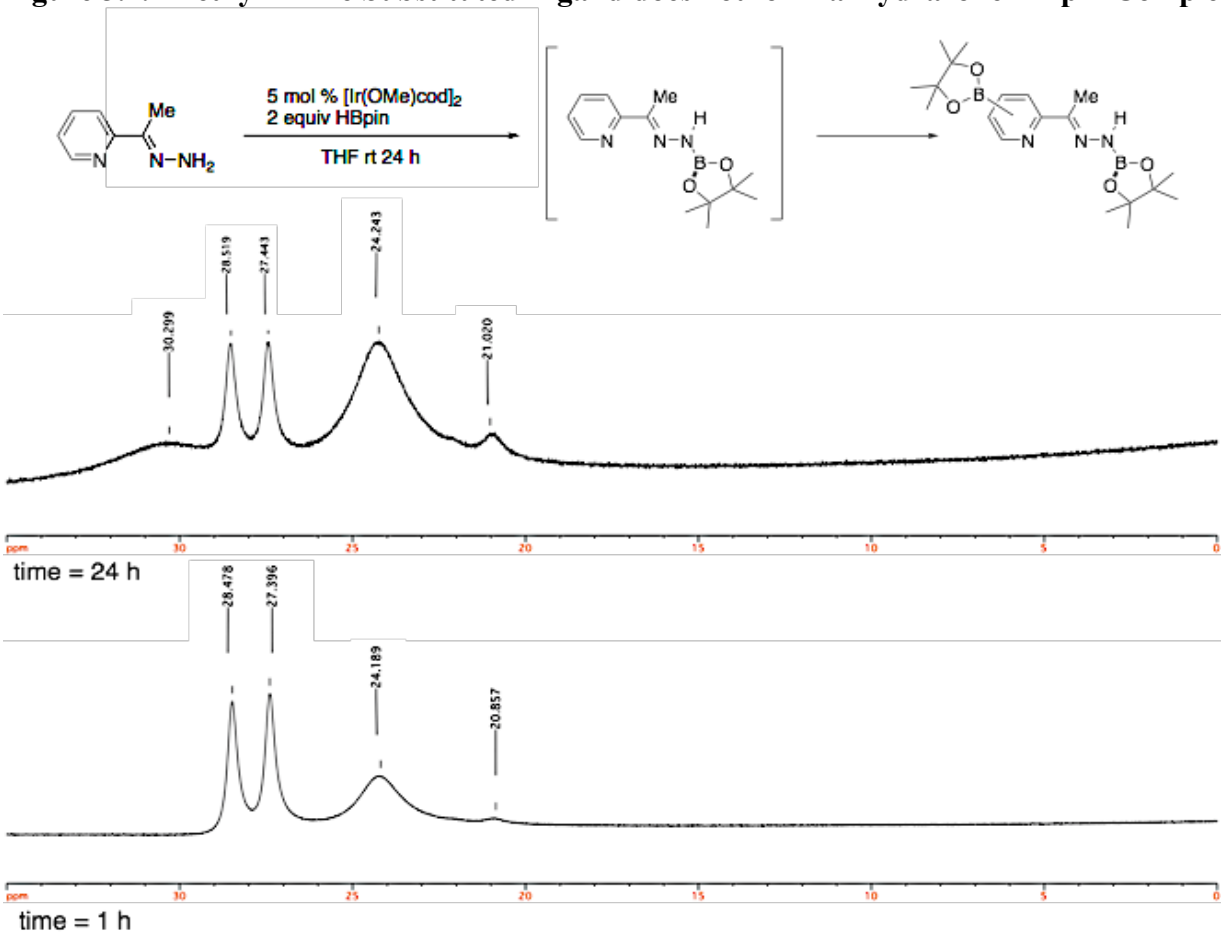

Figure 3.4. The methyl imine substituted hydrazone ligand **38** does not form a tetrahedral boron complex with HBpin. Ligand **35** undergoes N-B borylation instead, and no tetrahedral boron environments are evident in the ^{11}B NMR.

These experiments suggest that **29** does not readily undergo N-borylation like typical hydrazone ligands, such as ligand **38**. Further NMR studies showed that **29** forms a complex rapidly in the presence of $[Ir(OMe)cod]_2$, but one proton remains visible in the ^{1}H NMR. The spectrum did not change 24 or 48 h later, thus indicating that only 1 equivalent of HBpin formed an adduct in the presence of the Ir catalyst, and 1 H remains on the N atom of the hydrazone. Attempts to crystallize the **29**-HBpin complex are ongoing.

Although the crystal structure of the HBpin-**29** complex has not yet been obtained, the crystal structure of the isolated compound itself has been solved, and it offers clues to its reactivity.

Crystal Structure of DMAP Hydrazone Ligand. As seen in Figure 3.5, the hydrazone exhibits a strong hydrogen bond to keep its pyridyl face and imine arm locked in the same plane. It is likely that **29** binds to Iridium through the pyridyl imine backbone rather than through the dpm backbone.

Figure 3.5. Crystal Structure of DMAP-Imine Hydrazone Ligand

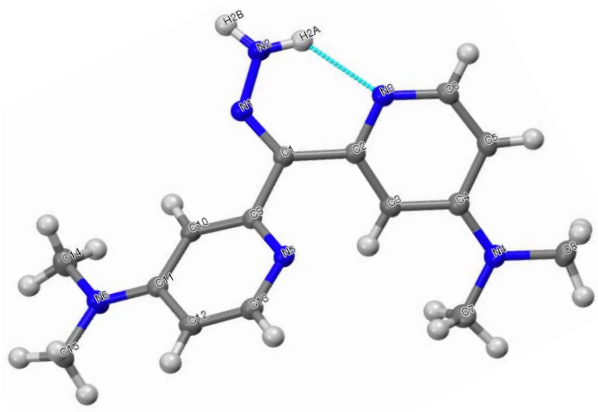

Figure 3.5. The crystal structure of **29** shows the pyridyl face and imine arm locked in the same plane by an H bonding interaction.

Effect of Ligand Structure on Borylation Selectivity of 1,3-Difluorobenzene. Considering the different mode of binding observed for **29,** the borylation of 1,3-difluorobenzene (**47**) was undertaken with various ligands to investigate the selectivity differences between the ligands. Previous work by Chotana and Rak[6] enables us to compare dtbpy (**31**) to Nishida's ligand (**32**) under forcing conditions.

They found that while dtbpy exhibits low selectivity resulting in four isomers, ligands bulkier than dtbpy achieve better selectivity and avoid 2-borylation between the F substituents.[6] We sought to expand this work in order to identify properties more subtle than large steric blocking groups on the ligands that shift selectivity. The ratios of products are listed in Table 3.3. The long

reaction times and high temperature of these conditions are unnecessary for this reactive substrate, so the conditions were modified in the current round of borylation studies, which were performed in collaboration with Behnaz Ghaffari and Jonathan Dannatt.

Table 3.3. Prior Ligand Studies of the Borylation of 1,3-Difluorobenzene

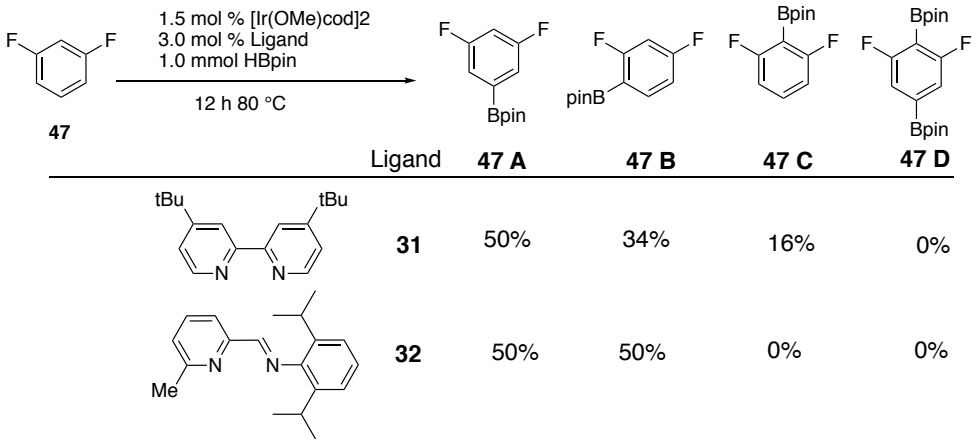

Ligand	47 A	47 B	47 C	47 D
31	50%	34%	16%	0%
32	50%	50%	0%	0%

Table 3.3. Previous work by Chotana and Rak show selectivity for ligands **31** and **32**. The bulky ligand **32** does not borylate the 2-position between the F atoms.

The pyridyl NMe_2 substituted and DMAP imine substituted ligands were prepared in the Maleczka group and included in the Smith group's ongoing imine ligand studies. The results relevant to the function of hydrazone activity and selectivity are presented on the next page in Table 3.4.

The first test was designed to probe the effect of substitution on the imine backbone, and the methyl imine substituted ligand **38**, was compared to the bare pyridyl imine hydrazone **39**.

Substitution of the methyl group at the imine carbon increases conversion and selectivity. The methyl imine substituted ligand **38** has greater selectivity for product **47C**, the 2-borylated isomer.

Within the second set of reactions, the effect of DMAP substitution at the imine carbon of **29** is examined and compared to imine-Me substitution of **38** and lack of imine substitution of **35** and **40**. The DMAP imine substituent improves reactivity and conversion, as the reaction is

complete within 2 h. The ratio of meta-substituted product **47A** obtained from **29** is dramatically increased, and is 18.2 times greater than the meta borylated product of unsubstituted **35** and **40** and Me substituted **38**.

Table 3.4. Selectivity Test of the Borylation of 1,3-Difluorobenzene

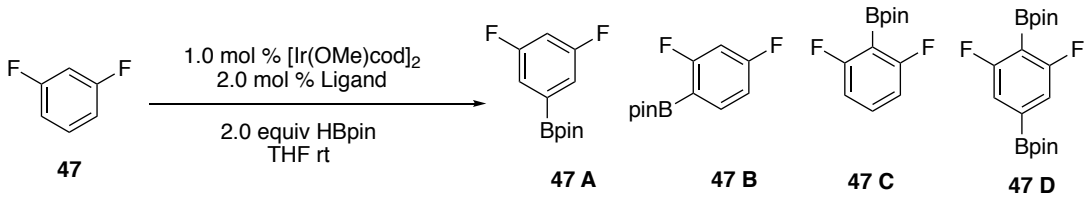

set	Ligand structures	Ligand	Time	Conversion	Ratio A : B : C : D
1)	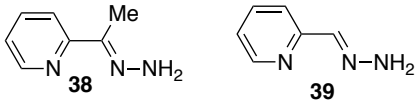	**38**	4 h	63 %	1.0 **:** 0.6 **:** **5.0** **:** 0.2
		39	4 h	36 %	1.0 **:** 0.8 **:** **2.4** **:** 0.4
2)	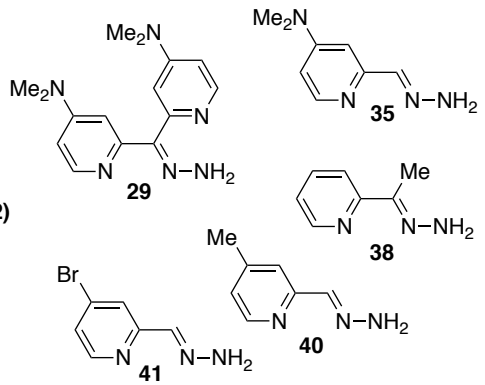	**29**	2 h	>99 %	**18.2** **:** 1.7 **:** 1.0 **:** 2.3
		35	2 h	91 %	1.0 **:** 0.4 **:** **2.8** **:** 1.3
		38	2 h	63 %	1.0 **:** 0.6 **:** **5.0** **:** 0.2
		40	2 h	62 %	1.0 **:** 0.5 **:** **2.2** **:** 0.75
		41	2 h	50 %	1.0 **:** 1.2 **:** **4.9** **:** 0.95
3)	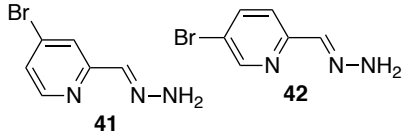	**41**	3 h	67 %	1.0 **:** 2.0 **:** **8.0** **:** 0.8
		42	3 h	65 %	1.0 **:** 1.8 **:** **13.0:** 0.6

Table 3.4. First set of experiments (1) tests the effect of an imine substituent on the ligand framework. Second set of experiments (2) compares pyridyl substituents vs effect of imine substituent, as well as the effect of electron donating or electron withdrawing substituents. Also considered, effect of borylation of pyridyl ring of **38** compared to pyridyl substituted ligands. Last set of experiments (3) tests the effect of 3 or 4 substitution of pyridyl ring.

The comparison of **35**, **40** and **38** within the second set of reactions is a good means to compare the of the effect of imine substitution to the effect of 4-substitution on the pyridine ring.

35 and **40** have no imine substituent, but have different electron donating group substituents on the pyridine ring. Ligand **38** has no pyridine ring substituent but has a Me imine substituent.

Also considered, it was shown that **38** itself is borylated in the course of an Ir-catalyzed reaction. Now the effect of borylated ligand **38** is compared to ligands where borylation is blocked by pyridyl substituents. The effect of pyridyl borylation is seen in the ratios of **47C**:(**47A**+**47B**+**47D**) for **35**, **40** and **38**. The results indicate that, while all three ligands favor 2-borylation over any other single product, **38** produced the highest ratio of **47C**:(**47A**+**47B**+**47D**) at 2.7:1. The other two ligands, **35** and **40** produce 1:1 ratios of **47C**:(**47A**+**47B**+**47D**). This lends support to the observation that methyl substitution of the imine carbon increases electronic selectivity, and also the borylation of pyridyl rings may shift selectivity to electronic products.

When comparing pyridine substituents of **35** (NMe_2) and **40** (Me), the selectivity is about the same, but the conversion is improved for NMe_2 substituted **35**, achieving 91% compared to 63%. The unsubstituted **38** and electron withdrawing group Br-substituted **41** fare the worst with 63% and 50% conversion respectively. **41** has slightly improved selectivity for 2-borylated product **47C**, with ratio **47C**:(**47A**+**47B**+**47D**) observed at 1.6:1. Br substitution of the pyridine ring appears have roughly the same effect as methyl substitution of the imine carbon. It is difficult to assign the increased product **47C** to borylation of the ring or the methyl imine substituent.

It was previously shown that ligand **38** undergoes borylation of the pyridine ring during borylation reactions, and Bpin is considered an electronegative group. Comparing **38** to **41** is an indirect probe of the effect of an electron withdrawing group, like Bpin, on the reactivity and selectivity of the ligand. The selectivities of **38** and **41** are approximately the same, hence borylation of the pyridyl rings likely influences selectivity. Br-substituted ligands **41** and **42** are

slated to be converted to Bpin substituted ligands by Miyaura coupling in order to test the real borylated ligands. These efforts are ongoing.

When borylation experiments were carried out on pyridyl ligands as substrates, two borylated isomers result, 4-borylation and 3-borylation on the pyridine ring, as seen with the borylation of 2-phenyl pyridine. In order to determine if the mixture of borylated ligands might shift selectivity of product **47C** for ligand **38** over the **47C**-selectivity of ligand **41**, a third set of experiments was designed. Using a Br substituent as an approximation of a Bpin substituent, 3-Br substituted **42** was synthesized. The reaction time was increased from 2h to 3h, and the ratio for **47C**:(**47A**+**47B**+**47D**) by **41** increased from 1.6:1 to 2:1, possibly from conversion of product **47D** into product **47C**. **42** achieved less conversion than **41,** but product **47C** selectivity is greater at a ratio of 3.8:1 for **47C**:(**47A**+**47B**+**47D**). When the Br-substituted ligands are converted to Bpin substituted ligands, they will be re-tested to see if selectivity for **47C** increases.

Effect of Solvent Polarity and Borane Source on Selectivity. Since free NH_2 can interact with solvents through H bonding, a last set of experiments was designed to observe the effects on

Table 3.5. Test of Solvent Polarity and Borane Source on Selectivity

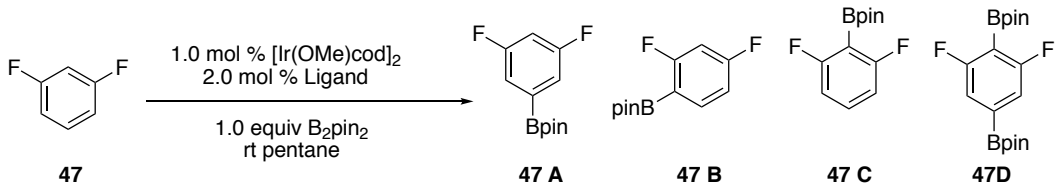

Ligand structures	Ligand	Time	Conversion	Ratio A : B : C : D
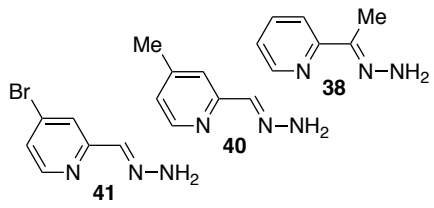	**38**	3 h	76%	1.0 **:** 1.3 **: 18.0 :** 01.0
	40	3 h	70%	1.0 **:** 1.0 **: 6.5 :** 0.8
	41	3 h	65 %	1.0 **:** 1.8 **: 13.0:** 0.6

Table 3.5. The effect of decreasing solvent polarity and the borane source are tested.

reactivity and selectivity of decreasing the solvent polarity from THF to pentane. Since many pyridyl imines also form complexes with HBpin, B_2pin_2 was used as the boron source, to minimize influence on the hydrazone from the environment. The results are presented in Table 3.5.

The decrease in polarity and use of B_2pin_2 resulted in a shift in selecitivty of product **47C** for for all ligands. **41** saw the largest increase in the ratio of **47C**:(**47A**+**47B**+**47D**) from 1.6:1 to 3.8:1 Non polar solvents and B_2pin_2 as the boron source favors electronic selectivity.

The borylation studies of 1,3-difluorobenzene indicate that 4-pyridyl substitution of NMe_2 improves conversion and reactivity. 4-Pyridyl methyl substitution improved conversion over unsubstituted pyriydyl imine ligands, but was not as advantageous as NMe_2. 4-pyridyl bromo substitution decreased conversion and resulted in a shift towards electronic selectivity. Imine substitution with 4-DMAP greatly enhances reactivity and meta selectivity, while methyl substitution at the imine shifts selectivity toward electronic products and improves conversion and reactivity.

Borylation of Electron-Rich Substrates. After probing the function of the pyridyl imine backbone, attention was turned to comparison of the pyridyl imine to bpy and tmp frameworks. A series of 1,3-disubstituted electron rich arenes was borylated with **29**, **31** and **tmp** as ligands in order to compare the reactivity of **29** to widely-used, general purpose ligands of good reactivity. The substrates chosen were 1,3-dimethoxybenzene (**48**), 1,3-diisopropylbenzene (**49**) and 3-dimethylaminotoluene (**50**). The reactions were heated to 65°C and stirred for 22 h. The results are presented in Table 3.6.

For dimethoxy benzene, **29** gave the most conversion. Tmp gave the best conversion for the other two substrates. In general **29** performed as well or better than dtbpy. Tmp produced more conversion in the time allowed. For these substrates, there was not a real test of selectivity so, the

next step is to test the ligands on electron rich substrates that give mixtures to compare the selectivity of tmp to the hydrazone, **29**. Efforts in this area are ongoing.

Table 3.6. Borylation of Electron Rich Substrates

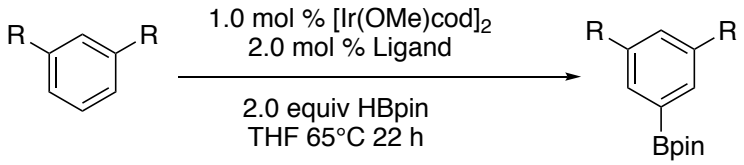

	conversion		
R group	**29**	**31**	**tmp**
R1 = R2 = OMe	61%	31%	34%
R1 = R2 = ipr	27%	16%	60%
R1 = NMe_2, R2 = Me	13%	13%	33%

Table 3.6. Borylation comparisons of electron rich substrates between ligand **29**, dtbpy and tmp show that ligand **29** is a viable ligand for electron rich substrates, performing as well or better than dtbpy.

In summary, the ligand design project is continuing to study ligand **29** with the aim of developing a highly active, meta selective ligand that is useful for a wide variety of substrates. The pyridyl imine framework has proven to be more active than the dpm framework, and pyridyl imines are thermally stable allowing borylation reactions to be heated, whereas dpm type ligated catalyst complexes break down when heated.

Preliminary tests indicate **29** is as reactive as dtbpy for neutral and electron withdrawing substrates, and more reactive towards electron rich substrates, though not as reactive towards these substrates as tmp. Studies are on-going to investigate whether **29** is more selective than tmp for borylation of non-symmetric elecron rich substrates that produce mixtrues of isomers.

The structure and reactivity studies of the pyridyl imine framework indicate that electron rich imine substituents increase activity and conversion. Methyl imine substitution shifts selectivity towards electronic products, while the DMAP imine substituent shifts to a high degree of steric selectivity. Electron donating 4-pyridyl substituents also increase reactivity and conversion of borylation reactions. The most beneficial 4-pyridyl substituent was found to be NMe_2. Electron withdrawing substituents decrease conversion, but are more selective for electronic products. 3-pyridyl substitution is not as beneficial as 4-pyridyl substitution. Efforts to enhance reactivity and meta selectivity hint that a larger, more electron donating aromatic substituent at the imine position may improve selectivity.

The 1,3-dicynobenzene borylation tests showed that the increased reactivity of ligand **29** is partly from the free NH_2 of the hydrazone. Substitution of the NH_2 leads to decreased reactivity, hemilabile behavior, and directed borylation with substrates that posess chelate directing functionality. The free NH_2 also facilitates HBpin complex formation which may block some electronic ortho borylation, and shifts selectivity towards steric products. The steric effect of HBpin is evident, as the tetrahedral boron complex provides a steric demand near the metal. It is not yet known what kind of electronic effects the HBpin complex engenders, and that will be explored by computaional modeling in the near future. Ligand **29** represents the design of a succesful ligand framework, and efforts to modify that framework to engineer selectivity are ongoing.

Although the dpm framework is much less reactive than the pyridyl imine framework, a unique opportunity exists to study the kinetics of HBpin borylation wth dpm ligands and to probe the catalytic cycles in order to shift selectivity outcomes.

REFERENCES

REFERENCES

1. Vanchura, I. I. B. A.; Preshlock, S. M.; Roosen, P. C.; Kallepalli, V. A.; Staples, R. J.; Maleczka, J. R. E.; Singleton, D. A.; Smith, I. I. I. M. R., Electronic effects in iridium C-H borylations: insights from unencumbered substrates and variation of boryl ligand substituents. *Chemical Communications* **2010,** *46* (41), 7724-7726.

2. Gasque, L.; Medina, G.; Ruiz-Ramírez, L.; Moreno-Esparza, R., Cu–O stretching frequency correlation with phenanthroline pKa values in mixed copper complexes. *Inorganica Chimica Acta* **1999,** *288* (1), 106-111.

3. Tagata, T.; Nishida, M., Aromatic C-H Borylation Catalyzed by Iridium/2,6-Diisopropyl-N-(2-pyridylmethylene)aniline Complex. *Advanced Synthesis & Catalysis* **2004,** *346* (13-15), 1655-1660.

4. Ros, A.; Estepa, B.; López-Rodríguez, R.; Álvarez, E.; Fernández, R.; Lassaletta, J. M., Use of Hemilabile N,N Ligands in Nitrogen-Directed Iridium-Catalyzed Borylations of Arenes. *Angewandte Chemie International Edition* **2011,** *50* (49), 11724-11728.

5. Ros, A.; López-Rodríguez, R.; Estepa, B.; Álvarez, E.; Fernández, R.; Lassaletta, J. M., Hydrazone as the Directing Group for Ir-Catalyzed Arene Diborylations and Sequential Functionalizations. *Journal of the American Chemical Society* **2012,** *134* (10), 4573-4576.

6. Chotana, G. A.; Rak, M. A.; Smith, M. R., Sterically Directed Functionalization of Aromatic C-H Bonds: Selective Borylation Ortho to Cyano Groups in Arenes and Heterocycles. *Journal of the American Chemical Society* **2005,** *127* (30), 10539-10544.

CHAPTER 4

GERMANIUM CROSS-COUPLING

Background and Significance. Harnessing the reliability of palladium-catalyzed Stille cross-coupling reactions while eliminating the health hazards and costs associated with handling and disposal of tin waste byproducts has been an interest in synthetic organic chemistry since the late 1980s and early 1990s, and efforts to replace tin with a less toxic alternative from group 14 have been on-going since that time.[1] The bulk of efforts have been directed towards silicon coupling chemistry, and the field has developed many successful and useful protocols from the primary work of Hiyama and Denmark and others.[2]

In the early 2000s, the Maleczka group took an interest in reducing the impact of tin in Stille couplings by developing the first Stille coupling process catalytic in tin, employing 6 mol% trialkyl tin rather than the standard stoichiometric transmetalating reagents.[3-5] With an eye towards eliminating toxicity concerns altogether, attention was turned to the study of germanium cross-coupling reactions with the aim of developing a similar catalytic coupling cycle employing germanium instead of tin. The results of the initial studies were published in 2009 by Torres, Lavis and Maleczka and formed the basis for this project.[6]

Several unusual features mark this germanium cross-coupling reaction compared to all other germyl cross-coupling efforts pursued up to that time. Like the early Si coupling efforts, directly replacing trialkyl tin reagents with analogous R_3Si or R_3Ge silyl or germyl reagents did not afford transmetalation. Activation of the more nonpolar C-Si and C-Ge bonds had to be accomplished by addition of fluoride ions to form a pentacoordinte intermediate which then could undergo cross-coupling. To the best of our knowledge, unlike all other published germanium cross-

coupling reports, Torres' account is the only direct R_3Ge analogue without fluoride additives or activation steps.

During the initial investigation of the cross-coupling reaction, an unexpected result was obtained. E-tributylvinyl germanes analogous to typical trialkyl stannane reagents were subjected to standard Stille arylation conditions in order to obtain vinyl arenes. Instead of the expected E-vinylarene product, however, the major product was the inverted Z-aryl olefin, as shown in Scheme. 4.1.

Scheme 4.1. Germyl-Stille Cross-Coupling Results in Inversion

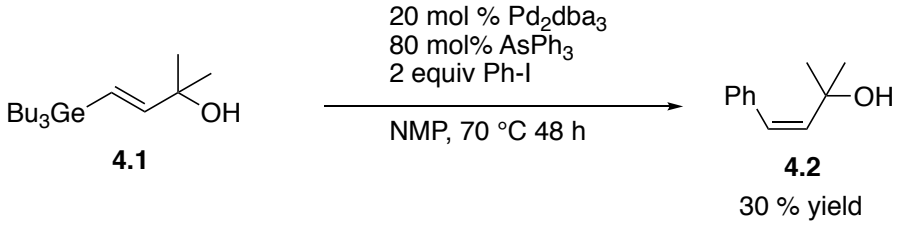

4.1 **4.2**

30 % yield

Scheme 4.1. The initial germyl-Stille reactions resulted in inversion of stereo chemistry to obtain Z isomer **4.2** as the major isomer.

Although the yield was low, if optimized, this unexpected result could offer a new tin-free Stille-type coupling with stereo control complementary to conventional Stille methodology. The early attempts by Torres to optimize this reaction under Stille conditions resulted in little improvement. Adding CuI, a typical means of rate acceleration for Stille reactions,[7] caused the reaction to fail altogether. Drawing insight from previous suggestions of Heck involvement in other contemporary Ge coupling studies,[8] it was recognized that a Heck mechanism could better explain the inversion of the olefin geometry found in the coupling product. Heck reaction conditions were subsequently investigated.

The standard conditions as shown in Scheme 4.2 were determined based on optimization studies with carbonate bases and quaternary ammonium additives previously tabulated for Heck reactions as catalogued by Jefferey in the mid 1990s.[9-10] This palladium Heck type system is also

referred to as [Pd/M_2CO_3/QX] where Pd is a simple palladium salt, usually palladium acetate, $Pd(OAc)_2$. M is an alkali metal, usually potassium or sodium, and QX is a quaternary ammonium halide, tetrabutylammonium bromide (TBAB) in this case. Triphenylphosphine (PPh_3) was utilized as the ligand, which is typical for this system, and iodobenzene (PhI) was the coupling partner.

Scheme 4.2. Optimized Heck Conditions for Published Germanium Cross-Coupling

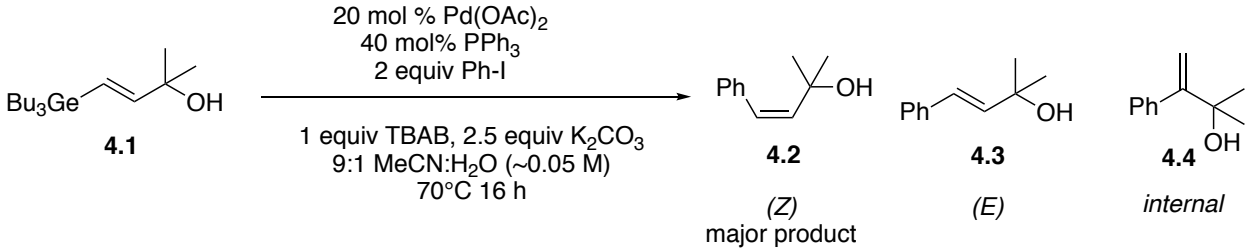

Scheme 4.2. The optimized conditions for the germyl Heck coupling published by Torres, Lavis and Maleczka in 2009[6] were similar to the conditions developed by Jeffrey[10] in the early 1990s.

Previously Proposed Catalytic Cycle. Operating under the premise that the reaction proceeded predominantly by a Heck-type insertion rather than a Stille-type transmetalation, Scheme 4.3 expands upon the putative mechanism offered in the 2009 paper. The mechanism is unusual in that instead of the expected β-H elimination which retains E olefin geometry, a bond rotation is suggested that puts Ge and Pd syn to each other, in preference to the usual coplanar arrangement of Pd and H. Instead of a β-hydride elimination, a β-germyl elimination is hypothesized, thus giving rise to the inverted Z olefin geometry. There is no precedence for this type of reaction in the literature, but over the next few years, after the project lapsed, attempts to rationalize the mechanism in order to explain the inversion prompted a reexamination of the proposed Pd-Ge elimination.

Alternate explanations involving reinsertion of a hydride,[11] oxy-palladation,[12-13] or Pd O-chelation[14] failed to account for the inversion of geometry. A look at the substrate scope provided hints for the basis of this unique reactivity.

Scheme 4.3. Putative Mechanism of Germyl Cross-Coupling Reaction as published in 2009

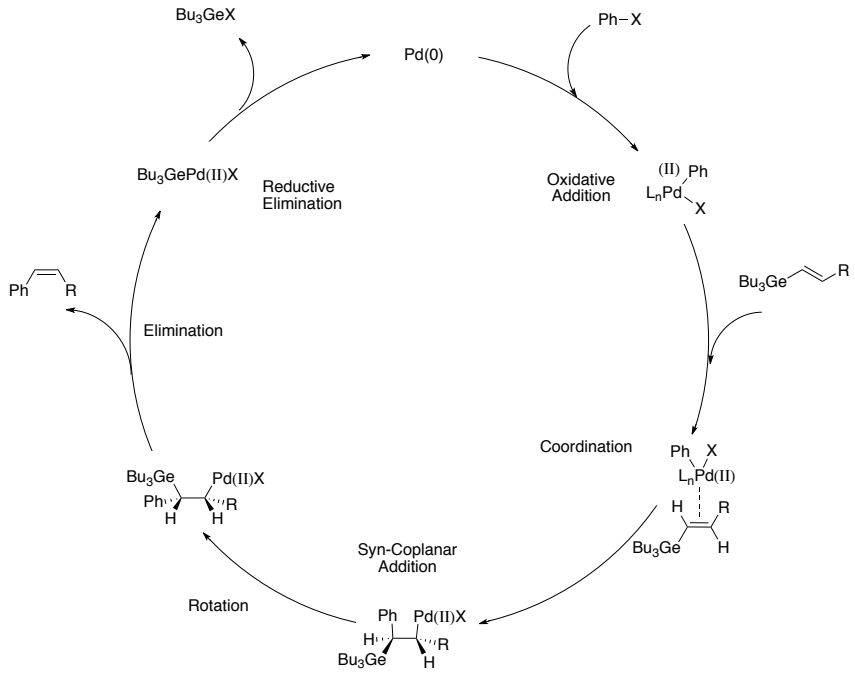

Scheme 4.3. The mechanism proposed by Torres, Lavis and Maleczka in 2009 involved a β-germyl elimination instead of the usual β-hydride elimination.

As seen in Table 4.1, successful coupling required the presence of a tertiary allylic alcohol, unlike simple Heck reactions which apply across a wide range of olefins and tolerate a variety of functional groups.[15-16] When the alcohol was protected, as compound **4.7**, no reaction occurred. This specific substrate scope cast doubt upon hydride reinsertion, as no oxygen functionality is required for the addition of a palladium hydride species. The failure of the ether to couple ruled out chelation chemistry,[14] as ethers and esters form a large part of the substrate scope of reported chelation chemistry. Oxy-palladation or cyclic germanium intermediates were ruled out, as

following the mechanisms for both possibilities leads to retention of stereochemistry, not inversion.

Table 4.1. Substrate Scope of Germyl-Heck Coupling Reaction.

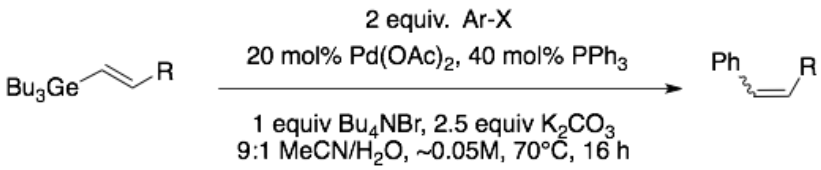

entry	vinyl germane	Ar-X	isolated yield	Z/E ratio
4.1	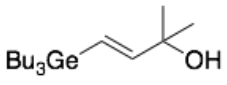	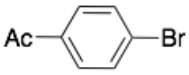	61	>20/1
4.5	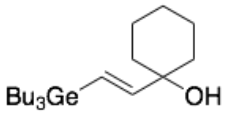		61	>20/1
4.6	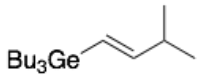		---	---
4.7	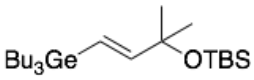	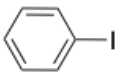	---	trace of Z (E not detected)
4.8	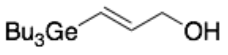		15	--- 100% cine

Table 4.1. The substrate scope of Torres' coupling reaction was limited to vinyl germanes bearing an unprotected allylic alcohol.

Substrate Scope. Torres used vinyl germanes with unhindered allylic alcohol groups, like compound **4.8** in Table 4.1, as a probe of competition for β-hydride elimination against the proposed β-germyl elimination, with the predicted outcome being retention of stereochemistry for β-hydride elimination and inversion for β-germyl elimination. When the allylic carbon is not tertiary, however, the reaction results in a complicated mixture, and Torres isolated only 15% internal product, with no formation of either E or Z coupling product, and no recovery of unreacted

starting material. The reaction mechanism is not straight forward, and may operate by a competing mixture of pathways.

Looking back to literature on desilylative couplings from the 1980s, Hiyama presents his observations of unactivated silanes coupling with allylic carbonates and epoxides under Pd catalyzed conditions which result in inversion of configuration, while activation with fluoride ion sources result in retention of configuration with the same substrates.[17] Scheme 4.4 shows his mechanistic reasoning for activation vs palladation.

Scheme 4.4. Hiyama's Activation vs. Carbopalladation Mechanisms

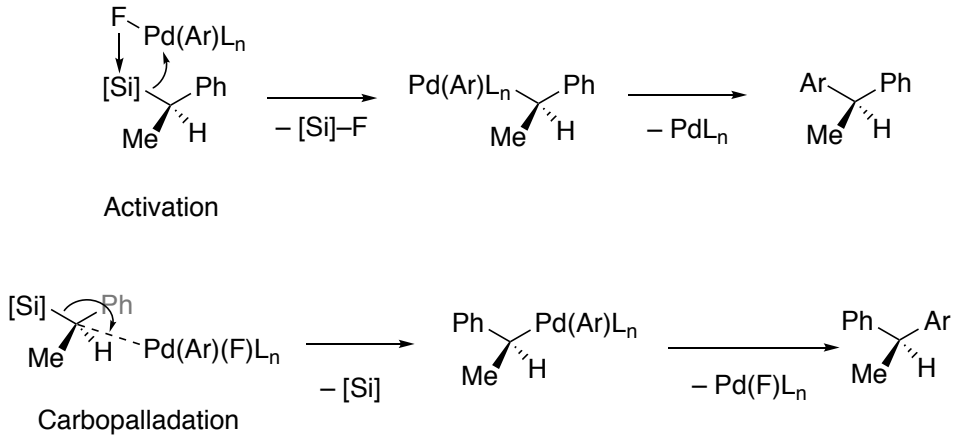

Scheme 4.4. Hiyama noticed that geometry of some desilylative couplings depended on reaction conditions. If a pentacoordinate species was generated by activation with fluoride additives, the geometry was retained. If the mechanism went through a direct carbopalladation across a C=C double bond without a fluoride ion source, the geometry was inverted. Only allylic carbonates and epoxides underwent unactivated coupling.

In Hiyama's mechanism, he shows the desilyation step for unactivated substrates as concurrent with the carbopalladation step. The first coupling reactions on the reboot of this project involved looking for evidence of degermylation to determine whether degermylation happened before or after carbopalladation. The initial reactions gave low conversion, and so careful recovery and quantification of the starting material was done in order to be sure than the vinyl germane was not degermylating or forming intermediates that were difficult to detect by NMR. In all cases,

the starting material recovery was nearly equal to the amount left over as indicated by GC-FID and ^{1}H NMR. We concluded that the starting material was not degermylating prior to the coupling reaction to liberate an allylic alcohol. This was consistent with the degermylation of a reaction intermediate.

Scheme 4.5. Degermylation of Vinyl Germanes makes Allylic Alcohols

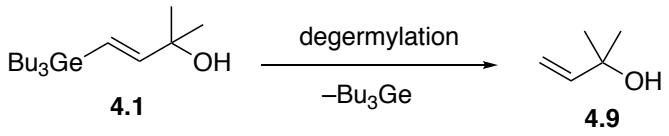

4.1 **4.9**

2-methyl-3-butene-2-ol

The allylic alcohol that would result from degermylation of vinyl germane **4.1** is 2-methyl-3-butene-2-ol, shown in Scheme 4.5 (referred to here as compound **4.9**). Looking back to the early Heck coupling reports from the 1970s, Chalk[18] and Heck[18] reported the first Heck coupling reactions of 2-methyl-3-butene-2-ol (**4.9**) in 1976, The results are shown in scheme 4.6.

Scheme 4.6. The First Reported Heck-Coupling of Allylic Alcohol 4.9.

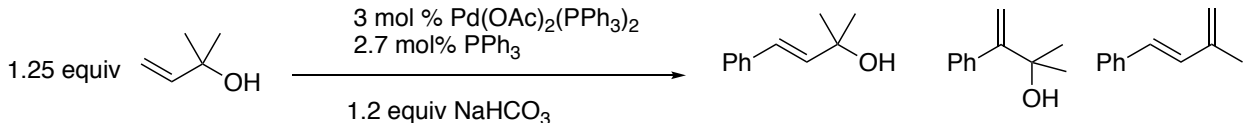

4.9 98% E **4.3** 1% internal **4.4** 1% dehyd. **4.10**

In the Heck coupling of the free allylic alcohol **4.9**, the Z isomer is not seen among the products. The E isomer is overwhelmingly the major product with only internal and dehydration products seen as side products. In the years that followed with successive improvements to Heck coupling, almost all coupling reactions with **4.9** produce 100% E isomer, with no traces of internal or Z isomer. A typical example of modern Heck coupling conditions are shown on the next page in Scheme 4.7.[19]

Scheme 4.7. Modern Heck-Coupling Protocols are E Selective

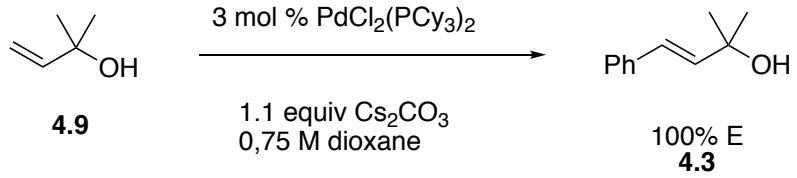

In all the literature searches we conducted of Heck reactions with allylic alcohols and similar vinyl silanes, Torres' coupling reaction was the only Heck reaction that afforded the Z isomer at all, let alone as the major product. Any coupling of the free allylic alcohol **4.9** under Heck conditions does not result in formation of the Z isomer. This suggests that the vinyl germane starting material forms a reactive intermediate that participates in the Heck reaction instead of liberating the alcohol.

Looking at the structures of the successful coupling partners, compounds **4.1** and **4.5** in Table 4.1, both can form an epoxide intermediates, reminiscent of Hiyama's early unactivated allylic epoxide and allylic carbonate substrates for desilyative coupling.[17, 20-21] Compound **4.6** does not have an allylic O atom, and **4.7** cannot form an epoxide due to the bulky O protection group. In our subsequent studies, we tried protecting the alcohol with a smaller methyl group, and that also resulted in no reaction. Formation of intermediate epoxides is a plausible reaction path since the substrate scope shows vinyl germanes lacking allylic oxygens or having protected allylic O atoms do not participate in the Heck coupling reaction.

The unhindered compound **4.8** has an allylic alcohol but the position is also flanked by β-H atoms. β-H elimination would result in a tautomerization likely to form a ketone or aldehyde. In our resumed studies, we found ketones present in some reaction mixtures, and the tell-tale CH_2 protons that are usually hidden under tetrabutylammoniumbromide (TBAB) peaks in the NMRs of the crude material and are difficult to see. The ketone products also come off the column near

the solvent front with the left over iodobenzene in the normal silica columns eluted with dichloromethane that were employed to analyze the reaction products. These less polar products can be easily missed without careful analysis of all eluted fractions. Investigation of unhindered vinyl germane alcohols is a priority of this project to enable a wider the substrate scope beyond tertiary allylic alcohols.

Probe of Steric Effects on the Inversion of Geometry. To test whether the O atom is directly involved in the inversion of the stereochemistry and to rule out steric influence, the analogous tributylvinyl germane with tertiary allylic carbon of 3,3-dimethylbutane, **4.11**, was synthesized and subjected to coupling conditions. Under the standard conditions, no coupling reaction occurred. Under the Torres' initial Stille coupling conditions with $Pd_2(dba)_3$ in NMP, still no coupling resulted. Adding tetrabutylammoniumfluoride (TBAF) to both the standard Stille and Heck reaction conditions from Torres' 2009 report[6] also resulted in no reaction.

Scheme 4.8. Germanium Cross-Coupling under Fluoride Activation

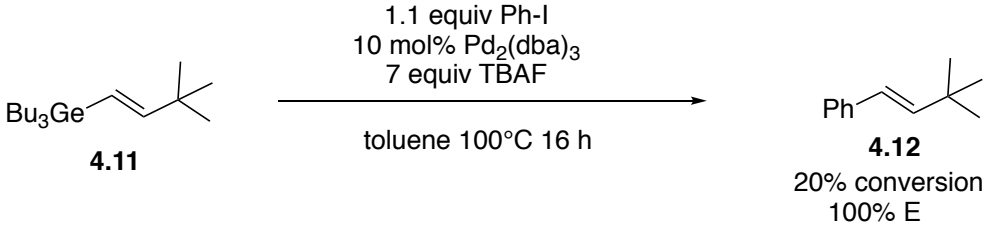

Scheme 4.8. When the vinyl germane lacks an allylic alcohol functional group, cross-coupling conditions must be harsher and activated with fluoride ions. Only E coupling product is observed under these conditions.

After searching for optimized conditions that might work, **4.11** was subjected to Stille coupling according to Wnuk's moist toluene approach using TBAF as an activating source, as detailed in Scheme 4.8.[22] The reaction exhibited only 20% conversion and only E product was seen by NMR and GC-FID. Although not much conversion was realized, the coupling product was isolated for a 16% yield and 72% of the starting vinyl germane **4.11** was recovered.

Updated Putative Mechanism Based on Reactive Intermediate Hypothesis. The recovery of the starting material supports the idea that the vinyl germane is robust and does not degermylate from fluoride attack under the reaction conditions to undergo subsequent coupling as a free allylic alcohol. In all cases of vinyl germane coupling, the unreacted vinyl germane is seen in the mass spec as a single peak m/z = 272 which corresponds to the molecular ion minus a butyl radical group (*m/z* = 56).

Scheme 4.9. Proposed Mechanism for Inversion of Stereochemistry of Ge Cross-Coupling

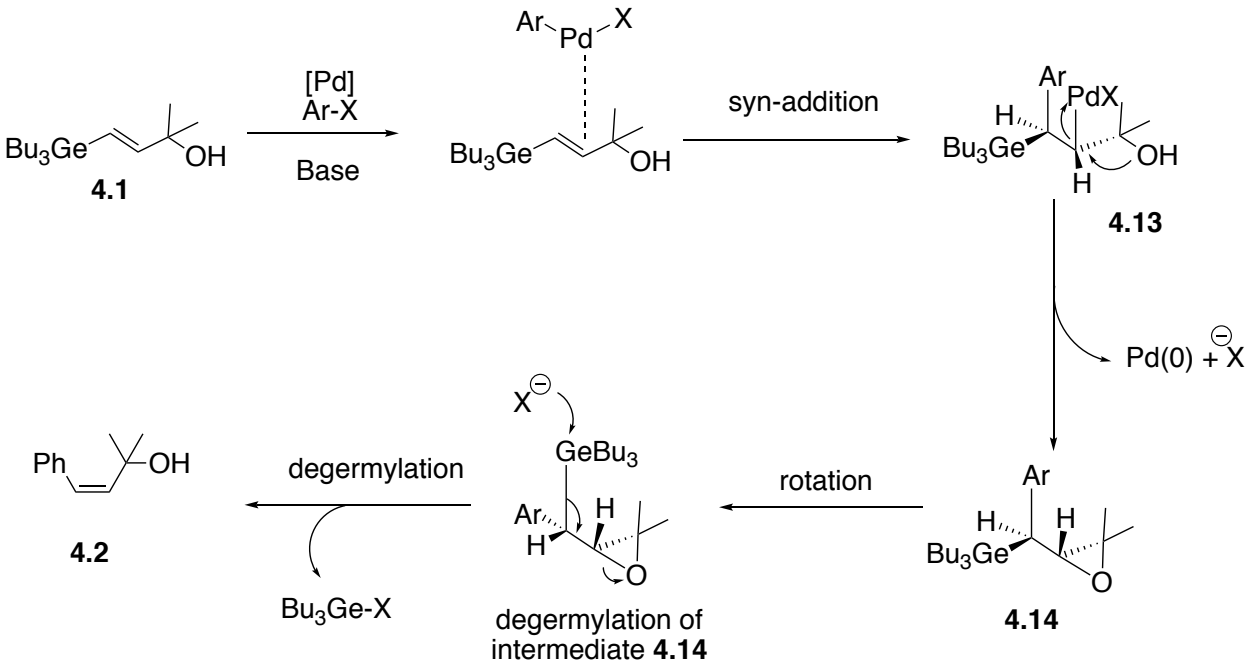

Scheme 4.9. The proposed mechanism of the germyl-coupling reaction proceeds through the generation of a reactive epoxide intermediate with subsequent degermylation of the intermediate.

The unreacted starting material is easily isolated and quantified to verify that it is not degermylating or forming an intermediate that is not detected by GC-MS or NMR. The ejected Bu_3Ge fragment is also seen in the GCMS with an m/z = 245. The mass of iodine is not found with it, so it is not unequivocally verified that degermylation occurs with attack of iodide to the intermediate, as illustrated with the proposed degermylation of 4.15, as shown in Scheme 4.9.

Further support for the degermylation of an intermediate is found in the fact that the Bu_3Ge fragment does not occur in the GC-MS of the starting material as a fragment pattern or artifact, nor does it appear in coupling reactions that have failed. The fact that this tributylgermyl fragment is only found in reactions where coupling products have been formed lends support to the fact that degermylation happens to an intermediate and not directly to the starting material.

Attempts to synthesize the putative secondary allylic germyl epoxide, **4.14** (as shown in Scheme 4.9) have not yet succeeded, and are ongoing. While work on the proposed intermediate progresses, primary allylic germyl epoxides were synthesized in the meantime. Although primary epoxides cannot provide information about the retention or inversion of stereochemistry, these reagents provided a means to test whether allylic germyl epoxides can undergo coupling reactions under the prescribed reaction conditions.

Scheme 4.10. Germyl Allylic Epoxides Degermylate under Acidic Conditions

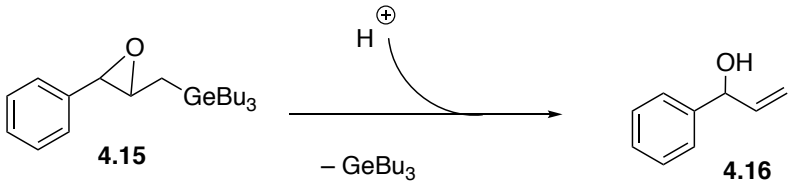

Scheme 4.10. The allylic germyl epoxide **4.15** was shown to degermylate on silica to generate an allylic alcohol. Efforts were made to determine whether the starting vinyl germane underwent degermylation to liberate the allylic alcohol or if degermylation occurred on a carbopalladated intermediate.

When epoxide **4.15** was passed through an activated silica plug, degermylation to the allylic alcohol **4.16** was seen. The NMR matched the reported spectrum of the known compound and GC-FID and GC-MS standards were taken in order to look for the free alcohol in the crude reactions. The epoxide survived passage through grade 2 silica (~3% water) and neutral and basic alumina.

Cross-Coupling with Allylic Germyl Epoxides. To test if the allylic germyl epoxide could undergo coupling in a reaction under the current conditions, a standard coupling reaction with vinyl germane **4.1** and iodobenzene was begun. After verification of coupling product formation around 4 - 8 hours, the vinyl germane was injected into the reaction. The analogous Heck coupling product of iodobenzene with 1-phenyl-prop-2-en-1-ol, **4.15**, was found in the literature to be the ketone 1,3-diphenylpropan-1-one, **4.16** (Scheme 4.9)[23]. After 24 hours, the GC-MS of the crude reaction was analyzed for the masses of the free allylic alcohol and the coupling product. The allylic alcohol was not found in the NMR or GC-MS, but the coupling product was seen in both NMR and GC-MS, and the spectrum of the isolated compound matched reported NMR data. Traces of unreacted germyl epoxide also remained in the crude reaction, but were not isolated.

Scheme 4.11. Reaction of an Allylic Germyl Epoxide in the Cross-Coupling Reaction

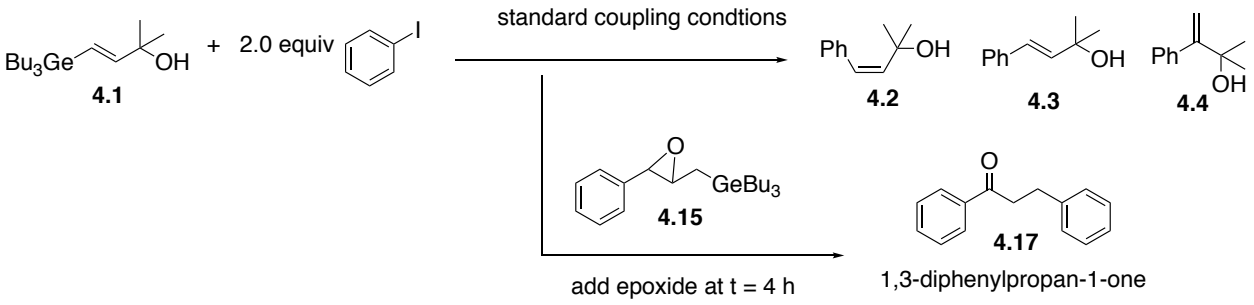

Scheme 4.11. The allylic germyl epoxide was injected into a coupling reaction already in progress to ensure the coupling conditions were viable upon addition of the epoxide, and to be sure the reaction was not hindered or stopped by the addition of the epoxide.

The procedure was repeated with iodotoluene as the coupling partner, and epoxide **4.15** was added into the reaction by syringe after 8 hours. The expected coupling product, **4.18**[23] was found in the GCMS and NMR of the crude reaction. Less conversion occurred for this reaction, and significant amounts of epoxide were seen remaining in the GC-MS and NMR of the crude reaction. The free allylic alcohol was not found in the crude reaction.

Scheme 4.12. Allylic Germyl Epoxide Reaction with Iodotoluene

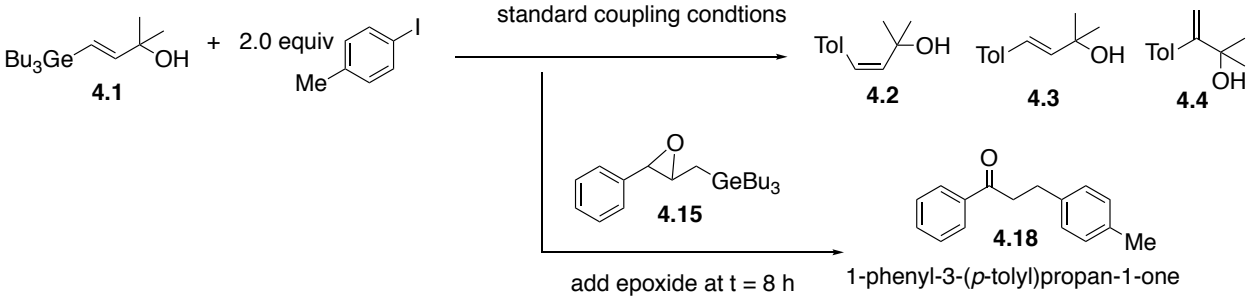

Scheme 4.12. The reaction was repeated with iodotoluene as the coupling partner to ensure no phenyl transfer reactions from PPh_3 or other reagents occurred.

These reactions showed that allylic germyl epoxides are capable of undergoing unactivated coupling reactions, thus lending support to the proposed epoxide intermediate in Scheme 4.7. In order to investigate the fate of unhindered allylic alcohols of vinyl germanes in the coupling reaction, the unhindered allylic vinyl germane **4.19** (Scheme 4.11) was synthesized and subjected to a coupling reaction under the same conditions with vinyl germane **4.1** and iodobenzene.

Scheme 4.13. Cross-Coupling Reaction of an Unhindered Allylic Germyl Epoxide

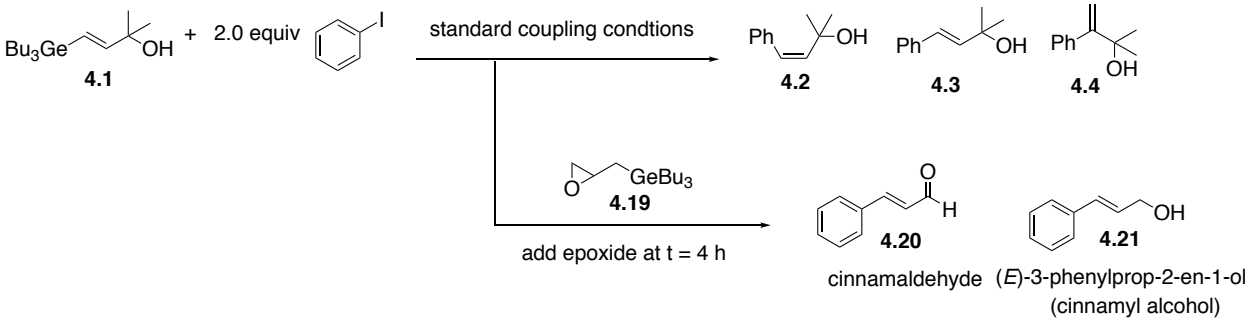

Scheme 4.13. The undhindered allylic germyl epoxide serves as a test to probe what might happen to unhindered vinyl germanes under the current coupling conditions.

At 4 hours, the epoxide was added into the reaction. After 24 h, the crude reaction smelled like cinnamon. Cinnamaldehyde and cinnamyl alcohol were found in the crude NMR and GCMS. The unhindered epoxide formed cinnamaldehyde and cinnamyl alcohol as byproducts of the coupling reaction.

Figure 4.1. NMR of the Cross-Coupled Unhindered Allylic Germyl Epoxide

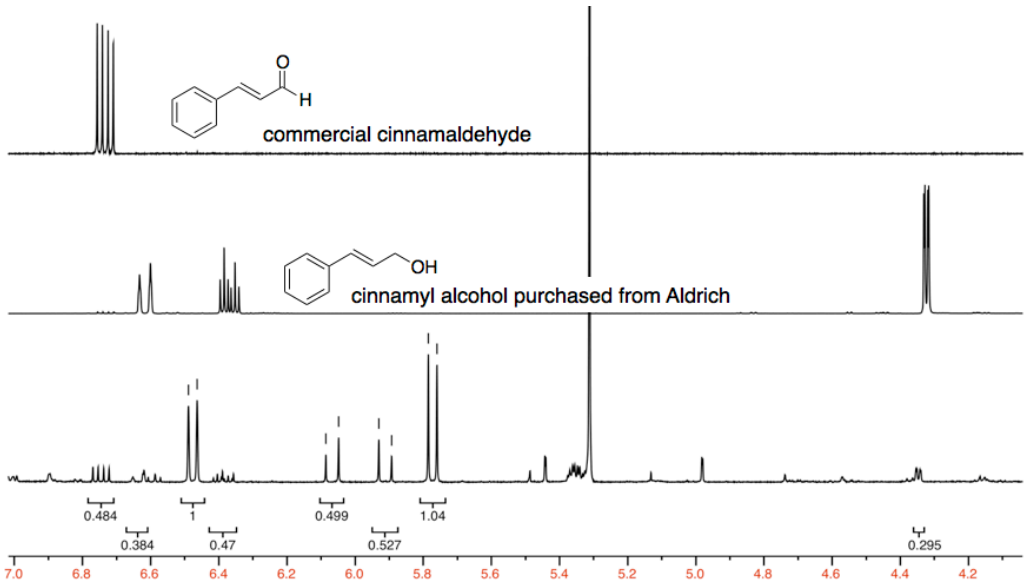

Figure 4.1. NMR of coupling reaction compared to known samples of cinnamaldehyde and cinnamyl alcohol show that the unhindered epoxide undergoes degermylative cross- coupling with iodobenzene

Scheme 4.14. Germyl Allylic Epoxides Participate in Heck-Coupling.

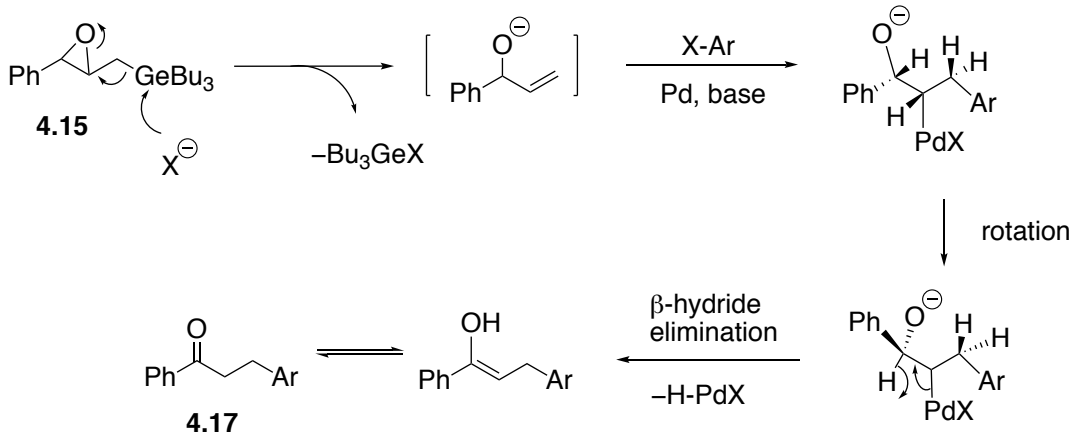

Scheme 4.14. Allylic germyl epoxides participate in Heck-coupling with aryl halides, thus lending support to the proposed reactive intermediate.

After support was found for the generation of a transient allylic germyl epoxide intermediate, an effort was made to improve the conversion and repeatability of the reaction, and to expand the substrate scope to include allylic carbonates, amines or thiols and vinyl germanes

with secondary allylic alcohols. Other catalysts systems less prone to β-hydride elimination may be investigated for the purpose of broadening the substrate scope.

The first task for optimization however, was to obtain consistent conversion and isomer ratios of Z to E, and to improve overall repeatability in general. Some early results indicated that water was necessary in higher ratios than 1:9 for the solvent. The best acetonitrile to water ratio was found to be 2:1. Greater solvent volume also helped to increase conversion and sparging with O_2 gas was also beneficial. Stirring the reaction for at least an hour before heating was found to increase conversion. Despite numerous optimization attempts, the reaction remained frustratingly inconsistent in conversion and Z:E ratios.

In collaboration with Kiyoto Tanemura, oxidative Heck-coupling conditions were investigated to see if improvements could be made. The results of some of these studies are presented in Table 4.2, seen on the following page.

Investigation of Oxidative Heck Conditions. When comparing additives and changes in conditions, it seems adding the oxidant benzoquinone, (BQ) was helpful for both conversion and yield, except in entry 10 when used in combination with O_2 sparging. Adding a radical initiator AIBN in Entry 11 resulted in no reaction. Bidentate ligand bis(diphenylphosphino)propane, dppp, decreased the Z:E ratio significantly for Entry 6. Triphenylphosphine oxide, TPPO, worked as a ligand in place of triphenylphosphine. Table 4.2 represents a sampling of Tanemura's optimizations. See the supporting information for more details. No clear trends emerged from studying the effect of additives or conditions designed to work in accordance with known Heck mechanisms, and again, the results were inconsistent.

Table 4.2. Investigation of Additives for Oxidative Heck Reactions

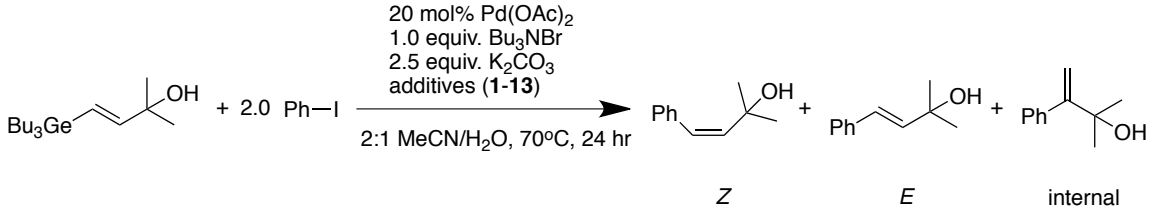

Entry	Additive	NMR conversion	Z:E:internal
1	40 mol % Ph_3P	40 %	46:1:2
2	40 mol % Ph_3P, O_2 sparge	76 %	10:1:0.3
3	40 mol % Ph_3P, air sparge	77 %	5.5:1:0.2
4	40 mol % Ph_3PO	60 %	13:1:0.2
5	20 mol % Ph_3P, 20 mol % Ph_3PO	52 %	6.5:1:0.2
6	40 mol % dppp, O_2 sparge	30 %	2.5:1:0.1
7	40 mol % Ph_3P, 20 mol % BQ	49 %	35:1:2
8	O_2 sparge	0%	-
9	20 mol % BQ, O_2 sparge	55 %	14:1:0.2
10	20 mol % BQ, 40 mol % Ph_3P, O_2 sparge	11 %	2:1:trace
11	40 mol % Ph_3P, 10 mol % AIBN	0 %	-
12	40 mol % S-Phos, O_2 sparge	71 %	14:1:0.4
13	40 mol % Ph_3P, 2.5 equiv. Ag_2CO_3	85 %	5:1:trace

Table 4.2. Additives typically used for oxidative Heck additions produced no clear trends. BQ = 1,4 benzoquinone, dppp = bis(diphenylphosphino) propane, a bidentate ligand, AIBN = azobisisobutylnitrile, a radical initiator, SPHOS = 2-Dicyclohexylphosphino-2′,6′-dimethoxy biphenyl, a bulky monodentate phosphine ligand.

When we turned to the literature for guidance on the conditions for the coupling, it became clear that the [Pd/M_2CO_3/QX] Heck coupling system was likely generating Pd nanoparticles,[24] and the coupling reaction was operating under a mixture of homogeneous and heterogeneous conditions.

Next, in collaboration with Shawn Haldar and Maryam Abbas, investigation of the substrate scope, effect of O_2 on the reaction, and testing for the presence of nanoparticles began.

Substrate Scope from Updated Optimization. A summary of the substrate scope is presented in Table 4.3. In keeping with the generation of nanoparticles, Abbas found that stirring the reagents for at least an hour, and making sure all solids were dissolved before adding the $Pd(OAc)_2$ was beneficial for higher yields and better Z:E ratio..

Table 4.3. Substrate Scope of Germanium Cross-Coupling Reaction

Entry	Substrate	Conversion	Z:E ratio	Yield
1)	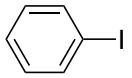	84%	20:1	78%
2)	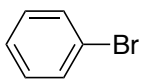	12%	14:1	5%
3)	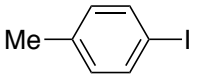	57%	10:1	47%
4)	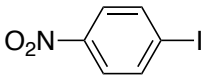	0%	—	—
5)	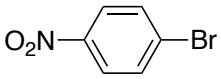	15%	5:1	7%
6)	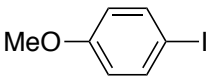	12%	5:1	5%
7)	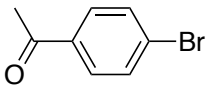	22%	8:1	10%

Table 4.3. General Conditions for 0.25 mmol: 1 equiv vinyl germane (**4.1)**, 2 equiv Ar-X, 40 mol % PPh_3, 1 equiv Bu_4NBr, 2.5 equiv K_2CO_3, 2:1 MeCN:H_2O, 20 mL (0.0125 M). Sparge O_2 gas (one balloon volume), 20 mol % Pd(OAc)2 added after stirring and sparging with O_2, but before heating. Stir under O_2 balloon 1 hour, heat 70 °C 23 more hours.

The reaction worked best for iodobenzene, then showed moderate to good conversion for electron donating groups, but the coupling barely worked for electron withdrawing coupling

partners like para-nitro-bromobenzene, resulting in low conversions of 5 -15%. No conversion was seen for para-nitro-iodobenzene

During the substrate screening, a test to determine the effect of O_2 atmosphere on the coupling reactions was conducted. One reaction of **4.1** with iodobenzene was made up with all reagents except $Pd(OAc)_2$ and allowed to stir for a half hour. Half of the reaction was removed to another flask by pipette. The flasks were labeled 1 and 2. Flask 1 was sparged with house N_2 gas for 2 hours, while flask 2 was sparged with two large balloon volumes of O_2 for a half hour then put under an O_2 balloon atmosphere. After 2 hours, the $Pd(OAc)_2$ was added. Flask 1 turned black immediately, while flask 2 looked normal, a bright orange color. The reactions were then stirred at room temperature for 3 hours. A GC-FID sample was taken and both reactions had about 10% conversion. The reactions were heated to 70°C overnight for 18 h, a total of 24 h since the reactions were started. Flask 1, carried out in the absence of O_2, achieved 55% conversion with 6:1 Z:E ratio. Flask 2, carried out under O_2, achieved 70% conversion with 14:1 Z:E ratio. It seems as if O_2 improves conversion and Z:E ratio, but is not crucial for the reaction to proceed.

Mercury Poisoning Test. The first test for nanoparticles was a Hg poisoning test in which a coupling reaction was set up and stirred for an hour, then half of the reaction was removed by pipette to another flask. A GC-FID sample was taken to ensure coupling products were being formed, with about 7% conversion seen in both. A drop of mercury was added to one flask while the other was allowed to proceed according to the standard conditions. The flask with mercury immediately turned clear and the conversion was low, around 10%, while the second flask without Hg showed 77% conversion. This was indicative that nanoparticles were probably being formed, and both heterogeneous and homogeneous conditions were operating.

Catalyst Recycling Test. A second test was done where germane **4.1** and iodotoluene were coupled to make product **4.22**, as shown in Scheme 4.12. The reaction was allowed to settle for 24 hours and then the reaction was slowly decanted out. The dirty flask and magnet were used for a subsequent coupling reaction of iodobenzene and **4.1** under standard conditions except no additional palladium was added. Conversion to **4.2** was seen and **4.22,** coupling product of the previous reaction, was not present in the GC or NMR. Although the conversion was low, the product was isolated and weighed to be sure the yield was consistent with the GC and NMR conversion. 10% isolated yield of pure **4.2** was obtained.

Scheme 4.15. Nanoparticle Recycling Test

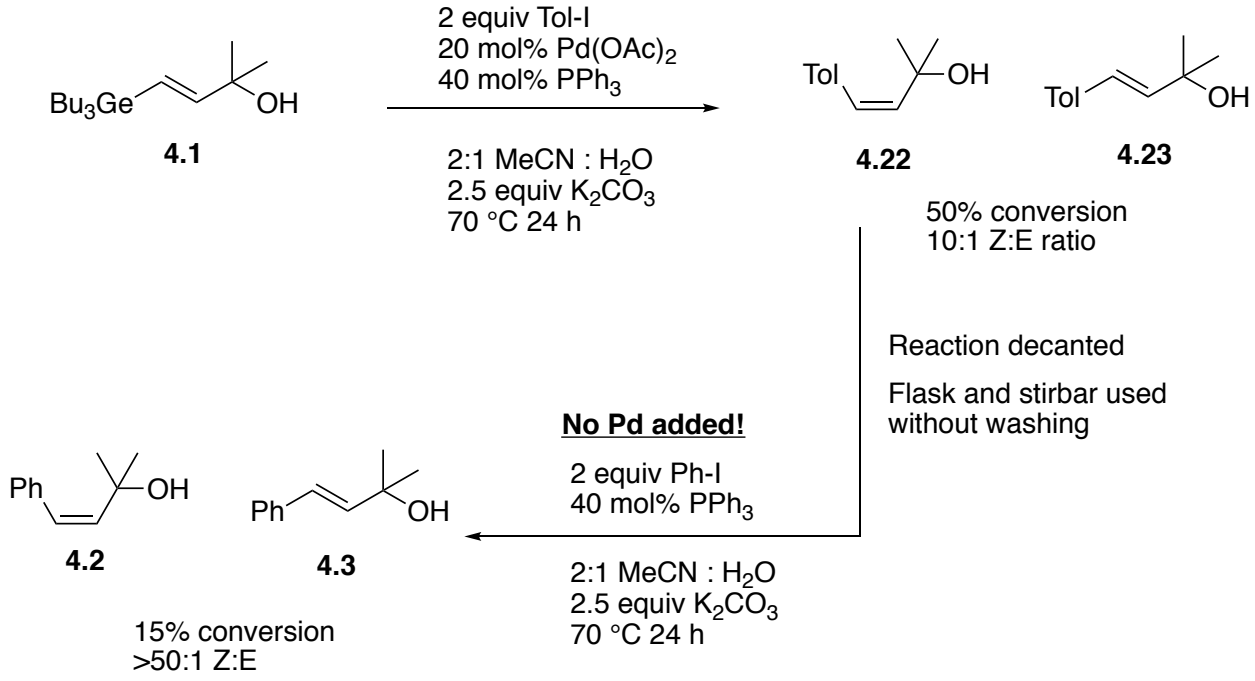

Confirmation *of Pd Nanoparticles by TEM and EDS*. Taken together, the results of the poisoning test and the catalyst recycling test were persuasive. A sample was prepared for Transmission Electron Microscopy (TEM). Images of the samples revealed the presence of poorly controlled nanoparticles varying in size from about 50 nm to 500 nm. An elemental analysis indicated about 1.9 % Pd present by weight in the sample, amidst organic residue.

Figure 4.2. TEM Images of Poorly Controlled Pd Nanoparticles

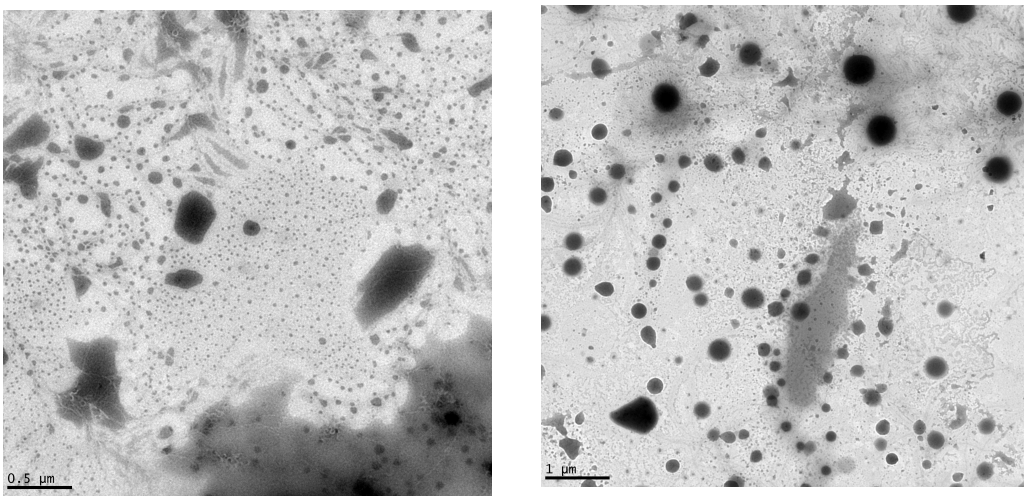

Figure 4.3. Elemental Analysis of Pd Nanoparticles by EDS Spectrum

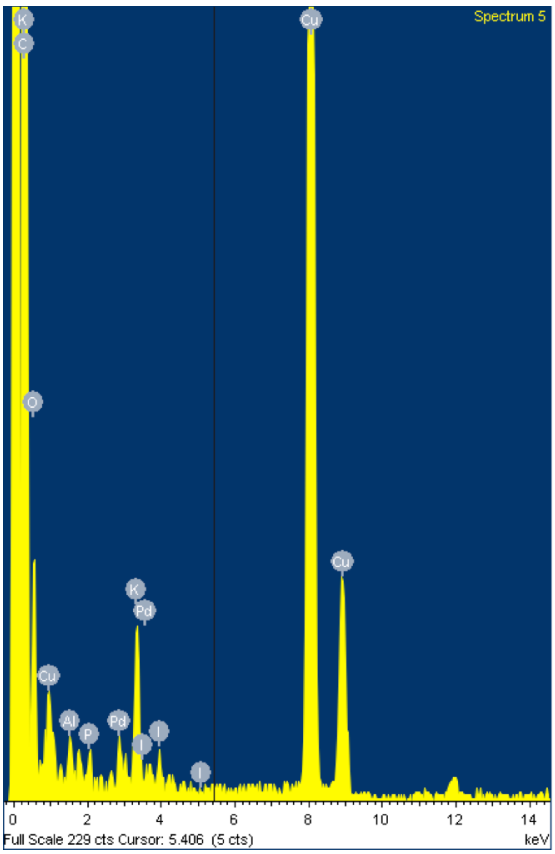

Spectrum processing :
No peaks omitted

Quantitation method : Cliff Lorimer thin ratio section.
Processing option : All elements analyzed (Normalised)
Number of iterations = 3

Standardless

Element	Weight%	Atomic%
C K	88.74	94.63
O K	4.78	3.82
Al K	0.57	0.27
P K	0.46	0.19
K K	2.18	0.71
Pd L	1.90	0.23
I L	1.38	0.14

Deconvolution Elements :
Copper
Sample thickness: 20.0 nm
Sample density: 3.32 g/cm3
Density estimate: 2.40 g/cm3
Beam broadening: 0.32 nm
No optimization has been performed.
Detector efficiency : Calculation

Although the discovery of Pd nanoparticles has complicated the investigation of this germanium cross-coupling reaction, there are still more interesting features to be discovered about the mechanism. When running a slow, long method in the GC-MS to look for intermediates and byproducts that can offer clues to the mechanism, a large acetamide peak was found. The reagent bottle of acetonitrile was tested and acetamide was absent. The reagents for a coupling reaction of **4.1** and iodobenzene were combined and stirred together for an hour, then a sample was removed and tested by GC-MS before the addition of $Pd(OAc)_2$. The combination of reagents did not contain any detectable aetamide. The $Pd(OAc)_2$ was added and the reaction was heated to 70 °C for 24 h. When a reaction sample was tested, a large acetamide peak was present. The reaction appears to catalyze the hydration of MeCN, and the solvent may be functioning as a ligand, thus becoming oxidized in the way that PPh_3 is oxidized to TPPO.

At the present time, efforts to quantify how much acetamide is produced from the reaction are in progress. We also wanted to know if the hydration of nitriles is general or if only acetonitrile can be hydrated. In a preliminary test for nitrile hydration, para dicyanobenzene was added into a coupling reaction. The next day the material was absent in the GC-MS and a peak of mass consistent with para cyanobenzoic acid was found. The results are preliminary and efforts to access the extent of hydration and conduct a brief test to determine the types of nitriles that will undergo hydration in this system are underway.

We are also working to test if nitrile hydration is linked to the mechanism of the germanium cross-coupling reaction, and if finding a better nitrile hydration catalyst will enable the cross-coupling reaction to proceed more reliably.

In summary, we have discovered that the palladium-catalyzed cross-coupling reaction of aryl halides and vinyl germanes bearing an allylic alcohol likely proceeds through a transient

intermediate, most likely an allylic epoxide species, which undergoes carbopalladation before degermylation. The structure of the allylic epoxide likely contributes to the ability to cross-couple without fluoride activation. The reaction has given inconsistent results due to the generation of poorly controlled Pd nanoparticles. The reaction has also been found to catalyze nitrile hydration, but it is not yet known if the reaction will proceed without the reagents for the cross-coupling present in the flask. Controls are being planned to determine if the nitrile hydration is a tandem cycle or if it operates independently of the coupling reaction. It has been noted previously that the reaction does not proceed without a mixture of acetonitrile and water, and other solvents such as methanol also have failed to facilitate cross- coupling.

REFERENCES

REFERENCES

1. Spivey, A. C.; Gripton, C. J. G.; Hannah, J. P., Recent Advances in Group 14 Cross-Coupling: Si and Ge-Based Alternatives to the Stille Reaction. *Current Organic Synthesis* **2004,** *1*, 211-226.

2. Denmark, S. E.; Regens, C. S., Palladium-Catalyzed Cross-Coupling Reactions of Organosilanols and Their Salts: Practical Alternatives to Boron- and Tin-Based Methods. *Accounts of Chemical Research* **2008,** *41* (11), 1486-1499.

3. Maleczka, R. E.; Gallagher, W. P.; Terstiege, I., Stille Couplings Catalytic in Tin: Beyond Proof-of-Principle. *Journal of the American Chemical Society* **1999,** *122* (2), 384-385.

4. Maleczka, R. E.; Gallagher, W. P., Stille Couplings Catalytic in Tin: The Sn-F Approach. *Organic Letters* **2001,** *3* (26), 4173-4176.

5. Gallagher, W. P.; Terstiege, I.; Maleczka, R. E., Stille Couplings Catalytic in Tin: The Sn-O Approach. *Journal of the American Chemical Society* **2001,** *123* (14), 3194-3204.

6. Torres, N. M.; Lavis, J. M.; Maleczka Jr, R. E., Reactions of vinyltributylgermanes and aryl halides under Heck conditions. *Tetrahedron Letters* **2009,** *50* (31), 4407-4410.

7. Mee, S. P. H.; Lee, V.; Baldwin, J. E., Stille Coupling Made Easier—The Synergic Effect of Copper(I) Salts and the Fluoride Ion. *Angewandte Chemie International Edition* **2004,** *43* (9), 1132-1136.

8. Faller, J. W.; Kultyshev, R. G., Palladium-Catalyzed Cross-Coupling Reactions of Allyl, Phenyl, Alkenyl, and Alkynyl Germatranes with Aryl Iodides. *Organometallics* **2002,** *21* (26), 5911-5918.

9. Jeffery, T., Heck-type reactions in water. *Tetrahedron Letters* **1994,** *35* (19), 3051-3054.

10. Jeffery, T., On the efficiency of tetraalkylammonium salts in Heck type reactions. *Tetrahedron* **1996,** *52* (30), 10113-10130.

11. Gordillo, A.; Ortuno, M. A.; Lopez-Mardomingo, C.; Lledos, A.; Ujaque, G.; de Jesus, E., Mechanistic Studies on the Pd-Catalyzed Vinylation of Aryl Halides with Vinylalkoxysilanes in Water: The Effect of the Solvent and NaOH Promoter. *Journal of the American Chemical Society* **2013,** *135* (37), 13749-13763.

12. Hay, M. B.; Wolfe, J. P., Palladium-Catalyzed Synthesis of 2,1,Äò-Disubstituted Tetrahydrofurans from Œ≥-Hydroxy Internal Alkenes. Evidence for Alkene Insertion into a Pd,àíO Bond and Stereochemical Scrambling via Œ≤-Hydride Elimination. *Journal of the American Chemical Society* **2005,** *127* (47), 16468-16476.

13. Hayashi, S.; Yorimitsu, H.; Oshima, K., Synthesis of Epoxides by Palladium-Catalyzed Reactions of Tertiary Allyl Alcohols with Aryl or Alkenyl Halides. *Journal of the American Chemical Society* **2009,** *131* (6), 2052-2053.

14. Ruan, J.; Xiao, J., From alpha-Arylation of Olefins to Acylation with Aldehydes: A Journey in Regiocontrol of the Heck Reaction. *Accounts of Chemical Research* **2011,** *44* (8), 614-626.

15. Beletskaya, I. P.; Cheprakov, A. V., The Heck Reaction as a Sharpening Stone of Palladium Catalysis. *Chemical Reviews* **2000,** *100* (8), 3009-3066.

16. Felpin, F.-X.; Nassar-Hardy, L.; Le Callonnec, F.; Fouquet, E., Recent advances in the Heck–Matsuda reaction in heterocyclic chemistry. *Tetrahedron* **2011,** *67* (16), 2815-2831.

17. Hayao, M.; Satoshi, A.; Kazunori, H.; Yasuo, H.; Atsunori, M.; Tamejiro, H., The Palladium-Catalyzed Cross-Coupling Reaction of Organosilicon Compounds with Allylic Carbonates or Diene Monoxides. *Bulletin of the Chemical Society of Japan* **1997,** *70* (8), 1943-1952.

18. Melpolder, J. B.; Heck, R. F., Palladium-catalyzed arylation of allylic alcohols with aryl halides. *The Journal of Organic Chemistry* **1976,** *41* (2), 265-272.

19. Yi, C.; Hua, R., An efficient palladium-catalyzed Heck coupling of aryl chlorides with alkenes. *Tetrahedron Letters* **2006,** *47* (15), 2573-2576.

20. Matsuhashi, H.; Hatanaka, Y.; Kuroboshi, M.; Hiyama, T., Palladium-catalyzed cross-coupling of allylic carbonates with alkenylfluorosilanes in the absence of fluoride ion. *Tetrahedron Letters* **1995,** *36* (9), 1539-1540.

21. Hiyama, T., How I came across the silicon-based cross-coupling reaction. *Journal of Organometallic Chemistry* **2002,** *653* (1–2), 58-61.

22. Zhang, Z.-T.; Pitteloud, J.-P.; Cabrera, L.; Liang, Y.; Toribio, M.; Wnuk, S. F., Arylchlorogermanes/TBAF/,Moist Toluene: A Promising Combination for Pd-Catalyzed Germyl-Stille Cross-Coupling. *Organic Letters* **2010,** *12* (4), 816-819.

23. Ambrogio, I.; Cacchi, S.; Fabrizi, G.; Goggiamani, A.; Sgalla, S., Regio- and Stereoselective Heck a-Arylation of Cinnamyl Alcohols. *Synlett* **2009,** *4*, 620-624.

LIST OF FIGURES